# PREDICTION OF
# HEAT TRANSFER AND FLOW CHARACTERISTICS
# IN A RECIRCULATING REATTACHING FLOW

BY
SAYEED AHMED

/

Thesis submitted to the Department of Mechanical Engineering
in partial fulfilment of the requirements of the degree of
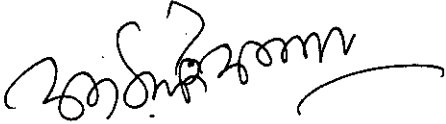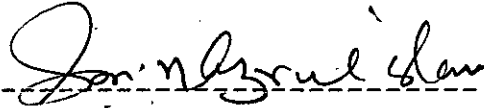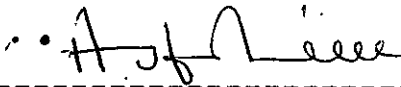Master of Science
in
Mechanical Engineering

December, 1989

BANGLADESH UNIVERSITY OF ENGINEERING AND TECHNOLOGY, DHAKA-1000
BANGLADESH.

The thesis titled " Prediction of Heat Transfer and Flow
Characteristics in a Recirculating Reattaching Flow " submitted
by Sayeed Ahmed, Roll No. 871419P, Registration No. 81379 of
M. Sc. Engg. (Mechanical) has been accepted as satisfactory in
partial fulfillment of the Master of Science in Engineering
(Mechanical) on 2nd December 1989.

BOARD OF EXAMINEERS

1.  _____
    Dr. A. K. M. Sadrul Islam                              Chairman
    Associate Professor                                   (Supervisor)
    Dept. of Mech. Engg.
    BUET, Dhaka.


2.  _____
    Dr. S. M. Nazrul Islam                                 Member
    Professor & Head
    Dept. of Mech. Engg.
    BUET, Dhaka.


3.  _____
    Dr. Md. Quamrul Islam                                  Member
    Professor
    Dept. of Mech. Engg.
    BUET, Dhaka.


4   _____
    Dr. Md. Abdul Halim                                    Member
    Professor & Head                                      (External)
    Dept. of Water Resources Engg.
    BUET, Dhaka.

ii

## CERTIFICATE OF RESEARCH


This is to certify that the work presented in this thesis is the outcome of the investigation carried out by the candidate under the supervision of Dr. A. K. M. Sadrul Islam in the Department of Mechanical Engineering, Bangladesh University of Engineering & Technology, Dhaka.


_____                    _____

Supervisor                                        Candidate

## ABSTRACT

Numerical solutions based on standard finite volume method are presented for the study of heat transfer and fluid dynamic characteristics in both laminar and turbulent flows behind a single-sided backward facing step. The calculation of the differential equations is performed using SIMPLE algorithm. For the turbulent flows, the standard $K-\epsilon$ turbulence model is used. The experimental studies of Armly et al(1982) for laminar flow and that of Eaton and Johnston (1980) and, Vogel and Eaton (1984) are used to validate the present predictions.

Prediction of velocity profiles and reattachment lengths for laminar flow cases are in good agreement with measured values except for higher Reynolds number cases. The prediction of heat transfer characteristics illustrates the augmentation of local heat transfer rate at the reattachment zone by three times the typical flat-plate value.

Predicted mean-velocity profiles and reattachment lengths, for turbulent flow, comply with the experimental data, but significant deviations occur in the predictions of turbulent intensities. The predicted heat transfer co-efficient are in good agreement upto the reattachment point and downstream of that point it matches qualitatively.

iv

## ACKNOWLEDGEMENTS

TO MY PARENTS
AND
NAZIAT

# C O N T E N T S

## LIST OF FIGURES

# NOMENCLATURE

$C_f$     Skin friction co-efficient $= \tau_\omega / \frac{1}{2}\rho v_o^2$

$C_p$     Static pressure co-efficient $= (P_w - P)/1/2 \rho U_o^2$

$c_p$     Specific heat

h     Developing channel height, heat tranfer co-efficient

$$= \dot{q}_o'' / (T_w - T_o)$$

H     Channel height, h + S

K     Conductivity

k     Turbulent kinetic energy, $1/2 \sqrt{u_i^2}$

P     Pressure

$P_o$     Reference static pressure.

$P_w$     Local wall static pressure

$P_r$     Prandtl number

$q_o''$     Wall heat transfer rate per unit area

Re     Reynolds number, $hU_o/\nu$

$Re_s$     Reynolds number based on step height, $SU_o/\nu$

S     Step height

ST     Stanton number $= h/U_o \rho c_p$

T     Temperature

$T_o$     Free stream temperature

$T_w$     Local wall teamperature

$U_o$     Freestream velocity

U     Mean streamwise velocity

u,v     Fluctuating velocities

$u^*$     Friction velocity, $\sqrt{\tau_\omega/\rho}$

V      Mean normal velocity

X      Streamwise distance from step edge

$X_r$      Reattachment length from step edge

Y      Distance from the step wall

$Y^+$      Non-dimensional distance from the wall, $Yu^*/\nu$

$X^*$      Non-dimensionalized reattachemnt length $(X-X_r)/X_r$


Greek Letters


$\delta$      Boundary layer thickness

$\nu$      Freestream kinematic viscocity

$\tau_\omega$      Local wall shear stress

$\Theta$      Non-dimensionalized local temperature difference

$$= \ (T-T_o)/(T_w-T_o)$$

$\rho$      Density

$\mu$      Viscocity

# CHAPTER 1

## INTRODUCTION

### 1.1  BACKGROUND

The reattachment of a shear layer, laminar or turbulent, has been the subject of study for many years because to its practical importance. These studies have attempted to explain the basic physics underlying the fluid-dynamics and heat-transfer behaviour in the separated and reattaching shear layer.

The heat-transfer process is intimately coupled with the fluid dynamics in reattaching flows. Very few studies have been made about the contribution of fluid mechanics in controlling the heat transfer rate in the reattachment zones.

In a large number of practical heat transfer devices such as heat exchangers and turbine engines, reattaching boundary layers can cause unexpected augmentation in the local heat transfer rate. This fact is creating great interest in numerical modeling of both the fluid dynamics and the heat transfer in a reattaching flow.

Among two dimensional flows the backward facing step is the simplest reattaching flow. This geometry fixes the point of separation, allows a spatially fixed free shear layer, and incorporates a relatively easily located reattachment zone and redevelopment region. In addition, the streamlines are nearly

parallel to the wall at the separation point, so the principal elliptic interactions occur downstream of separation.

Although the backward-facing step is the simplest reattaching flow, the flow field is still very complex. Fig.1.1 illustrates some of the complexities of the backward-facing step flowfield. A boundary layer separates from the step edge, becoming a free shear layer, which is almost unaffected by the presence of the upper and lower walls. This shear layer grows by entrainment from both the freestream and the recirculation region beneath it. Due to the pressure gradient and its own expansion, this shear layer turns and reattaches at the lower surface. Within the reattachment zone the shear layer is subjected to the effects of strong curvature, adverse pressure gradient and strong interaction with the wall. One or more of these mechanisms cause(s) a rapid decay of the turbulence energy within the reattachment zone. Part of the shear layer fluid is deflected upstream into the recirculating flow to supply the entrainment. So between the wall and the separated shear layer, a recirculation region of some complexity exists, with a primary vortex and a small corner eddy close to the step face. The backflow region is a layer of fluid near the wall. Downstream of reattachment, in the redevelopment region, the reattached shear layer gradually transforms back into a wall dominated flow structure.

The heat transfer is generally low in the recirculation region where velocities are less than the freestream. It then

rises very rapidly approaching the reattachment region, where it peaks at values typically 50% greater than under ordinary boundary layers. Downstream of reattachment, the heat transfer rate reduces back to the flat plate solution.

## 1.2 LITERATURE REVIEW:

There are two main streams in the literature for this study, the fluid dynamics of the backward-facing step and heat- transfer studies of separated and reattaching flows. In recognition to this fact, the following literature survey contains two main sections. The first is a brief survey of the fluid dynamics in a backward facing step following a brief survey of the heat transfer studies in separated flows.

## 1.2.1 Fluid dynamics of the Backward-Facing Step:

Many studies of separated and reattaching flow have been incorporated in air and water, at subsonic and supersonic speeds, with a wide variety of geometries. The following survey concentrates on subsonic, backward facing step flows.

In the last few years, there has been extensive work on the fluid dynamics of the backward-facing step, including several recent literature surveys. For example, Vogel and Eaton (1984) conducted an extensive experiment on heat transfer and fluid mechanics measurements in the turbulent reattaching flow behind a backward-facing step. Eaton and Johnston (1980) provided a

comprehensive review of subsonic, reattaching turbulent flow (See Table 1.1). Watkins and Gooray (1982) cover some of the same material, but also included a survey of heat-transfer experiments in reattachment. Other pertinent literature surveys include Bradshaw and Wong (1972) and Westphal's (1982) extensive coverage of separation and reattachment.

Brief description of the relevant recent experiments follow in chronological order.

Hsu (1950) was the first to measure both mean flow and turbulence profiles in a low-speed flow behind a large step. He noted little unsteadiness in the position of the reattachment points. His turbulence data, which were measured with hot-wire anemometers are in serious disagreement with other worker's results.

Another early study was made by Abbot and Kline (1961), who measured mean-velocity profiles for both single and double steps of various heights. They used water flow with flow-visualization techniques, and observed that the flow near reattachment was very unsteady. They concluded that most of the backflow fluid was entrained into the shear layer in the early region of shear-layer development. Turbulence measurements were attempted with hot-film anemometers.

Tani et al (1961) measured mean velocity, turbulence intensity and turbulent shear stress for flow with various step

heights. These measurements, which were made with hot wires, were the first reasonably accurate turbulence data for the backward-facing step flow-field. They noticed little change in the flow when the state of separating boundary layer was changed from laminar to turbulent.

Bradshaw and Wong (1972) studied the recovery of the boundary layer downstream of reattachment. They concluded that (i) there was a very fast rate of decrease in the Reynolds stresses just downstream of reattachment, (ii) the developing boundary layer did not follow the log law of the wall in the normal way, and (iii) the wake component of the mean velocity profile was abnormal. In fact, ordinary turbulent boundary layer characteristics still were not fully recovered at their last data station which was 52 step heights downstream of separation. Their results demonstrated the importance of understanding the turbulence structure in the reattachment zone.

Narayanan et al (1974) measured wall-static-pressure distributions behind steps of various heights. They found similarities in the pressure distributions and were able to infer the reattachment length from the pressure distribution.

Bordered and Bradshaw (1975) investigated three-dimensionality of the flow in the recirculating region. They also measured the effect of aspect ratio ( channel width/step height ) on the reattachment length and base pressure and found that end wall effects were negligible for aspect ratios greater than ten.

Seki et al (1976) and Rushed et al (1978) made turbulence measurements with hot-wires, but neither study contributed much to the understanding of the flow.

Chandrasuda (1975) made extensive measurements in the separated and reattached flow using hot wires. Measurements included mean velocity, Reynolds stresses, higher-order turbulence quantities and intermittence. Chandrasuda found rapid changes in turbulence structure for some distance downstream of reattachment. Despite the rapid changes, the free-shear-layer structure which was developed ahead of reattachment was still important at the last data station, $X/S = 14.3$, well downstream of reattachment. In a preliminary flow-visualization experiment, Chandrasuda observed that large eddies were not torn in two at reattachment, as had been implied by Bradshaw and Wong (1972) from reattachment and others went upstream with the recirculating flow in a more or less alternating fashion.

Kim et al,(1978) measured mean velocity, Reynolds stresses and intermittence in a sudden-expansion channel flow using hot-wire anemometers. Their measurements comprise the best-documented data set to date for the backward-facing step flow (Eaton and Johnston,1980). The motion of wall tufts in their experiments indicated large-scale unsteadiness in the reattachment region and suggested the spanwise variations at reattachment.

Smyth (1979) used a laser-doppler anemometer to measure mean-velocity and Reynolds-stress components in a double-sided, sudden-expansion flow. Unfortunately, the measurement resolution was not adequate to provide much information about the separated flow region. He found that the turbulence profiles were still far from equilibrium 48 step heights downstream of separation. This demonstrated the remarkable persistence of the flow structure characteristic of the separated shear layer.

Eaton and Johnston (1980) were among the first to make measurements in the highly unsteady and reversing flow behind a backward-facing step, using instruments that could accurately quantify the flow. They used a pulsed-wire anemometer, thermal tuft and pulsed-wall probe to take data in the reversing region and measure the skin friction. They found that the laminar separated layer grows faster than for the turbulent case. In the redeveloping boundary layer, the turbulence intensity decreases rapidly downstream of reattachment, with the turbulence actually beginning to decay upstream of reattachment some one or two step heights. Upstream of this region, the shear layer was found to be essentially identical to a plane-mixing layer. The observed vortex pairing for laminar but not turbulent separation, using two point velocity correlations. They believe that the presence of vortices in the laminar case and the rapid mixing associated with them was responsible for the more rapid growth rate of laminar shear layer. Using several thermal tufts to track the location of the reattachment point, they found a low-frequency "flapping" of the reattachment region as it oscillated back and

forth approximately one step height around the mean reattachment point.

Durst and Tropea (1981) used a water channel to study a backward facing-step flow, acquiring the data with a laser-doppler anemometer. In their study, by varying the expansion ration they found a strong dependence of the reattachment length on this quantity. Similar profiles on the plots of the reattachment distance versus the Reynolds number might mean that the effect of area ratio could be uncoupled from those of Reynolds number.

Driver and Seegmiller (1982) acquired wind-tunnel fluid-dynamic data for the backward-facing step using a laser-doppler anemometer. From their data they extracted many of the important turbulence quantities, such as production and dissipation rates in the flow. They studied the effect of pressure gradient on the separated flow. However, they found that the Reynolds stresses are similar for cases both with and without overall pressure recovery.They also found a sudden increase in the Reynolds stresses right after separation, increasing until two step heights upstream of reattachment, where the stresses begin to decay. The side of the shear layer toward the wall showed substantially higher turbulence levels than the other, which appeared like a free shear layer. Turbulent triple cross-products disappear rapidly approaching reattachment,possibly because the large vortices which produce this correlated motion are torn

apart at reattachment. Generally, they rank the production and dissipation terms as being the most dominant, though convection and diffusion are also important.

Pronchick (1983) investigated the backward -facing step flow in a water channel with a fairly thick boundary layer ( $\delta/S =$ 0.8 ) at separation, using laser-doppler anemometer and flow visualization. The main objective of his work was to examine the interaction of large shear-layer structures with the wall in the unsteady reattachment region. Pronick concluded that all of the observed unsteadiness was caused by three-dimensional eddies. Three different paths were observed for the vortices as they passed into the reattachment region. Some of the eddies do not impinge on the wall at all, but "over ride" the reattachment region and go on downstream into the outer edge of the redeveloping boundary layer essentially intact. These overriding eddies are the source of the large length scales in the outer part of the boundary layer downstream of reattachment and are responsible for the slow recovery of the reattached layer. The vortices that impinge (do impact) on the wall are broken up, and parts are either swept upstream to be entrained back into the shear layer, enter the recirculation region, or are swept down stream into the redeveloping boundary layer. No large, coherent motions are visible in the recirculation region, indicating a loss of organized structure due to the large shear-layer eddies.

Pronchick supported these ideas by noting that the turbulence kinetic energy is generated primarily far from the

wall in the reattachment region. This production decreases rapidly as the fluid moves downstream, while the near-wall region changes more slowly.

Further experiments were carried out by Westphal (1982) in a backward facing step geometry wind tunnel, using the pulsed-wall probe and other instruments. For all turbulent boundary layers at separation, he found a stronger than expected dependence of reattachment length on the boundary-layer thickness at separation. Among the cases he studied were perturbations to the flow, such as the effect of embedded longitudinal vortices and Reynolds number variations. Special attention was paid to what he identified as a region of strong, viscous flow close to the wall in the upstream-flow region of the separation bubble. Significantly, the data for all cases seems to collapse best on a normalization based on the reattachment length, $X^* = (X-X_r)/X_r$ where, $X_r$ is the reattachment length. Further, he proposed a definition of the reattachment region as extending roughly 20% of the reattachment length on either side of the mean reattachment point. Scaling on $X^*$ collapse all the data in the recirculation region independent of perturbation to the flow, even though the reattachment length itself may change considerably as various flow parameters are changed.

Walterick et al (1984) performed some experiments on a backstep flow using mainly hot films and hot wires. They also observed free-stream turbulence levels of 2% which they attribute to unsteady motion in the recirculation region. The lack of any

flow conditioning upstream of the test section and the high free-stream turbulence level make their work of uncertain value.

Adams (1984) made an extensive study of the fluid dynamics behaviour in a backward-facing step. He used a variety of instruments, including a laser-doppler anemometer operating in air, to obtain a wide variety of data. From his experiments, Adams arrived at several significant conclusions. First, he showed the importance of all three of the parameters that affected this flow, namely, the upstream condition as determined by the boundary-layer thickness at separation, the step height Reynolds number, and the expansion ratio. Initial boundary-layer thickness has an effect on flow variables such as the reattachment length. The state of the boundary layer is also important, as laminar separation has considerably shorter reattachment length than does turbulent. However, the region around recovery is relatively insensitive to the initial conditions as long as s/S < 0.4. Since the pressure recovery first becomes affected at roughly this same value, he suggests this as a dividing line between the cases where separation and reattachment have a " strong" (s/S < 0.4) or " overwhelming" effect (s/S > 0.4) on the downstream boundary layer.

From a comparison of his work with those of others, Adams concluded that different expansion ratios produce qualitatively different reattachment zones and thus cannot be compared using flow similarity. Over the range of step-height Reynolds numbers studied, the flow did not reach Reynolds- number independence

(maximum $Re_s$ = 36,000). Because the maximum recirculation region velocities are typically 20% of the free stream, much higher free-stream velocities would be required to attain Reynolds-number independence in that zone ($Re_s$ = 200,000).

Adams examined the thin boundary layer in recirculating flow in some detail. He found strong evidence to support the earlier supposition by Westphal (1982) that the backflow boundary layer was laminar, even at the maximum Reynolds number ($Re_s$ = 36,000). The evidence for this conclusion included measurements of the streamwise component of the velocity close to the wall. Which showed that the burstling process typical of a turbulent flat-plate boundary layer was missing. There are high levels of fluctuations in the fluid, but it is not correlated motion. The reverse-flow velocity profiles appear more like a laminar layer than a turbulent one. The fluctuations scale on the distance from reattachment and the local mean velocity for y+> 20 and approximate a stokes solution for y+< 20. This means that the low frequencies are damped out in the region close to the wall.

Simpson et al(1981a, 1981b, 1983) carried out significant experiment on separation boundary layer. They have taken extensive laser-doppler anemometry data in a effort to model the mean-velocity profile in backflow regions. Upstream of separation, the velocity profiles follow the Law-of-the wall. Downstream of separation, in the backflow region, the turbulence intensities are very high.

Vogel and Eaton (1984) made an extensive experiment on heat transfer and fluid mechanics measurements in the turbulent reattaching flow behind a backward-facing step. The overall goal of their research was to investigate the relationship between the fluid dynamics and heat transfer in a separated and reattaching flow.

## 1.2.2 Experimental Studies in Backward Facing Step Heat Transfer:

Heat-transfer studies of a separated and reattaching boundary layer have been carried on for some time. Few of the previous experiments include only mean-velocity or turbulence profiles. Since the reattachment length was not measured directly, it was usually inferred from the heat-transfer results. However, all these experiments show the same general features of heat transfer in a reattaching flow, that is, a low value of the heat-transfer rate in the fully separated region, followed by a rapid rise to a maximum near reattachment, followed by eventual recovery to flat-plate levels. Many of the studies are perturbations of the geometry or other parameters of the flow studies that contribute significantly to the physical understanding and modeling of the flow will be pointed out.

Seban (1964) measured velocity and temperature distributions downstream of a backward facing step using a constant heat flux surface. He found, for a one-inch step and a free-stream velocity of 150 ft/sec (Re = 76,000), that mean reattachment, as inferred from the heat-transfer data, was about six step height downstream

of the step. Further, he did not find the wall similarities typical of a wall-controlled boundary layer in neither the separation nor the reattachment regions. A hot wire was used for making the velocity measurements which can not give correct results in reversing or highly turbulent flows. Seban found large temperature gradients near the wall downstream of the step. In fact, 1.2 step heights downstream of separation, 80% of the temperature drop from the wall to the free stream was within 0.2 step heights of the wall.

In an earlier effort, Seban et al (1958) found similar results, with the addition that the maximum Nusselt number behind the step appeared to depend on Re $^{0.8}$ In a later paper, Seban (1966) made the important point that the maximum heat-transfer rate occurs at the point of low or zero skin friction. He attributed this fact to high diffusivity along with a low thermal resistance typical of a newly developing layer.

Filetti and Kays (1967) measured the local heat-transfer co-efficient on a constant-temperature surface behind a symmetric sudden expansion (double step ). Large expansion ratios, typically 1:2, were used. They concluded that the peak heat-transfer rate occurred at the reattachment point, which was approximately four step heights downstream of the step. They did not independently measure the reattachment length, and the shortest estimated length suggests that the peak heat transfer actually occurred upstream of reattachment. The peak heat transfer rate based on Nusselt number was found to vary as Re$^{0.6}$

over the range 70,000 < Re < 205,000. They found significant augmentation of the heat-transfer rate downstream of reattachment, up to six times the flat-plate value for the same conditions. Measurements were taken from the step edge to 14 step heights downstream. At that point, the Nusselt-number profiles had still not returned to a typical flat-plate value.

Aung and Goldstein (1972) acquired data in an air flow behind a backward-facing step using a Mach-Zehnder interferometer with an estimated uncertainty of 7%. Since the upstream step was heated to the same temperature as the downstream surface, the boundary conditions for this flow were generally different from those of other studies. Also, the range of free-stream velocities was smaller, ranging from 1.65m/s to 4.55m/s, with a step height of 6.5mm. This corresponds to a Reynolds-number range based on step height of 700 to 1290. For all cases, the boundary-layer thickness at separation was one step height.

They concluded, from the temperature profiles, that 90% of the temperature drop from the wall to the free-stream occurred in the shear layer at the station 0.53 step height downstream of separation. Further downstream, the thermal resistance became more concentrated in the near wall region. At the point midway between separation and reattachment ($X^* = -0.5$), 50% of the temperature drop was across the shear layer and the rest was across the fluid near the wall. The location of reattachment was inferred to lie at the maximum heat-transfer point, which was 4.5 step heights downstream of reattachment for all Reynolds-number.

This was further upstream than found in similar experiments with higher-speed flows. The mean heat-transfer co-efficient downstream of reattachment shows the expected profile, with the maximum 50% greater than the far-downstream value. They showed that after 12 step heights the heat-transfer co-efficient is recovering to the flat-plate value.

Seki et al (1976a & b) constructed a double-sided, backward-facing step using air as the working fluid. Typical Reynolds number ranged from 4,000 to 250,000. They also varied the step heights between 0.035 and 7.0, normalized on the distance between the upstream surfaces. They obtained temperature and velocity measurements in the flow over their constant heat flux surface using a fine thermocouple and hot wire, respectively. The authors mentioned that the hot wire was inadequate in a highly turbulent flow.

Aung (1983 ) investigated the heat-transfer for a completely laminar flow over a backward-facing step. His relevant to this work was that the streamwise curvature upstream of separation had significant impact on the local heat-transfer rate. This finding was of importance when describing the initial conditions for numerical calculations. The mean reattachment point did not have associated with it any particular heat-transfer characteristics. In general, the agreement with the theory of Chapman was very good.

Kottke (1984) attempted to provide a more unified approach to the subject of heat, mass and momentum transfer in a variety of separated flows. He chose air as the fluid and used a single-sided, backward-facing step as his test apparatus. His observations were based on flow visualization of a subliming material from the lower surface. From his own study and by correlating the work of others, he decided that the reattachment length is the relevant length scale.

Vogel and Eaton (1984) made the most extensive study on the turbulent reattaching flow behind a backward facing step. Heat transfer and fluid dynamic measurements were made in the turbulent separated and reattaching flow behind a backward-facing step. The primary goal was to investigate the causes of high heat transfer rate in the reattachment region. Specific objectives included extending the engineering correlations for the heat transfer rate, characterization of the redeveloping boundary layer, and analysis of the near wall region. The experimental facility used for this work was a two-dimensional, sudden-expansion rectangular duct 45 cm in span with an expansion ratio of 1.25. Filtered ambient air was the working fluid used for measurements over a velocity range of 3 - 15 m/sec. The boundary layer thickness at separation was varied between 0.1 to 1.5 times the 3.81 cm step height.

Heat transfer data were acquired using a constant heat flux heat transfer surface. Mean temperature profiles were obtained using a traversing thermocouple probe. The thermal tuft and the

pulsed wall probe were used to measure the forward flow fraction and the wall skin friction, respectively. A Laser Doppler Velocimeter was used in conjuction with a traversing resistance thermometer to make measurements of the correlation of the local fluctuation temperature and normal component of the velocity.

### 1.2.3 Numerical Studies of Heat Transfer in Backward Facing Step Flows :

Within the last fifteen years, numerical modelers have made a great deal of progress in the computation of complex turbulent flows. In the last five years, these computations have been extended to include the temperature field, with limited, but significant success. Most of these computations have been carried out using variations on the $k - E$ model for the turbulence, although algebraic stress models also received some attention.

In all of these computations, an important consideration is the treatment of the boundary condition at the inner edge of the grid. At this point, usually around $y+ = 70$, some sort of wall model for the flow is used to give the velocity and temperature boundary conditions. This model plays a crucial role in the success or failure of the numerical method. Significant effort has been made to " fix up " various numerical methods to work satisfactorily in backward-facing step flows with heat transfer. However, these modes are successful over a very limited range of geometrics and boundary and initial conditions. Recently, the

realization that the near-wall and turbulence models are the important keys to successful, general computational techniques has spurred development in these areas.

Chieng and Launder (1980) calculated the velocity and temperature fields downstream of an abrupt pipe expansion (expansion ratio = 1:2),using a k - $\epsilon$ model of turbulence. Wall functions were used to connect the grid to the solid surfaces. These wall functions are based on a universal length scale for the turbulence, with the scale increasing linearly with distance from the wall. This model was used for the near-wall region of the flow outside the viscous sublayer.

For higher Reynolds-number calculations ranging from 4860 to 66,260, they claim agreement within 15% of the heat transfer rate measured by Zemanick and Dougall (1970).However, the location of the maximum heat-transfer point, calculated by their model, was upstream of that found experimentally by one step height. To check the generality of their results, they calculated all the way to the wall with a low Reynolds-number case and found a 500% overprediction of the heat-transfer rate. They believe that this effect can be attributed to the large overprediction of the length scales in the near-wall region.

Based on the work of Chieng and Launder (1980), Amano (1982) developed a new near-wall model to improve the predictive capability of the Navier-stokes equations using a k-$\epsilon$ turbulence model. This new model evaluates the generation and dissipation

rates of the turbulence for the grid point nearest the wall, at $y+ = 30$. The turbulent kinetic energy is assumed to have a parabolic profile, giving the same linear profile for the fluctuating component of the velocity as used by Chieng and Launder (1980).The main difference between the two methods lies in the treatment of the $\mathcal{E}$- equation. Amano (1982) does not need local equilibrium between production and dissipation in the near-wall region, but uses the zero gradient at the wall and a mean velocity model to generate a set of equations describing the behavior in this region.

Comparing their results to those of Chieng and Launder (1980) for the same pipe flow, they found it improved the predictions of the mean heat transfer by 20%. However, their calculations predict the maximum heat transfer point to lie at five step heights downstream of separation, simultaneously predicting reattachment at $X/S = 7$. Compared to the data of Zemanick and Dougall (1970), their data underestimated the distance to the maximum heat - transfer point by 30 - 50%.

Watkins and Gooray (1982) performed extensive computations to compare their numerical models to experiments with heat transfer in both backward - facing steps and sudden-expansion pipe flows. Their basic method was built on the TEACH-T code, modified by including heat transfer and quadratic differencing for the convective terms. Essentially, they used a two-pass system, the first pass finding the reattachment point using the standard k - E model. Once mean reattachment was found, they

recomputed using the same grid, substituing the low Reynolds-number model in the redeveloping region.

They studied a variety of closure techniques, including mixing length models, k - $\varepsilon$ models, and modifications to the latter. Their reported results are based on their own development of a co-efficient that determines the length scales from the viscosity and a relation for the turbulent Prandtl number. These new relations are based on, but do not use, the algebraic stress models. The key inclusions into the standard k - $\varepsilon$ model are terms involving the streamline curvature and " wall-damping ".

As in the earlier studies, their treatment of the near-wall region is generally the same as they prescribed boundary conditions using " wall-functions". At y+<5,the flow is assumed laminar; between 13<y+<250, the flow is assumed to follow the log-law for fully turbulent flow. Their velocity – field boundary conditions depend on a specification of the shear stress at the wall. Their computations start closer to the wall than do those of earlier modelers, in this case at y+ = 15.

Compared to the experimental results of Zemanick and Dougall (1970), their results show improved agreement using their two-pass system over earlier modelers. The location of the maximum Nusselt number is within the experimental error and correlates on Re $^{0.75}$. Their heat transfer profiles recover more slowly than do the experimental results, with a maximum deviation of 15% just

downstream of reattachment at $Re_S$ = 66,260. They note generally greater deviation for lower Reynolds - numbers.

For a single-sided backstep flow, they found a variation in the maximum heat-transfer rate with boundary-layer thickness at separation. They reported a computed decrease of 8% in the maximum Nusselt number as the boundary-layer thickness decreases from $\delta$/S = 2.0 to $\delta$/S = 0.4 at Re = 5000.

Chieng (1983) investigated a number of different turbulence models for the abrupt pipe expansion.Compared to the results of Zemanick and Dougall (1970), the standard two-equation k - $\varepsilon$ model underpredicted the maximum heat-transfer rate, even with the modification to include secondary turbulence terms, a near-wall model, and high pressure - gradient effects. The low-Reynolds-number models overpredicted the heat-transfer rates.

He believes that solutions to these problems involve the use of the correct turbulent " Prandtl number " and higher vorticity transport. For his computations, he empirically arrived at the correct values for these terms by comparison with the experimental results.

Sinder (1983a,1983b) compared four different closure methods for the Reynolds stresses in calculating the flow behind a backward facing step. The four different methods were the k-$\varepsilon$ "modified" k - $\varepsilon$, algebraic stress, and "modified" algebraic stress. He also used a new non-equilibrium wall-function treatment in the models. His conclusions are as follows: changes

in the pressure gradient mainly affect the reattachment length. Then effects are greater at lower expansion ratios. The pressure gradient does not change the magnitude of the Reynolds stress, but moves the location of the maximum in space. All four numerical models show the proper relationship between the expansion ratio and the size of the separation region. None of the numerical models works well in all region of the flow. The "modified" algebraic stress model works best in the recirculation region, but performs more poorly than the others in the redevelopment region. He then concluded that combining several models in a kind of zonal approach to take advantage of their region dependency would give good results.

The above numerical studies help point out the lack of good near-wall models to use in developing numerical methods for predicting the heat transfer in a reattaching flow.

1.3. Objectives of the Present Research :

The overall goal of this project is to develop a computer code which can predict the fluid dynamic behaviour and the heat transfer rate in strongly recirculating reattaching flows with sufficient accuracy. In particular, the main motivation behind this work is to investigate the causes of large augmentation of the heat transfer in the reattachment region. To achieve this goal, experiment of Armaly et al (1982) for laminar case and that of Eaton & Johnston (1980) and Vogel & Eaton (1984) for

turbulent case are taken for data base. This goal is broken down into several specific objectives :

a) Prediction of laminar recirculating reattaching flows.

b) Prediction of turbulent recirculating reattaching flows.

c) Prediction of heat transfer rate in laminar flows with constant heat-flux and constant temperature boundary conditions.

d) Prediction of heat transfer rate in turbulent flows with constant heat flux boundary conditions.

e) Investigation of the effect of varying Reynolds number on reattachment length.

f) To study the variation of pressure co-efficient and skin-friction co-efficient in the flowfield.

g) To predict the behaviour of the heat transfer co-efficient along the wall.

## CHAPTER 2

## MATHEMATICAL MODEL

### 2.1 Governing equations :

The partial deferential equations for conservation of mass, momentum and a conserved scalar property for steady incompressible turbulent flow in cartesian tensor notation ( for detail see Hinge 1975 ) are :-

$$\text{mass :} \qquad \frac{\delta U_i}{\delta X_i} = 0 \qquad\qquad (2.1)$$

$$\text{momentum :} \quad \frac{\delta}{\delta X_j} (U_i U_j) = -\frac{1}{\rho} \frac{\delta P}{\delta X_i} + \frac{\delta}{\delta X_j} \left( \frac{\delta U_i}{\delta X_j} - \overline{u_j u_j} \right) \qquad (2.2)$$

$$\text{Scalar :} \quad \frac{\delta}{\delta X_j} (U_i \, \theta) = \frac{\delta}{\delta X_i} \left( \frac{\Gamma_0}{\rho} \frac{\delta \theta}{\delta X_i} - u_i \theta \right) \qquad (2.3)$$

Where, upper case $U_i$ and $\theta$ represents the averaged values of velocity and scalar and lower case $u_i$ and $\theta'$ represent their fluctuating quantities, an overbar represent a mean value of that quantity. For laminar flow calculations, the governing equations are equations(2.1)-(2.3) except the fluctuating quantities.

Equations 2.1 to 2.3 do not form a closed system because of the unknown fluctuating correlations. Thus the equations 2.1-2.3 can only be solved if the unknown correlation "$-u_i u_j$" and "$-u_i \theta'$" are determined through some modeling known as turbulence modeling.

## 2.2 Turbulence Model of the Present Study :

The model used in the present study is the standard k-model(Launder & Spalding 1972).The set of equations constituting this model is:

Reynolds stress :-

$$- \overline{u_j u_j} = \nu_t \left( \frac{\delta U_i}{\delta X_j} + \frac{\delta U_i}{\delta X_i} \right) - \frac{2}{3} k \; _{ij} \dots \quad (2.4)$$

where $\delta_{ij} = 1$ for $i = j$ and $\delta_{ij} = 0$ for $i \neq j$

Turbulent heat flux :-

$$- \overline{u_i \theta} = \frac{\nu_t}{\sigma_{\theta,t}} \left( -\frac{\delta \theta}{\delta X_i} \right) \dots \quad \dots \quad \dots \quad \dots \quad (2.5)$$

where eddy viscosity.

$$\nu_t = C_\mu \frac{k^2}{\epsilon} \quad \dots \quad \dots \quad \dots \quad \dots \quad (2.6)$$

where $C_\mu$ is a const.

The modeled k-equation.

$$\frac{\delta}{\delta X_i} (\rho U_i k) = \frac{\delta}{\delta X_i} \left( \frac{\mu_{eff}}{\sigma_k} \cdot \frac{\delta k}{\delta X_i} \right) + G - \rho \epsilon \quad \dots \quad (2.7)$$

The modeled $\epsilon$-equation.

$$\frac{\delta}{\delta X_i} (\rho U_i \epsilon ) = \frac{\delta}{\delta X_i} \left( \frac{\mu_{eff}}{\sigma_\epsilon} \cdot \frac{\delta \epsilon}{\delta X_i} \right) + C_{\epsilon 1} \rho \frac{\epsilon}{k} G - C_{\epsilon 2} \frac{\epsilon^2}{k} \quad (2.8)$$

where G and other constants are given in table 2.1

## 2.3 Boundary Conditions :

The transport equations  2.1-2.3 and 2.7-2.8 are of elliptic type and their solutions require  known conditions at the boundaries. The following boundary conditions are employed in the present study.

i.   At the inlet boundary, known quantities are specified from the experimental sources.

ii.   At the outlet boundary a zero gradient for stream wise velocity, $k, \varepsilon$ and scalar temperature are employed.

iii. At the solid wall, all velocities and turbulent kinetic energy are specified to be zero. For temperature equation two types of wall conditions are considered : (a) constant wall temperature and, (b) constant heat flux condition.

## 2.4 Calculation of Heat Transfer Coefficient :

(a) for constant wall temperature condition heat transfer coefficient is calculated as follows.

$$h \ ( T_w - T_o) = K -\frac{\delta T}{\delta y} \bigg|_{y \ = \ o} \qquad \ldots \ldots \qquad \ldots \ldots \qquad \ldots \ldots \qquad (2.9)$$

(b) for constant heat flux condition, the wall temperature is calculated by the following equation:

(i) $$K -\frac{\delta T}{\delta y} \bigg|_{y \ = \ o} = K \ \frac{T_w \ - T_w +1}{\nabla Y} = q'' = Const. \ (for \ laminar \ flow)$$

$$\ldots \ (2.10)$$

(ii) $$T_w = T_{w+1} + \frac{q''}{\rho C_p \checkmark K_{w+1}} \ ( \frac{U_{w+1} \ K_{w+1}}{\tau_w / \rho} - 1.77 \ )(for \ turbulent \ flow)$$

$$\ldots \ldots \ (2.11)$$

where (w+1) represents the nearest grid to the wall.

Equation 2.11 is taken from Joyatilek (1978).

## 2.5   Method of Numerical Calculation :

The partial different equations 2.1-2.3, 2.7 -2.8 can be reduced to the standard from :

$$-\frac{\delta}{\delta X_i}(\rho U_i \theta) = -\frac{\delta}{\delta X_i}(\Gamma_\theta -\frac{\delta \theta}{\delta X_i}) + S_\theta \ldots \ldots \ldots \qquad (2.12)$$

Where $\theta$ is a general dependent variable, $S_\theta$ is the source term and     is their diffusive transport coefficient. Table 2.1 illustrates these terms for equations 2.1 - 2.3 & 2.7 - 2.8.

These elliptic partial differential equations   are solved by a standard finite volume method. The detail derivation and formulation of this method  can be found for example in Patankar (1980).

In the present study,  the convective terms on the left hand side of equation ( 2.12) are discretised by using third order accurate quadratic upstream weighted scheme known as QUICK (Quadratic Upstream Interpolation for Convective Kinematics) [Leonard, 1979]. The diffusive fluxes and the source terms (right hand terms of equation 2.12 ) are discretised by using second order accurate central differencing. The use of QUICK scheme reduces numerical inaccuracies due to false diffusion related to the first order UPWIND scheme ( Leschzincer & Rodi 1981, Leonard et al 1978 ).

## TABLE 2.1

## The Conservation Equations

| Equation | $\theta$ | $\Gamma_\theta$ | $S_\theta$ |
|---|---|---|---|
| Mass | 1 | 0 | 0 |
| U-momentum | U | $\mu_{eff}$ | $-\frac{\delta P}{\delta X} + \frac{\delta}{\delta X}(\mu_{eff}\frac{\delta U}{\delta X}) + \frac{\delta}{\delta y}(\mu_{eff}\frac{\delta V}{\delta X})$ |
| V-momentum | V | $\mu_{eff}$ | $-\frac{\delta P}{\delta X} + \frac{\delta}{\delta X}(\mu_{eff}\frac{\delta U}{\delta Y}) + \frac{\delta}{\delta Y}(\mu_{eff}\frac{\delta V}{\delta Y})$ |
| Temperature | T | $\frac{\mu}{\sigma_\theta} + \frac{\mu_t}{\sigma_{\theta t}}$ | 0 |
| Turbulent kinetic energy | K | $\frac{\mu_{eff}}{\sigma_k}$ | $G - \rho\varepsilon$ |
| Dissipation of k | $\varepsilon$ | $\frac{\mu_{eff}}{\sigma_\varepsilon}$ | $\frac{\varepsilon}{k}(C_1 G - C_2 \rho\varepsilon)$ |

$$\mu_{eff} = \mu + \mu_t, \quad \mu_t = C_\mu \rho \frac{k^2}{\varepsilon}$$

$$G = \frac{\mu_t}{\rho}(\frac{\delta U_i}{\delta X_i} + \frac{\delta U_j}{\delta X_i})\frac{\delta U_i}{\delta X_j}$$

| C | $C_1$ | $C_2$ | $\sigma_k$ | $\sigma_\varepsilon$ | $\sigma_\theta$ | $\sigma_{\theta t}$ |
|---|---|---|---|---|---|---|
| 0.09 | 1.44 | 1.92 | 1.0 | 1.22 | 0.72 | 0.90 |

The discretised equations are solved simultaneously using the SIMPLE (Semi Implicit Method for Pressure - Linked Equations) algorithm of Patankar & Spalding (1972) by repeated sweeps of a line-by-line application of the Tridiagonal Matrix Algorithm (TDMA) (Patankar 1980). Since the mass and momentum equations are not coupled with temperature, the temperature equation is solved after the convergence of the momentum equations.

The calculations of the cases considered in this study are carried out using 40 X 25 (x,y) grid. Two more grid systems (coarse) are also used in two cases to test grid dependence. This will be discussed in the following chapter. The grid spacings used are non-uniform with grid lines more closely spaced near the step.

CHAPTER 3

# PREDICTION OF LAMINAR FLOW AND HEAT TRANSFER

## 3.1   Introduction :

In this chapter the results obtained from the prediction of Armaly et al's (1982) experiment of laminar flow in the backward facing step is discussed. The experimental set up of Armaly et at incorporated of a two dimensional backward facing step that provided an expansion ratio of 1:1.94. The large channel, downstream of the step, had a height of 1.01cm and an aspect ratio of 18:1. A laser-Doppler anemometer was employed to define quantitatively the variation of separation length with Reynolds number and to obtain detailed information of the velocity profiles downstream of the step. Armaly et al also presented two-dimensional numerical predictions of mean velocity distributions. His prediction also based on finite volume approach but the convection terms were discretised with hybrid scheme.

In this present prediction, four different Reynolds number cases are considered  and the results are compared with the experimental and predicted values of Armaly et al (1982).

The present prediction also contains heat transfer co-efficient for two different boundary conditions: constant wall temperature and constant heat flux.

## 3.2   Computational details:

Grid dependence test was made to determine the most optimum grid size of the calculation domain. The test was done for Reynolds number 100 and 1290. In figures 3.1 & 3.2 the U-velocity profiles are presented for three grid sizes: (20 X 11), (30 X 14), and ( 40 X 25 )(x,y). For both Reynolds number, it was found that the optimum grid size was ( 40 X 25 ). However, due to the memory limitation of the computer, finer grids could not be used. This grid size was  chosen for all the cases considered in this prediction. All these calculations were done on an IBM/AT computer at Mech. Engg. Dept., BUET.

## 3.3   Results and Discussion:

### 3.3.1   Fluid dynamic characteristics :

The U-velocity profiles of the four different Reynolds number cases are presented in figures 3.3 to 3.6. The velocity profiles for Reynolds number of 100 and 389 show good agreement with the experimental values of Armaly et al. For different axial locations the velocity profiles matches almost entirely. For Reynolds number of 1000, the present predicted velocity profiles were compared with that of Armaly et al's experimental and predicted profiles. The present predicted profiles resembles to the experimental profiles up to X/S = 15.5. Then the profiles deviate considerably up to 24 and  again show a good agreement

when the profiles are fully developed. But Armaly et al's predicted profiles deviated considerably after a distance of 4 step height. The predicted velocity profiles for Reynolds number of 1290 showed good agreement with that of the experimental data upto an axial distance of 15 step height. After that the profiles deviated considerably.

The variation in reattachment length with Reynolds number from Armaly et al's experiment and prediction is presented in fig. 3.7 and compared with the present prediction. The reattachment length is clearly a function of Reynolds number. The present predicted reattachment length almost coincide with the experimental data. Armaly et al could not predict this length after Reynolds number of about 400. This profile also showed that recirculation length increases with the increase of Reynolds number of about 1200, after which the value decreases where the flow becomes transitional.

Except primary zone of recirculating flow attached to the backward facing step, additional regions of flow separation downstream of the step and on both sides of the channel test section was also found in the present prediction as had been reported by Armaly et al. One additional region at the upper wall for Re = 1000 and two additional regions, one at the upper and the other at the lower wall, are found in the present prediction but their sizes could not be predicted accurately due to the limitation of grid refinement.

The variation of wall static pressure for both upper and lower wall are shown in figures 3.8(b) - 3.10(b). For all Reynolds number wall static pressure is found to be maximum in the reattachment zone and in the downstream of reattachment, static pressure for both walls is identical.

Profiles of skin-friction co-efficient are shown in figures 3.8(c)-3.10(c).The skin-friction co-efficient is found to be zero in the vicinity of reattachment point which corresponds to the definition of reattachment length given by Westphal (1983). The upper wall skin-friction co-efficient is maximum at the step, decreases to a minimum in the reattachment zone and then remains almost constant.

3.3.2 Heat transfer characteristics :

Convective heat transfer co-efficient profiles for constant wall temperature are presented in figures 3.8(d)-3.10(d). For all Reynolds number, the peak value occurs in the vicinity of the reattachment zone. The maximum heat transfer rates in the present prediction range from 2.24 times that of the far downstream value for 1000 Reynolds number and 2.9 times for Re=100. The peak heat transfer coefficient gradually shifts towards the reattachment point as the Reynolds number increases (see fig. 3.11).

All of the convective heat transfer co-efficient have the same general features. There is a low heat transfer rate in the recirculation region, followed by a steep rise to a maximum near the reattachment point. The ratio of the maximum value to the value near recirculation region is found to depend on the Reynolds number. The heat transfer rate then declines less than 50% from the peak value, downstream of reattachment, to a typical flat-plate level.

The effective origin of the redeveloping thermal boundary layer is found by matching the flat-plate solution to the profile downstream of reattachment, as shown in figure 3.12. The following correlation (Kreath 1958) is used to generate the flat plate profile

$$h_x = 0.332 \ K/x \ Re_x^{1/2} \ Pr^{1/3}. \ \dots \dots \dots \dots \dots \dots \dots \dots \tag{3.1}$$

This procedure locates the effective origin approximately two step heights downstream of reattachment, for Reynolds number of 100. But far downstream of reattachment, present prediction overestimates the heat transfer rate by about 25%.

Figure 3.14 shows that normalizing the local convective heat transfer co-efficient for all Reynolds number on the maximum value of the heat transfer co-efficient collapses to one point at the reattachment point. At this point convective heat transfer co-efficient is maximum. Figure 3.13 shows that the normalized zero stream function line for all the Reynolds number collapses to one profile.

To investigate the effect of constant heat **flux** boundary condition on the wall temperature, only one case is considered i.e. Re = 100. The constant heat flux q" is taken from the results of constnat wall temperature condition, i.e.

$$q" = [-\frac{1}{L} \int_o^L h (T_w - T_o) \, dx ] \qquad T_w = Cont. \qquad L = 50S.$$

In figure 3.15 the wall temperature calculated from this boundary condition is presented. Figure 3.15 shows that the wall temperature decreases sharply after the separation, reaches to a minimum at about 0.2 step height after reattachment point, then gradually rises in the redeveloping zone. About 6 step height after reattachment point, the wall temperature overshoots the temperature for constant wall temperature condition. In the far downstream of reattachment point the temperature rises about 16% above the constant wall temperature condition.

Six temperature profiles are shown in fig. 3.16 at various axial locations. The rise of temperature at different locations above the free-stream is nondimensionalized by the difference of temperature between the wall and the free stream. The temperature profiles show the steepest temperature gradients, and therefore most of the thermal resistances in the region very close to the step height where thermal boundary layer lies. Near the wall, the

steepest temperature gradient is found to be at X/S = 3.45 which is close to reattachment point as the bulk of the low temperature fluid comes in contact with the hot wall. The temperature gradient for X/S = 1.0 is almost constant from wall to the step height because in the recirculating region there is mixing motion of the fluid. Far downstream of reattachment point, the temperature profiles show that steep temperature gradient gradually shifts away from the wall because of the thick thermal boundary layer in the redeveloping zone which approaches flat plate solution.

CHAPTER 4

PREDICTION OF TURBULENT FLOW AND HEAT TRANSFER

## 4.1 Introduction :

This chapter describes the prediction of turbulent recirculating reattaching flow for three different Reynolds number. The Reynolds numbers considered here are 11000, 28000, and 40000 based on step height. Data base for Reynolds number 11,000 and 40,000 are taken from Eaton and Johnston (1980) and for 28,000 from Vogel and Eaton (1984). In the two former cases, only fluid dynamic data are available whereas in the later case relevant heat transfer data are also found. In the present prediction both fluid dynamic and heat transfer characteristics of recirculating reattaching flow are investigated and compared with the experimental data.

Eaton and Johnston (1980) used a blower wind tunnel. With the step height set at 5.08cm the test section was a sudden expansion from 7.62cm to 12.70cm. The instruments used in their study were (i) a thermal tuft, (ii) a pulsed - wire anemometer, and (iii) a pulsed wall probe.

Vogel and Eaton (1984) used 3.8cm high backward-facing step with an expansion ratio of 1.25 (h = 15.2cm, H = 19cm).They measured heat transfer characteristics of reattaching flow along with fluid dynamics with precision instruments such as (i)

traversing thermocouple probe (ii) thermal tuft (iii) traversing and non-traversing pulsed wall probes (iv)Laser-Doppler anemometer and (v) resistance thermometer.

In the present prediction,the computational domain was divided by a 40 X 25 (x,y) mesh for all cases and the calculations were performed in an IBM PS/2-50 computer in the Dept. of Mech. Engg., BUET.

## 4.2 Results and Discussion :

### 4.2.1 Fluid dynamic characteristics :

Vogel and Eaton (1984) measured the reattachment length $(X_r)$ by taking the distance from the backward-facing step face to the point of zero mean skin friction co-efficient, corresponding to the point of 50% forward flow fraction defined as the point at which the flow is going upstream one half the time and downstream the other half [Westphal (1983)]. In the present prediction this length is taken as the distance of zero stream function line from step face along the lower wall which corresponds to the point of zero mean skin friction coefficient. The predicted and measured values of $X_r$ are presented in Table 4.1. The prediction of reattachment length are in good agreement with the experimental values.

Table 4.1

Reattachment Length of Turbulent Flows

| $Re_s$ | Boundary layer thickness at separation /S | $X_r/S$ | | Reference |
|---|---|---|---|---|
| | | Predicted | Measured | |
| 11,000 | 0.18 | 7.6 | 6.97 | Eaton & Johnston, 1980 |
| 28,000 | 1.10 | 6.95 | 6.68 | Vogel & Eaton, 1984 |
| 40,000 | 0.23 | 7.72 | 7.95 | Eaton & Johnston, 1980 |

Mean-velocity profiles for all three cases are shown in figs. 4.1 through 4.3. The velocity profiles show the shear layer growing by entrainment as it proceeds downstream and then intercepting the wall at the reattachment point. Underneath the shear layer, the near-wall boundary layer starts near reattachment and flows upstream toward the step. The predicted mean velocity profiles agrees quite well with the experimental one but slight deviation occurs in the downstream of reattachment. The maximum backflow velocity found in the present prediction is about 24% of the freestream velocity which is very close to the experimental value of 20% ( Vogel and Eaton ,1984). The location of maximum backflow velocity is about 0.1 step height from the wall and about 3.5 to 4.0 step height downstream of the step face.

Figure 4.4 presents the normal mean velocity (V) profiles normalized on the reference freestream velocity for $Re_s$ = 28,000. Near the step edge, there is an upward mean flow as the large recirculation eddy sweeps the fluid near the wall up toward the

shear layer, indicated by the positive going velocity profile at
X/S = 0.7 and 2.0. The V-velocity profiles further
downstream,(say X/S = 4.67) but still within the recirculation
region, are small downward velocities. This negative V-velocity
is due to the fact that the free shear layer is bending towards
the wall. Fluid from the lower edge of the shear layer then turns
at the wall and takes on a streamwise component of velocity in
the upstream direction. Just upstream of reattachment, the mean
flow is towards the wall across the entire shear layer.
Downstream of reattachment, the normal velocity gradually
decreases, indicating the formation of wall bounded flow.

Figures 4.5 through 4.7 present the fluctuating component of
the streamwise velocity for three Reynolds number cases. The peak
intensity grows and the region of turbulence broadens as the
shear layer develops. The turbulence intensity then decays,
beginning near in the reattachment zone. The location of the peak
in the turbulence-intensity profiles starts at about Y/S = 1.0
downstream of separation. The peak dips down towards the wall in
the recirculating zone then moves back out towards Y/S = 1.0
downstream of reattachment (not shown in the figure).

In the present prediction the trend of the turbulent normal
stress profiles is similar to that of the experiment. The maximum
underprediction is found about 50% which occurs near the step
edge for all cases. The predicted profiles gradually approaches
to that of the experiment in the reattachment zone and then about
15% overprediction occurs far downstream of reattachment zone

(see fig.4.6h). The peak level of $u^2$ for $Re_s = 28,000$ around 14.5% normalized on the freestream velocity, is found in the recirculation region at $X^* = -.12$ whereas in the experiment (Vogel and Eaton, 1984) the peak level and location was 16% and $X^* = -0.32$ respectively. The location of the maximum moves from $Y/S = 0.7$ at $X^* = -.12$ to $Y/S = 0.94$ at $X^* = 1.5$. The magnitude of the maximum drops from 14.5% to 12.5% in this distance. These predicted values are in good agreement comparable to that of the experiment of (Vogel and Eaton (1984).

In fig. 4.8 turbulent shear stress $(-\overline{uv})$ profiles for $Re_s = 40,000$ are presented and compared with experimental values of Eaton & Johnston(1980).The peak value of turbulent shear stress show a pattern very similar to that of the turbulent normal stress.In most of the axial locations, present model overpredicts the experimental data of Eaton and Johnston, (1980), although underprediction of about 25% in observed in the vicinity of the step face (at $X/S = 1.0$). The maximum predicted value of the turbulent shear stress is $-\overline{uv}/U_o^2 = 0.016$ where as the experimental value was 0.01.

4.2.2 Heat Transfer Characteristics:

In this section, the behaviour of the heat transfer characteristics of the recirculating reattaching flow is discussed. Fig. 4.9 shows the Stanton number variation for the Reynolds number cases considered here. Constant heat flux ($q_o'' = 130$ W/m$^2$) boundary condition in assumed at the step wall

according to the experimental setup of Vogel & Eaton (1984).

All of the Stanton number profiles have the same general features. There is a low heat transfer rate in the recirculation region $(X^* <0)$, followed by a steep rise to a maximum near the reattachment point. By comparing the location of the reattachment point to the location of the peak heat transfer rate, Vogel and Eaton (1984) found that the maximum occurs slightly upstream of reattachment. In present prediction it is found that the maximum Stanton number is about $0.13X^*$ to $0.17X^*$ upstream of reattachment point depending on the Reynolds number whereas the experimental value was about $0.1X^*$ for Re = 28,000. The heat transfer rate then declines 40% to 50% from the peak value depending on the Reynolds number, downstream of reattachment, to a typical flat-plate level.

The effective origin of the redeveloping thermal boundary layer is found by matching the flat-plate solution to the profile downstream of reattachment as shown in fig. 4.9(c). The following correlation, taken from Kays and Crawford (1980), is used to generate the flat-plate profile.

$$ST\ Pr^{0.4}\ = .030\ Re^{-0.2} \dots\dots\dots \quad\dots\dots\quad\dots\dots\dots \quad (4.1)$$

This procedure locates the effective origin approximately two step heights downstream of reattachment.

Profiles showing the variation of the heat transfer rate

with Reynolds number are presented in fig. 4.10. The streamwise coordinate is non-dimensionalized on the reattachment distance for each particular profile. The variation of the heat transfer co-efficient with the Reynolds number is smooth and monotonic. The entire Stanton number profiles are shifted in value, indicating a general scaling of the heat transfer rate on the Reynolds number, the same effect as for the flat-plate heated boundary layer. Far downstream of reattachment, the Stanton number assures a flat-plate turbulent boundary layer value. The maximum heat transfer rate in the present prediction range from 1.7 times for the largest Reynolds number to 2.0 times for the smallest of the far downstream values.

Figure 4.11 shows that normalizing the reference Stanton number profile on the maximum value of Stanton number collapsed almost to one profile although there is slight deviation downstream of reattachment. The experimental data (Vogel & Eaton, 1984) for $Re_s$ = 28,000 is identical with the predicted profile upto reattachment zone and then deviates considerably.

The predicted mean temperature profiles for $Re_s$ = 28,000 are presented at various streamwise locations downstream of the separation. The temperature profiles show the steepest temperature gradients, and therefore most of the thermal resistance, in the region very close to the wall, which is conduction dominated. Only in one of the profiles, that closest to the step at X/S = 0.33, there is a significant temperature gradient in the flow far from the wall, most of it across the

free shear layer. This gradient also exist for X/S = 1.66 but gradually decreases and almost diminishes after reattachment. The predicted profiles deviate considerably in the recirculation region and after reattachment point (X/S > 6.7), these are very close to the experimental data. This deviation is due to the shortcomings of diffusion modeling of temperature equation., Greater convective mixing effects in other regions of the flow does not allow steep temperature gradients except near the wall and accross the shear layer near the separation. The temperature drop accross the shear layer suggests that the warmer slow moving recirculation fluid is not rapidly transported accross the recently separated shear layer.

# CHAPTER 5

## CONCLUSION

Prediction of the fluid dynamic and heat transfer quantities in the separated and reattaching flow behind the backward facing step is made to develop a computer code with sufficient accuracy. Both laminar and turbulent flows are studied and compared with the existing experimental data base. A brief summary of the important conclusions of this work follows.

1.  This model predicts the laminar flow with sufficient accuracy for low Reynolds number (100 and 389). For higher Reynolds number, such as Re = 1000, the prediction of velocity profile is very good from step face to reattachment point, after that it deviates to some extent from the experimental data. In case of reattachment length, present prediction is identical with the experimental results.

2.  The heat transfer coefficient for a laminar reattaching flow is about three times that of a flat plate boundary layer around reattachment and also depends on Reynolds number. This augmentation is caused by thinning of the viscous layer adjacent to the surface resulting from the impinging mean flow. The higher the Reynolds number, the higher is the heat transfer rate. The maximum heat transfer rate lies at 10% the reattachement length upstream of reattachment point for the lowest Reynolds number and gradually shifts towards reattachment point for higher Reynolds number cases.

3.  The maximum temperature in laminar flows drop occurs across the shear layer very close to the seperation. So it can be concluded that the warmer slow moving recirculating fluid is not easily transported across the free shear layer at this region.

4.  For turbulent flow the present model predicts mean velocity profile almost accurately for all three Reynolds number cases considered, although there are small deviation in the profiles after reattachement point. Prediction of location and magnitude of backflow velocity is fairly good.

5.  Prediction of turbulent fluctuating component is not very good. There is underprediction of about 50% in the maximum turbulent normal stress near the separation point. The difference gradually decreases and close to the reattachment point, prediction approaches experimental data. Similar result is also found in the cases of turbulent shear stress prediction.

6.  The heat transfer coefficient in turbulent flows is about 2 times that of a flat plate boundary layer around reattachment which is close to the experimental value. The maximum heat transfer rate lies from $0.13X^{*}$ to $0.17X^{*}$ upstream of reattachment.

7.   The temperature profiles show the steepest gradients in the region very close to the wall which is conduction dominated. There is a significant temperature drop accross the shear layer in the recirculation region. The temperature profiles in upstream of reattachment can not be predicted with accuracy due to the shortcoming of the diffusion modeling of temperature equation.
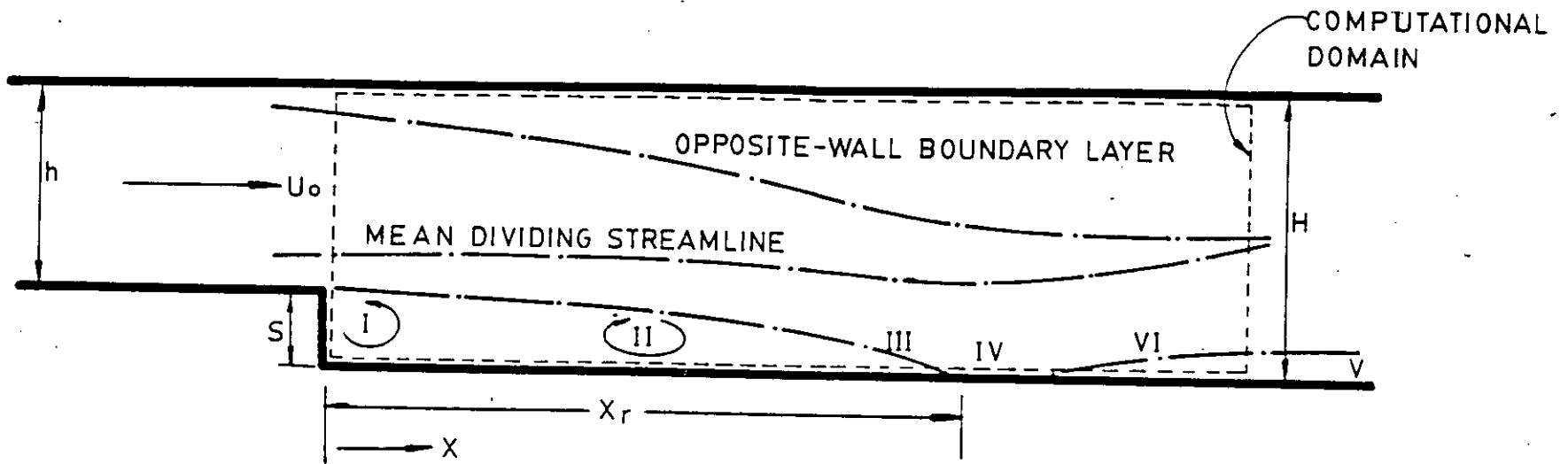
FLOW ZONES:

I    CORNER EDDY

II   BACKFLOW ZONE

III  SEPARATED SHEAR LAYER

IV  REATTACHMENT ZONE

V   REDEVELOPING NEAR-WALL FLOW

VI  RELAXING OUTER SHEAR LAYER

FIG. 1.1  SCHEMATIC OF THE SINGLE-SIDED BACKWARD-FACING STEP.
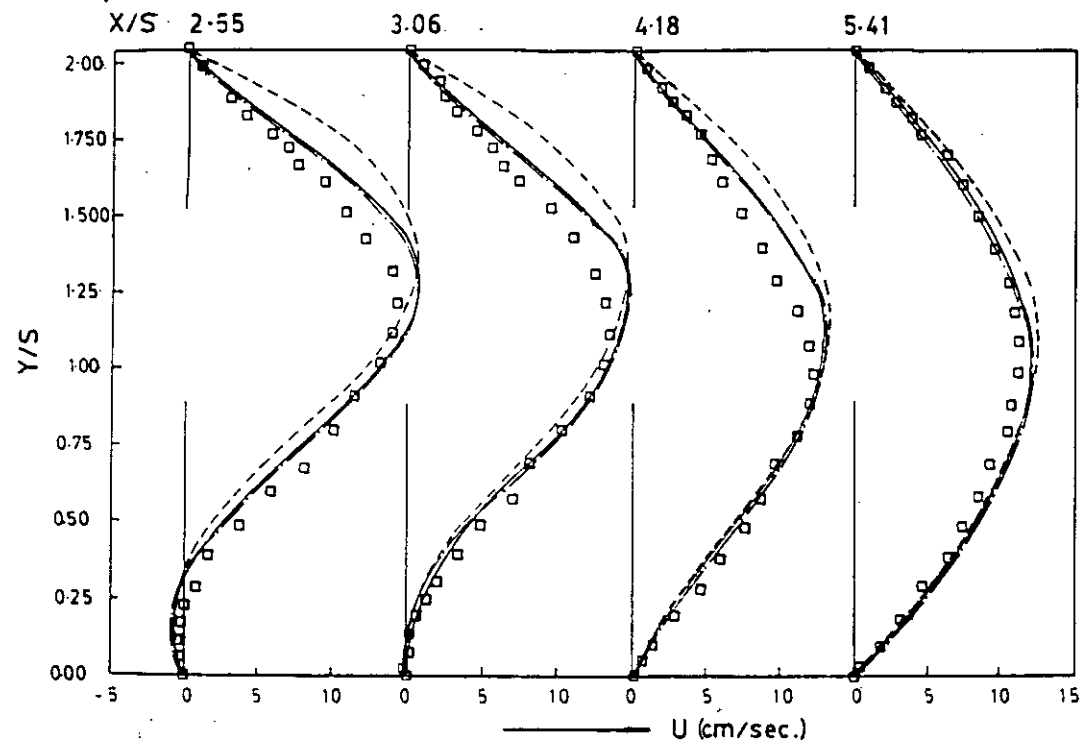
FIG. 3.1 GRID DEPENDENCY TEST FOR Re = 100

PRESENT PREDICTIONS ——— (40×25) —·— (30×14) & ----- (20×11)

□   EXPT. (ARMALY ET AL 1983)
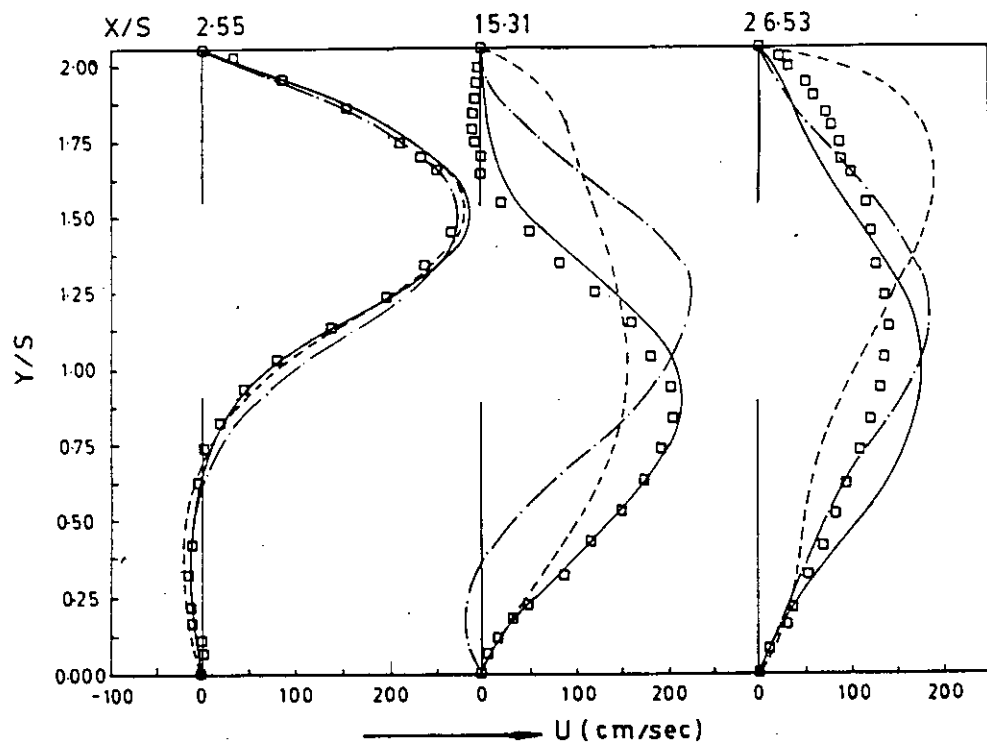
FIG. 3.2  GRID DEPENDENCY TEST FOR Re = 1290

PRESENT PREDICTIONS ——(40x25)———(30x14) & ———— (20x11)

□    EXPT. (ARMALY ET. EL 1983)
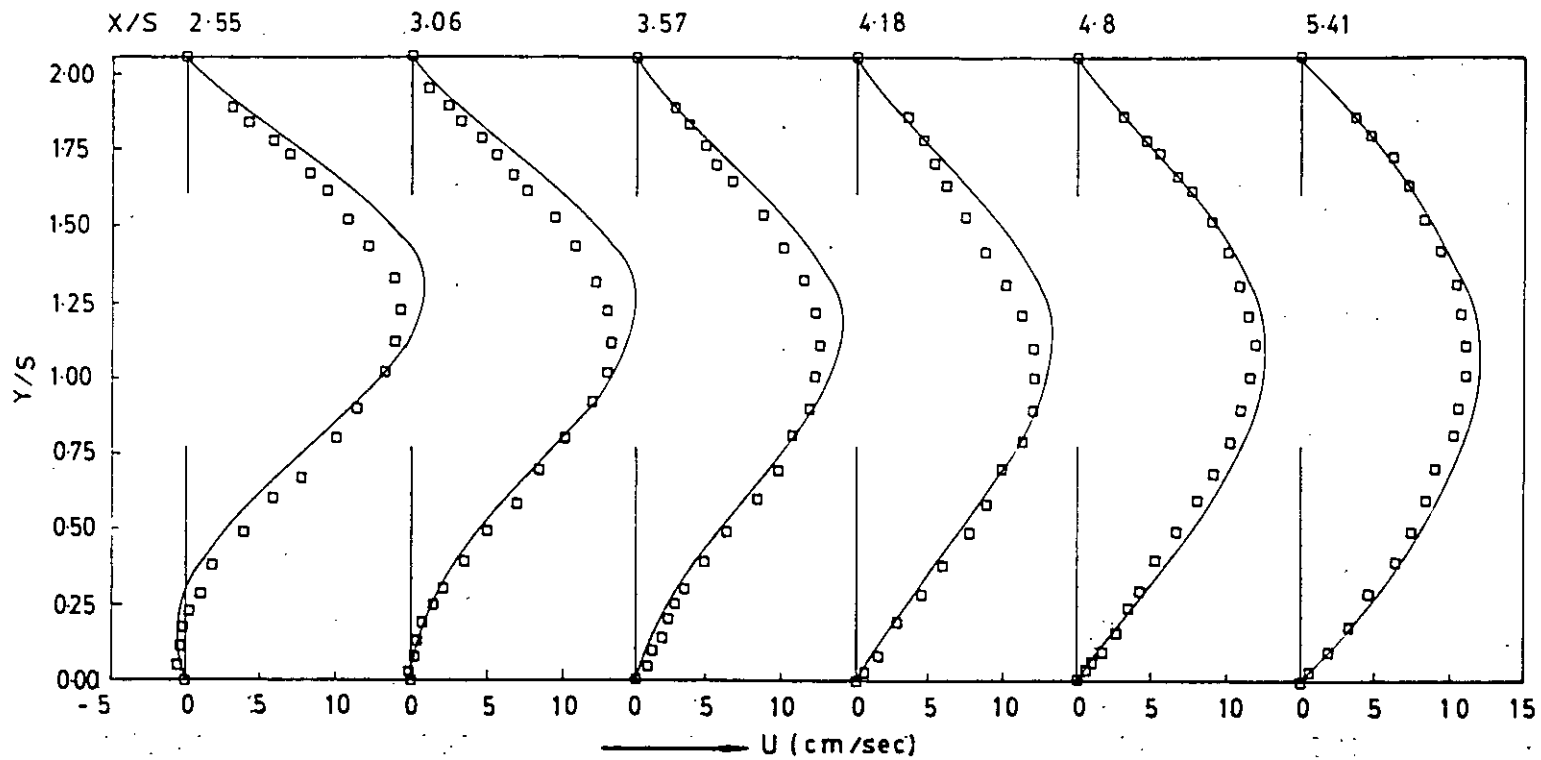
FIG. 3.3   VELOCITY PROFILES FOR Re = 100 AT DIFFERENT AXIAL LOCATIONS

□      EXPT. (ARMALY ET AL 1983)

———PRESENT PREDICTION
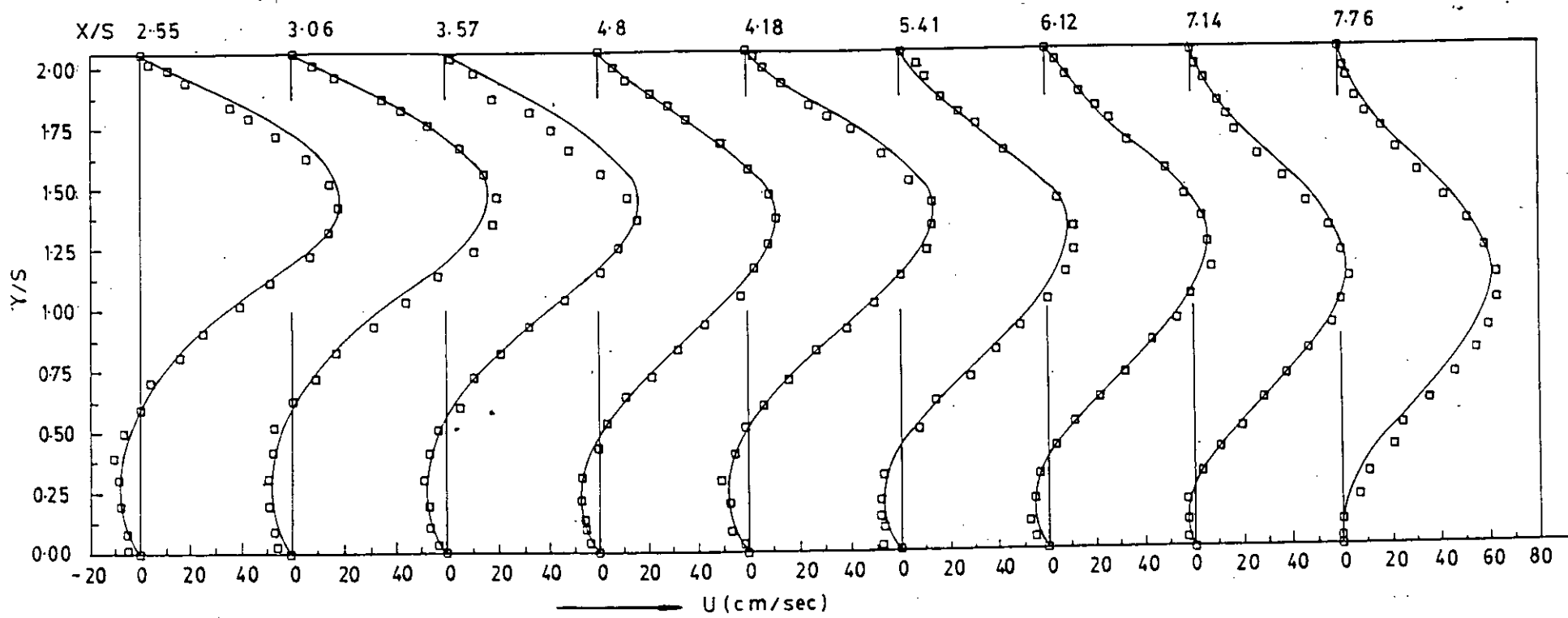
FIG. 3.4   VELOCITY PROFILES FOR Re=389 AT DIFFERENT AXIAL LOCATIONS

□   EXPT. (ARMLY ET AL 1983)

———PRESENT PREDICTION
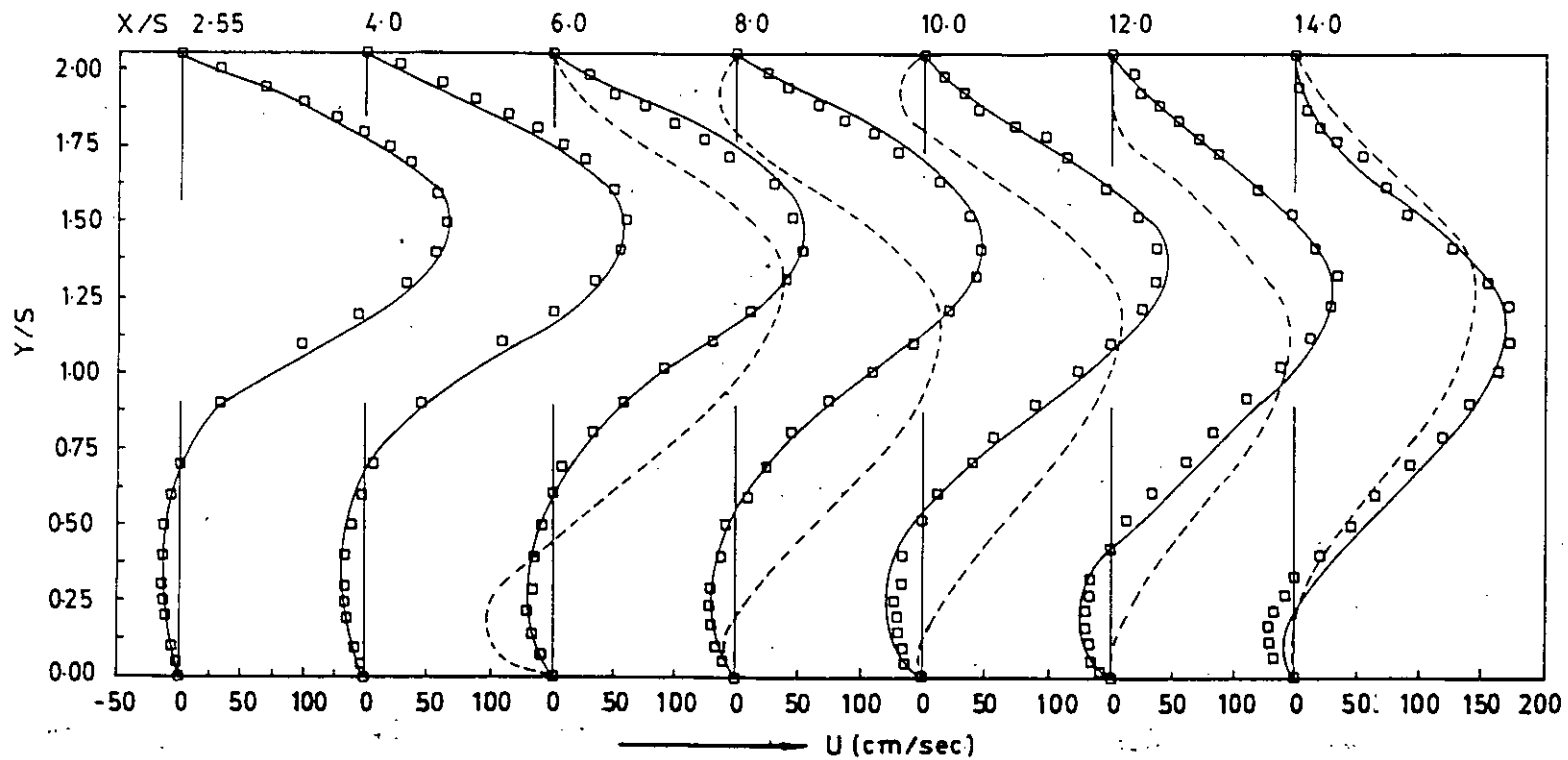
FIG. 3.5 VELOCITY PROFILES FOR Re = 1000 AT DIFFEREN AXIAL LOCATIONS
□ EXPT. (ARMALY ET AL 1983), ———— PREDICTION (ARMALY ET AL 1983)
———— PRESENT PREDICTION
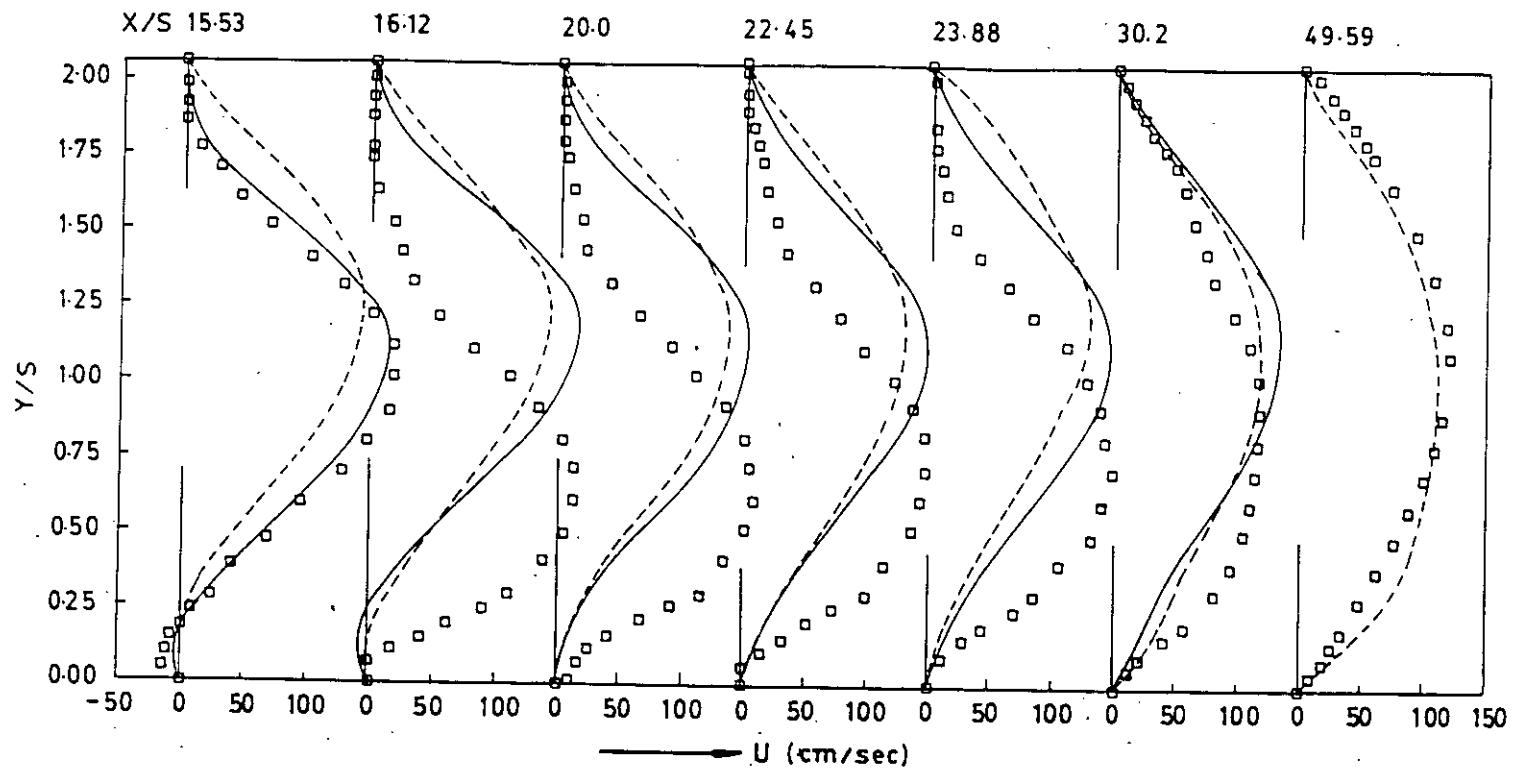
FIG. 3.5   VELOCITY PROFILES FOR Re=1000 AT DIFFERENT AXIAL LOCATIONS

□   EXPT.(ARMALY ET AL 1983) ,————PREDICTION (ARMALY ET AL 1983)

————PRESENT PREDICTION
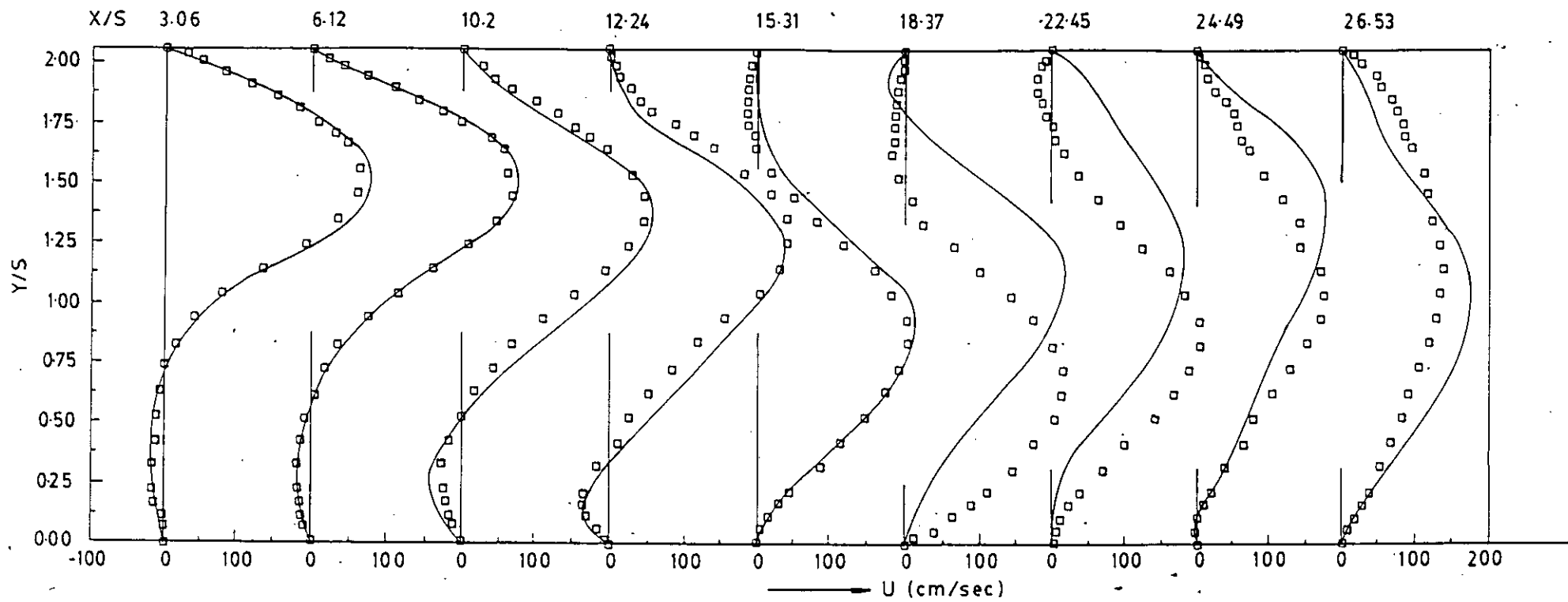
FIG. 3-6  VELOCITY  PROFILES  FOR  Re = 1290  AT  DIFFERENT  AXIAL  LOCATIONS

      □     EXPT. (ARMALY ET AL 1983 )

      ——    PRESENT PREDICTION
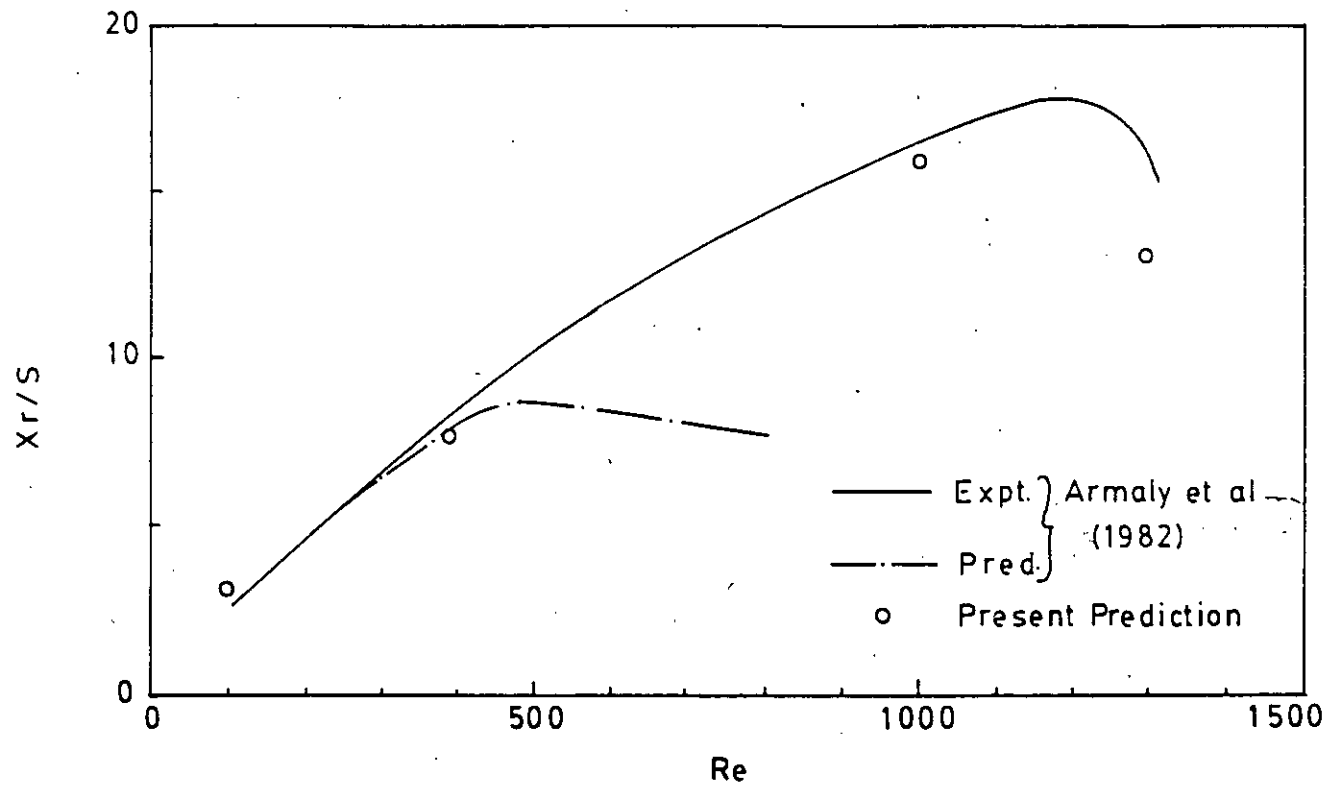
FIG.3·7  REATTAEHMENT LENGTH FOR DIFFERENT REYNOLDS NUMBER
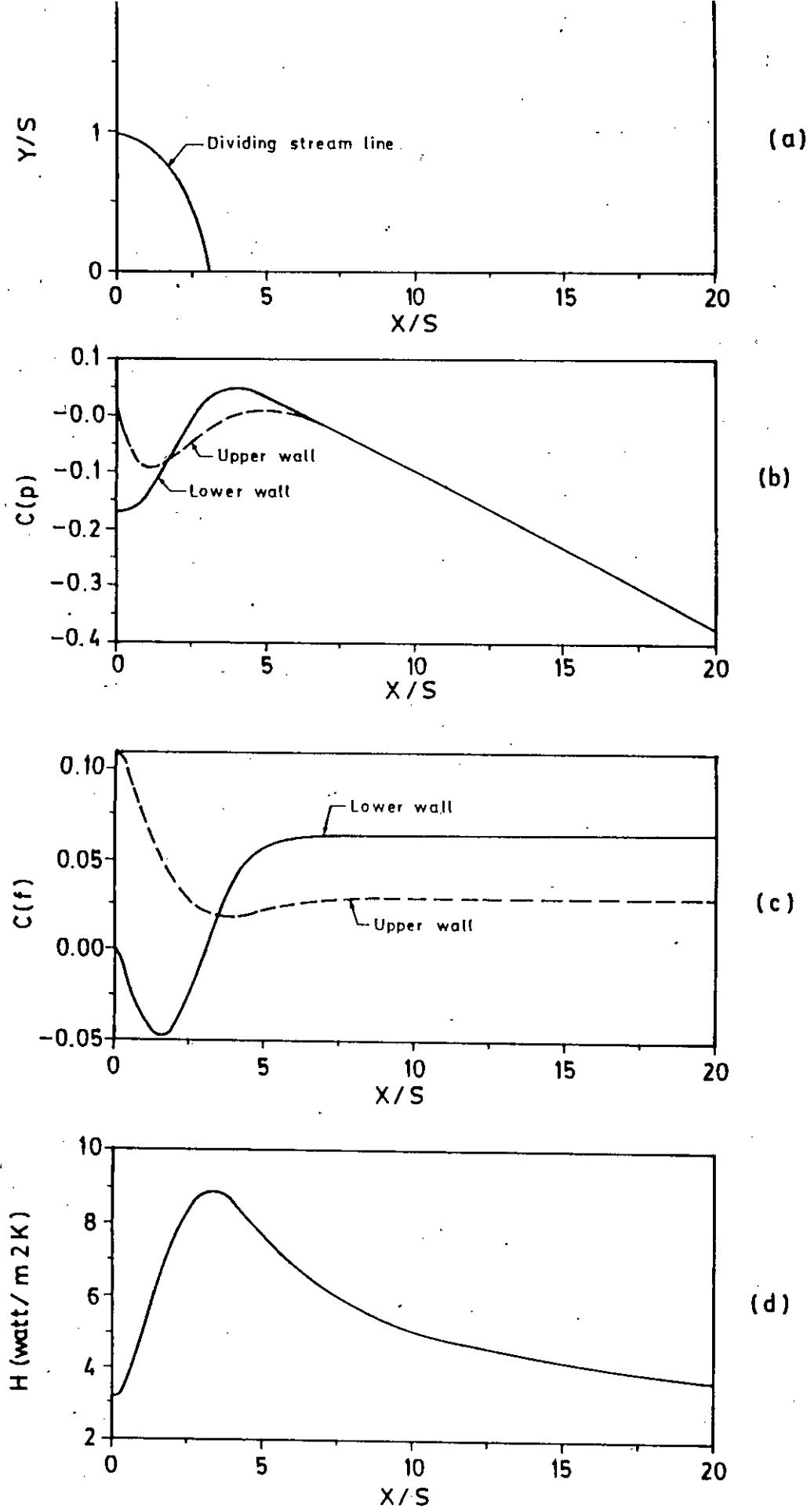
Fig. 3·8   Predicted profiles of (a) dividing stream line (b) static
pressure co-efficient at the wall (c) skin friction co-effi-
cient and (d) convective heat transfer co-efficient for Re = 100
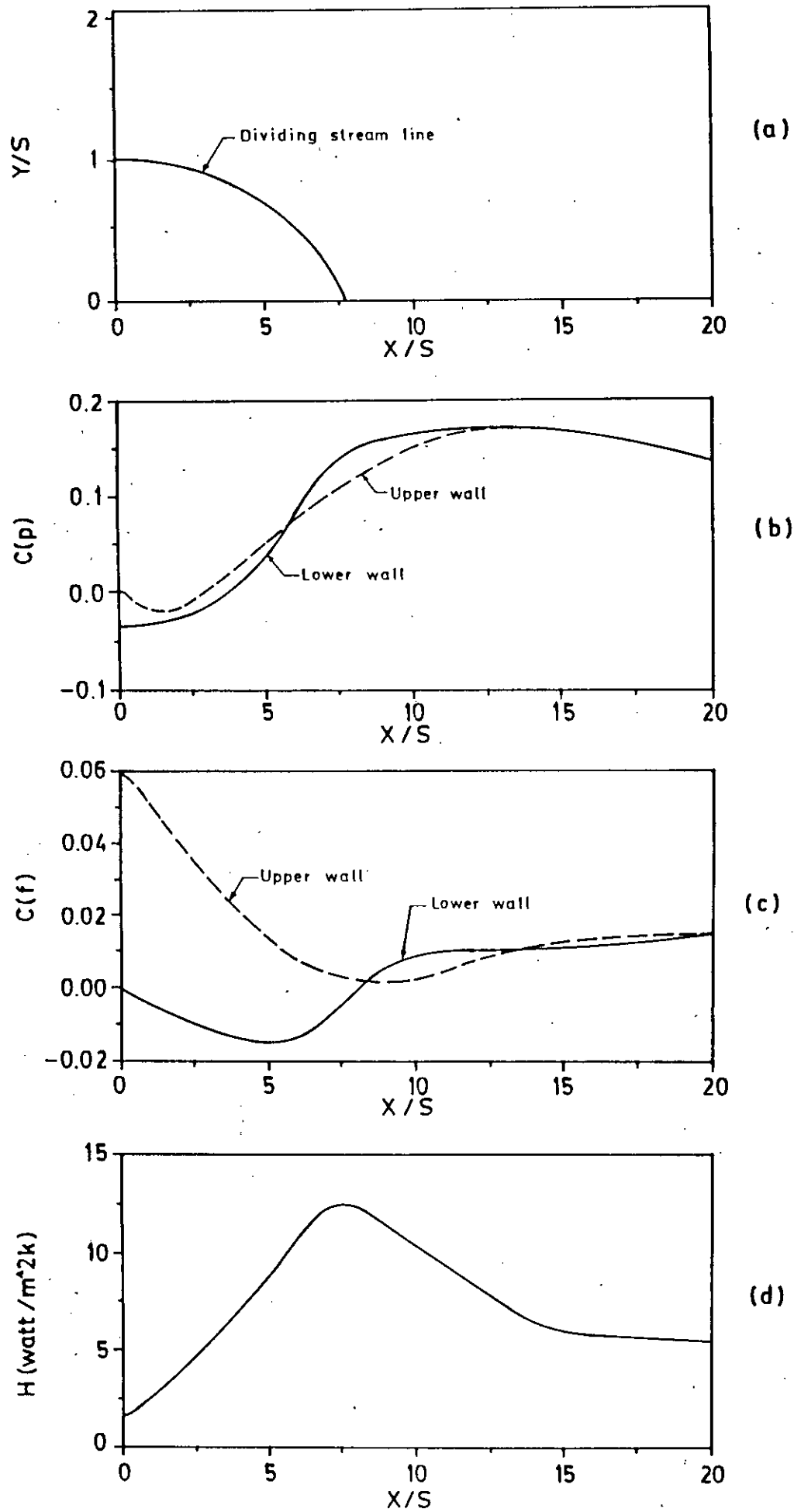
Fig. 3·9 Predicted profiles of (a) dividing stream line (b) static pressure co-efficient at the wall (c) skin friction co-efficient and (c) convective heat transfer co-efficient for Re = 389.
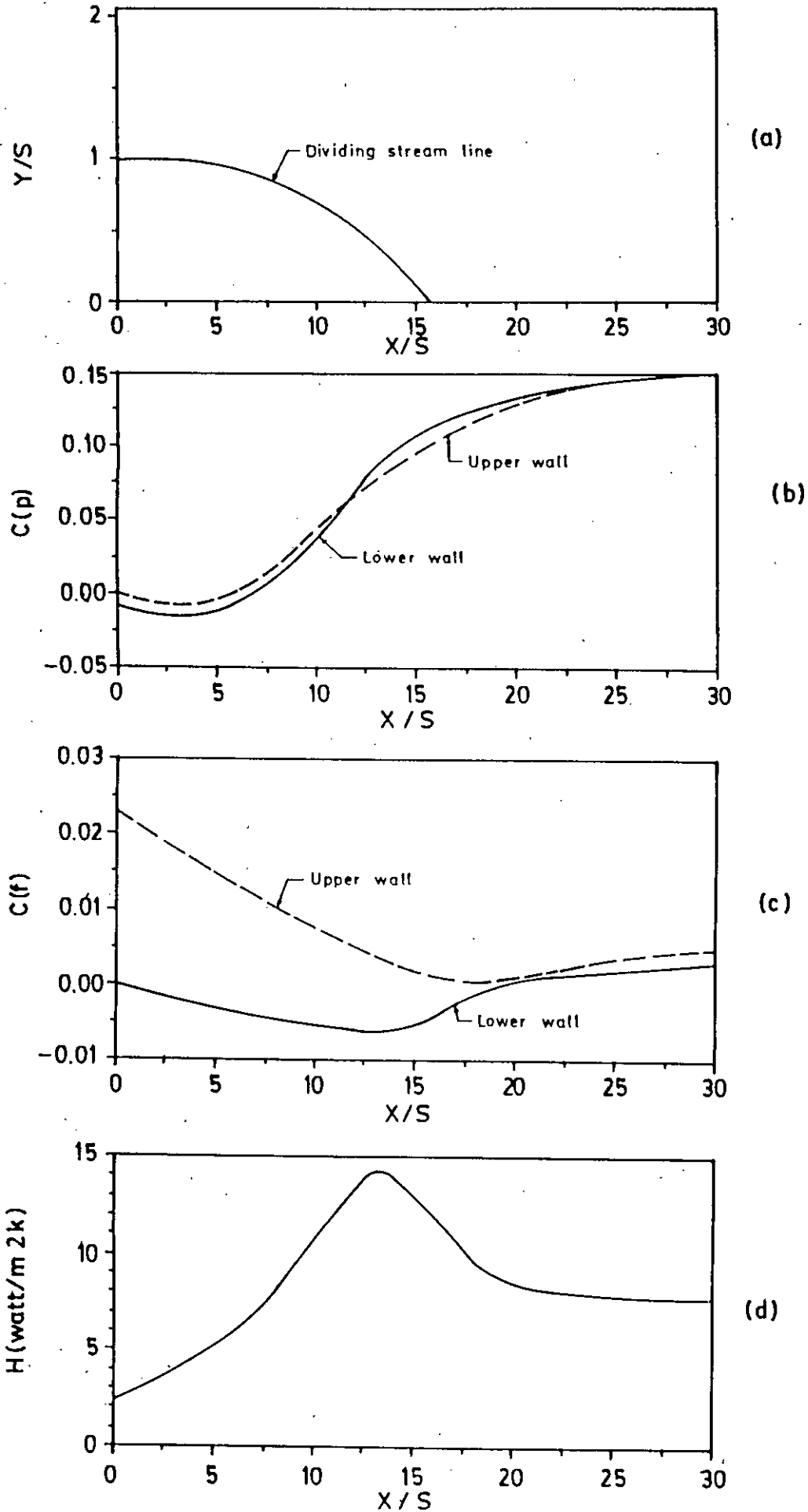
Fig. 3.10. Predicted profiles of (a) dividing stream line (b) static
pressure co-efficient at the wall (c) skin friction co-efficient
and (d) convective heat transfer co-efficient for Re = 1000.
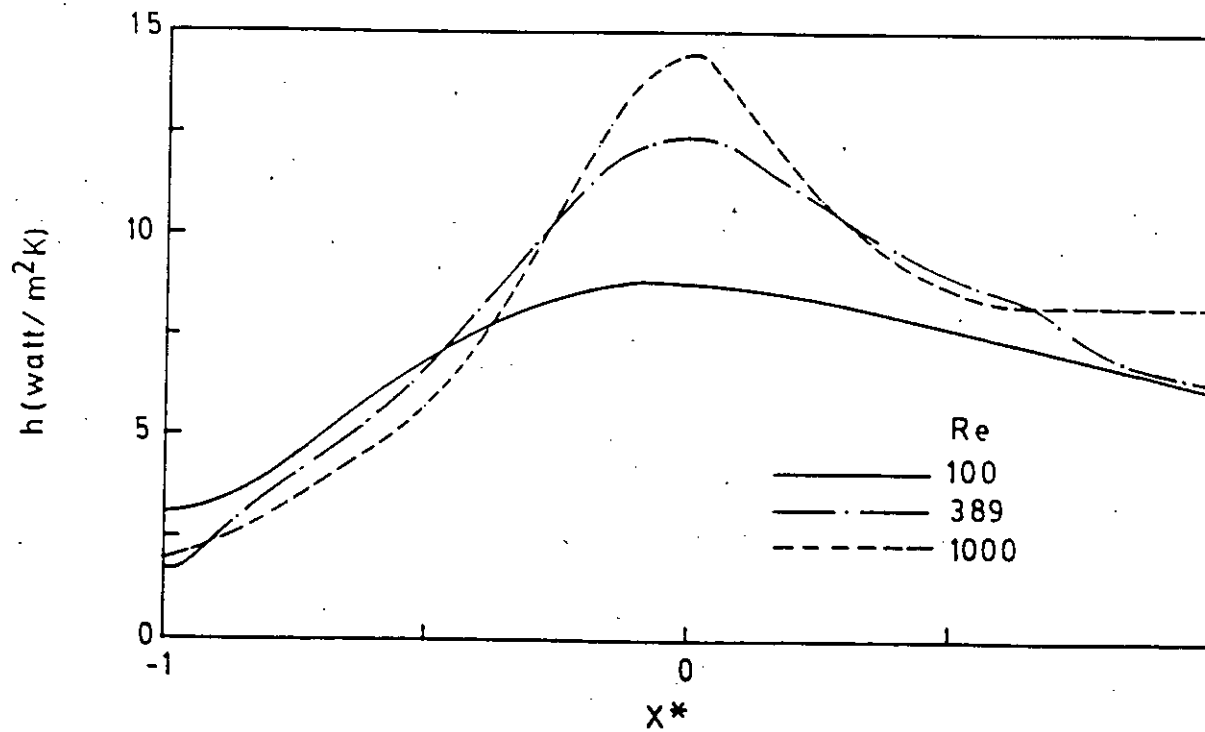
FIG.3.11 HEAT TRANSFER COEFFICIENT FOR DIFFERENT REYNOLDS
        NUMBER

76326
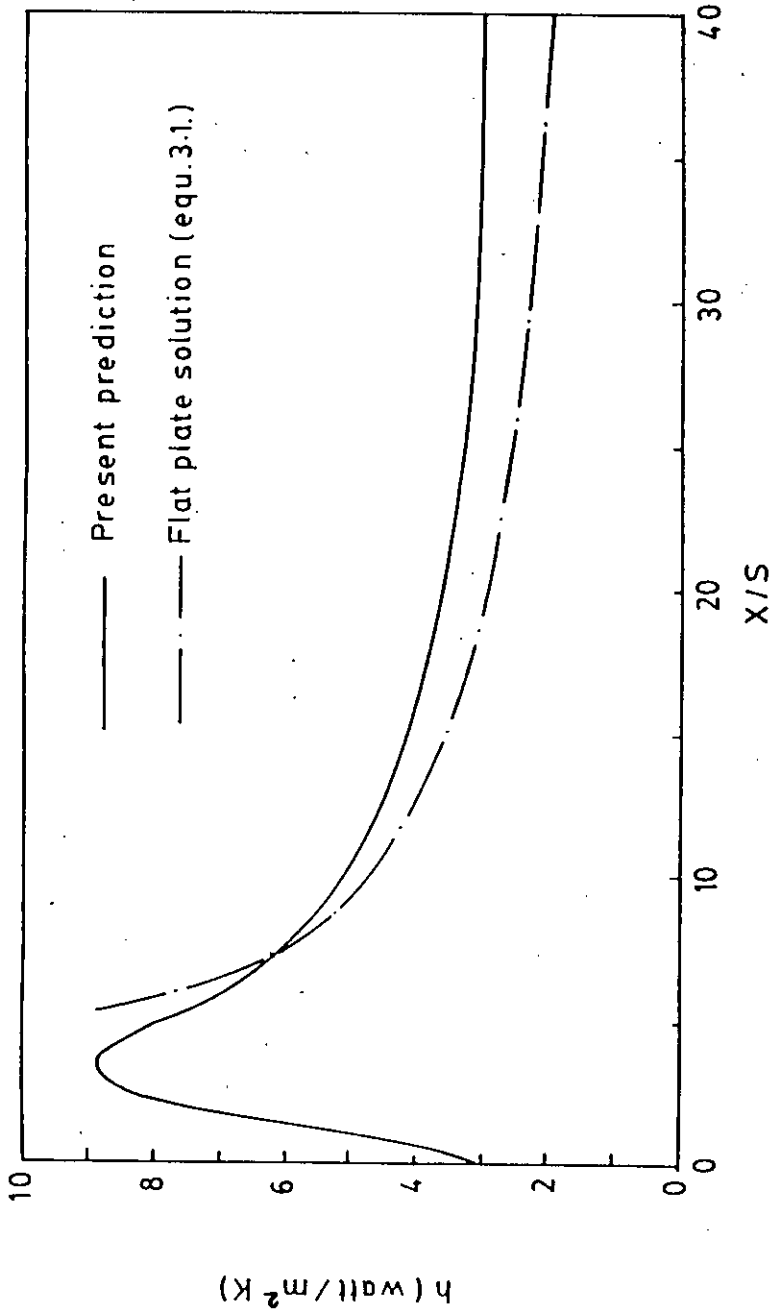


FIG.3.12 VARIATION OF HEAT TRANSFER COEFFICIENT ALONG AXIAL
DISTANCE FOR Re = 100
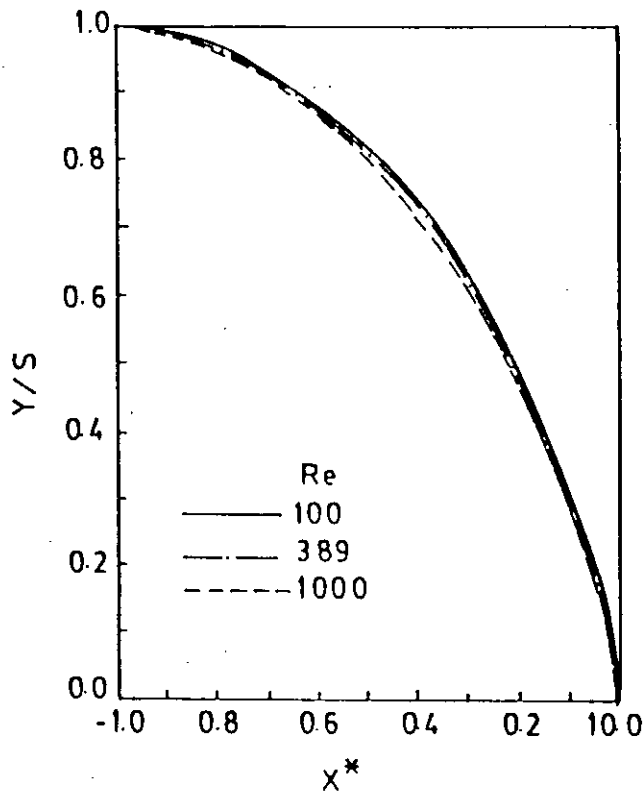
FIG.3.13 DIVIDING STREAM LINES FOR LAMINAR FLOW
AT DIFFERENT REYNOLDS NUMBER
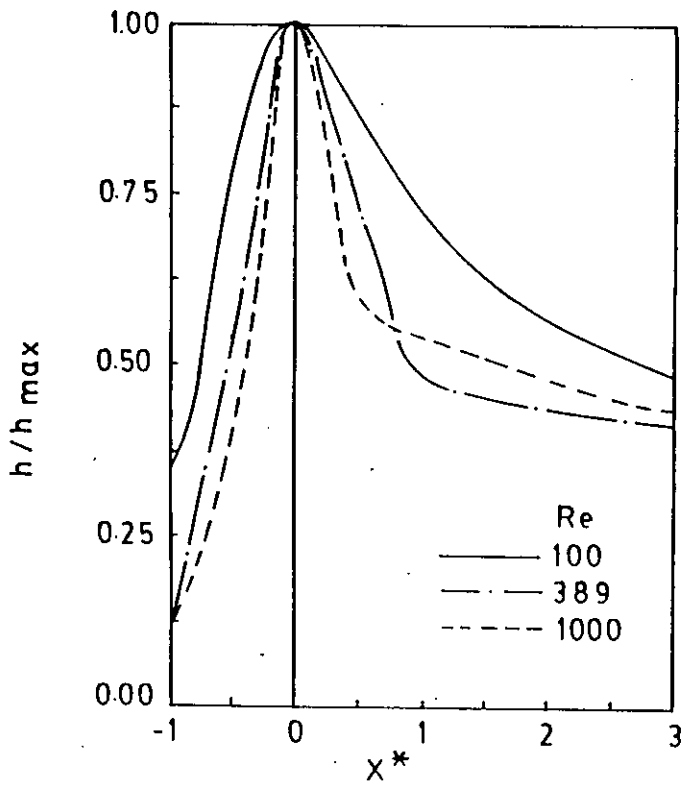
FIG.3.14 HEAT TRANSFER COEFFICIENT FOR LAMINAR
FLOW AT DIFFERENT REYNOLDS NUMBER
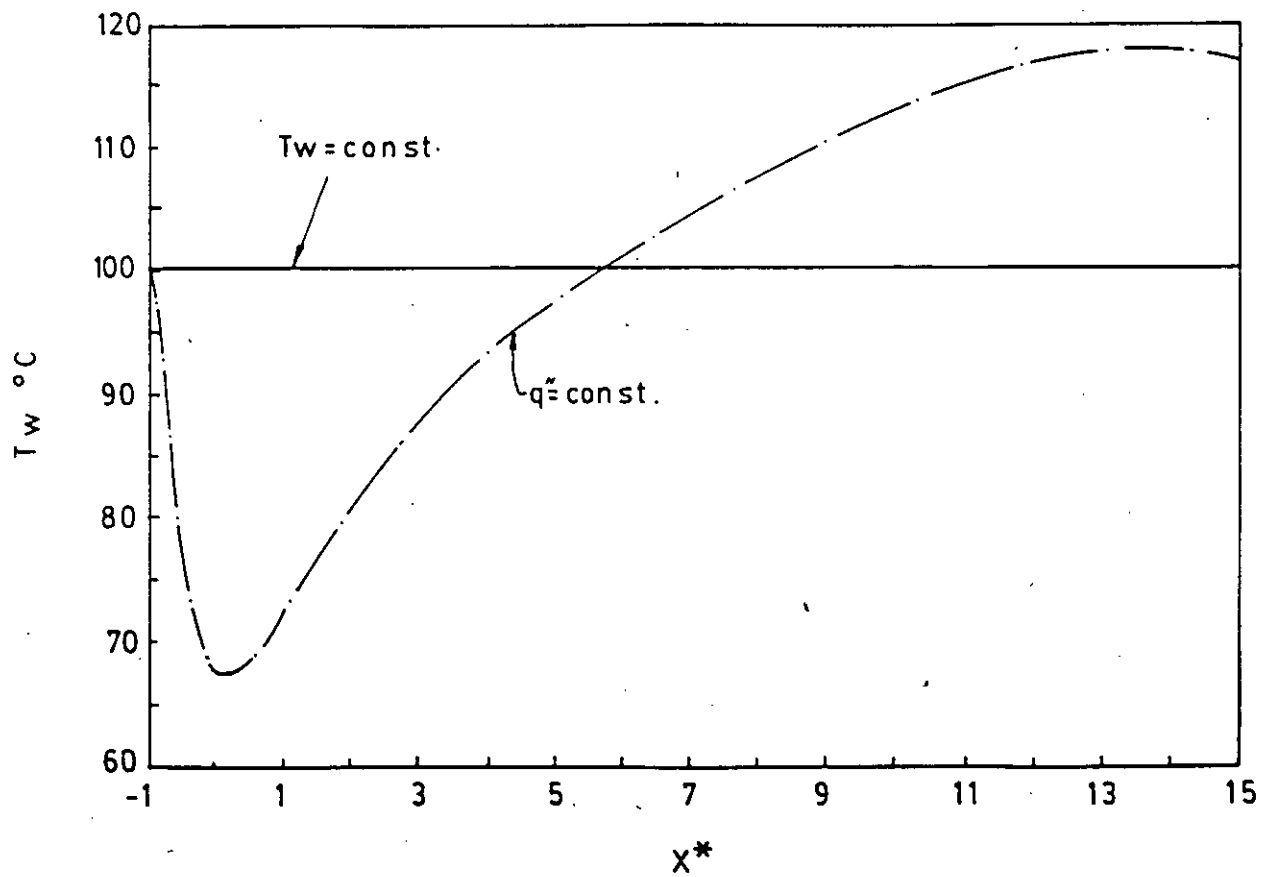
FIG.3.15 WALL TEMPERATURE DISTRIBUTION FOR Re =100
———— CONST. WALL TEMP.,—·—— CONST. HEAT FLUX CONDITION

FIG.3.16 CONTD.

X/S = 7.49

(e)



X/S = 49.8

(f)
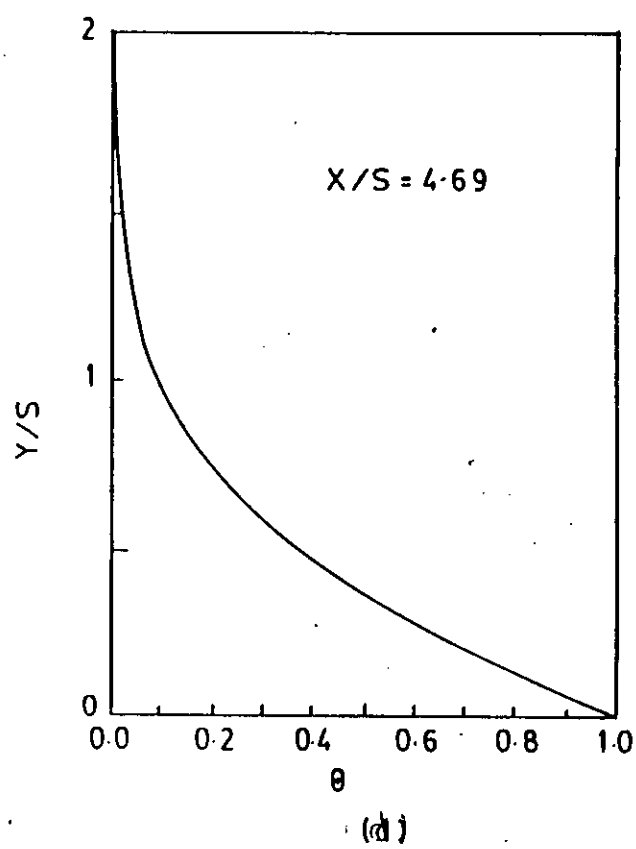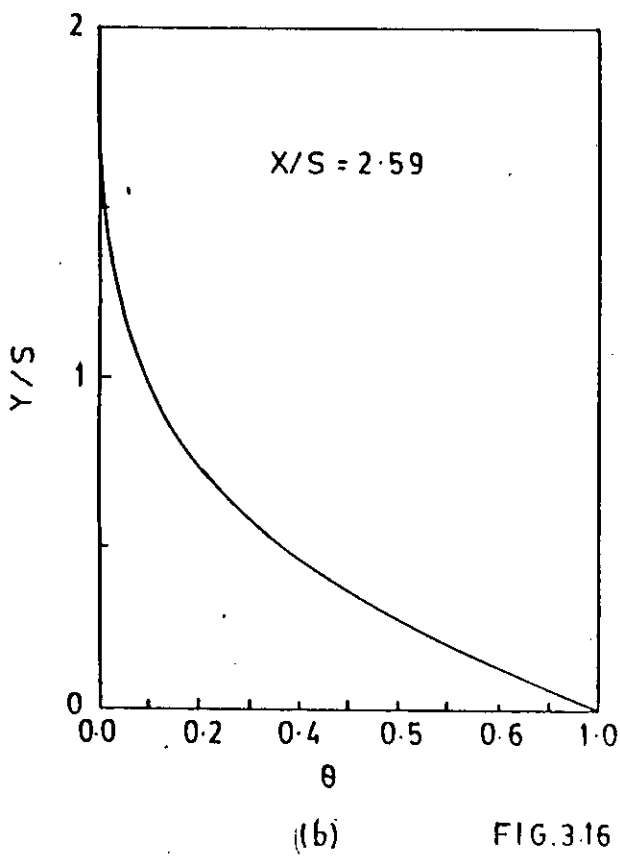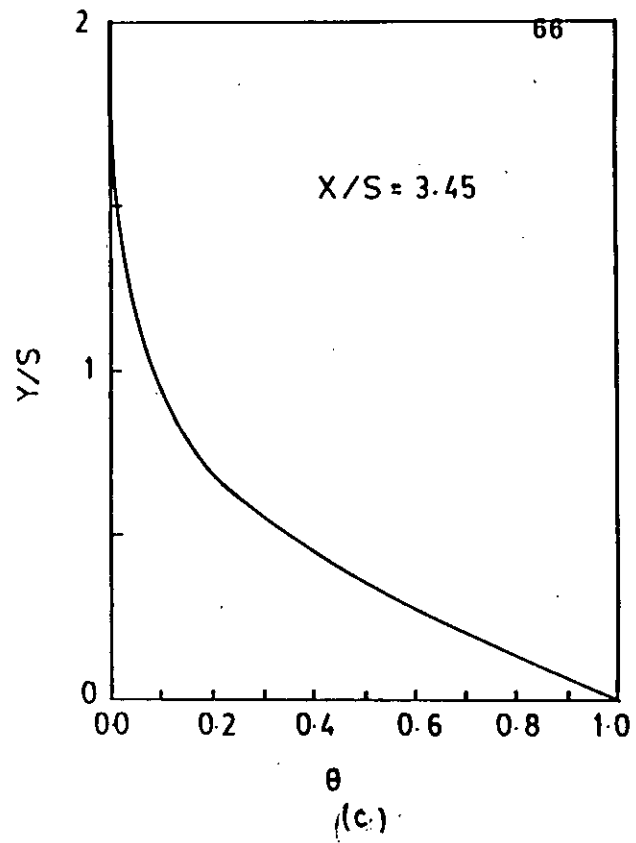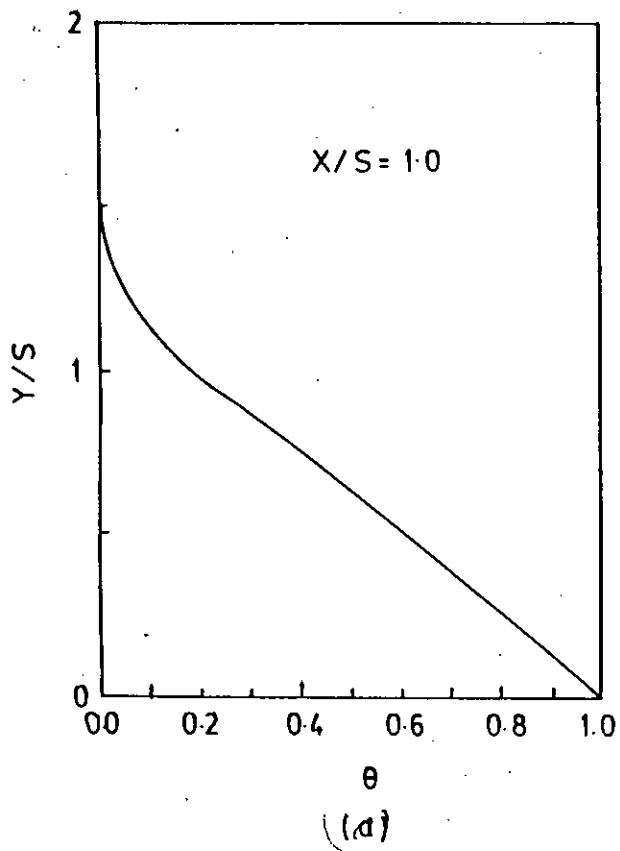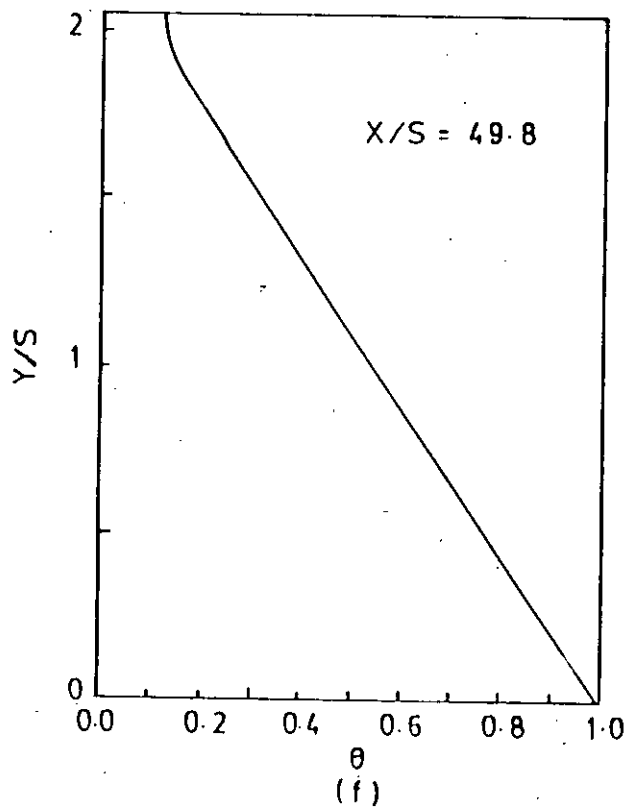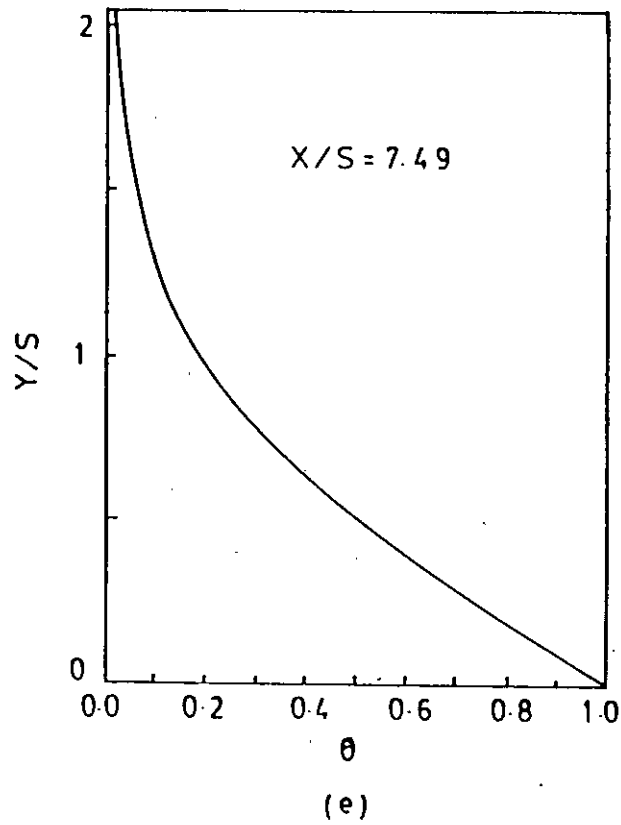
FIG.3.16 NORMALISED TEMPERATURE PROFILES AT
DIFFERENT AXIAL LOCATIONS FOR Re = 100
(FOR CONSTANT WALL TEMPERATURE CONDITION)

Fig. 4·1    Contd.

(c)

U /Uo



(d)

U /Uo

Fig. 4.1    Contd.

(e)

$U / U_o$



(f)

$U / U_o$
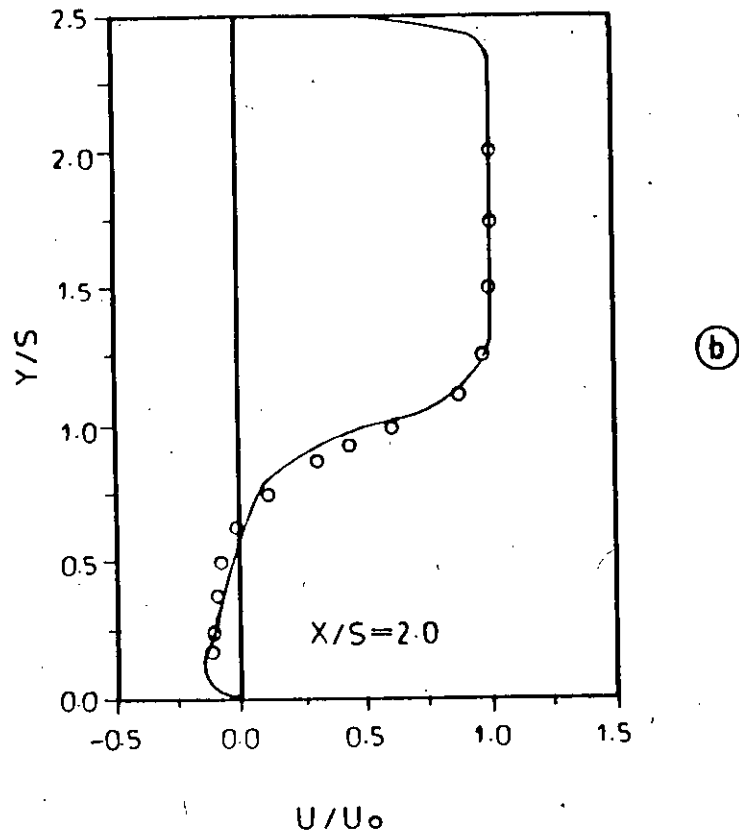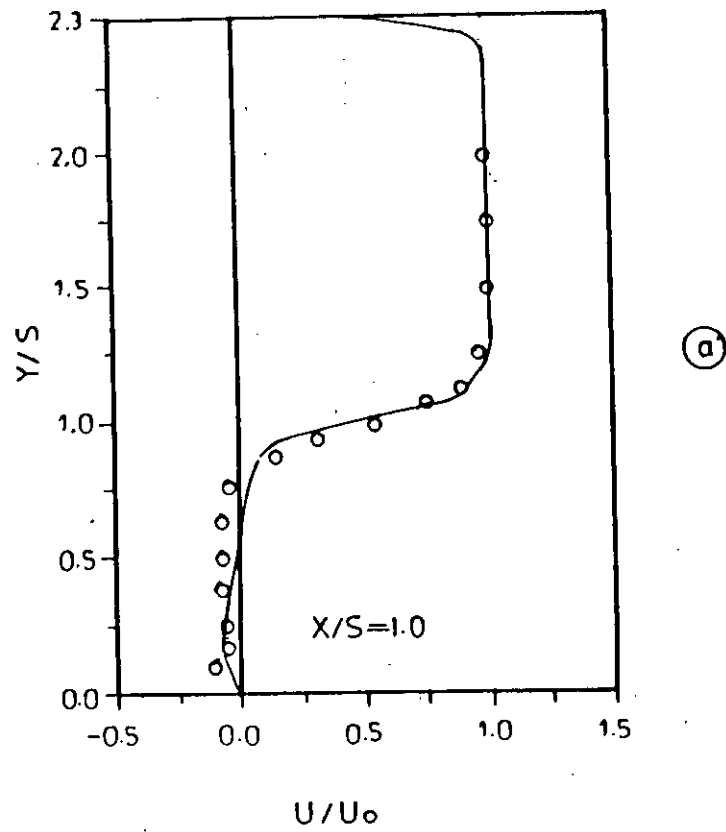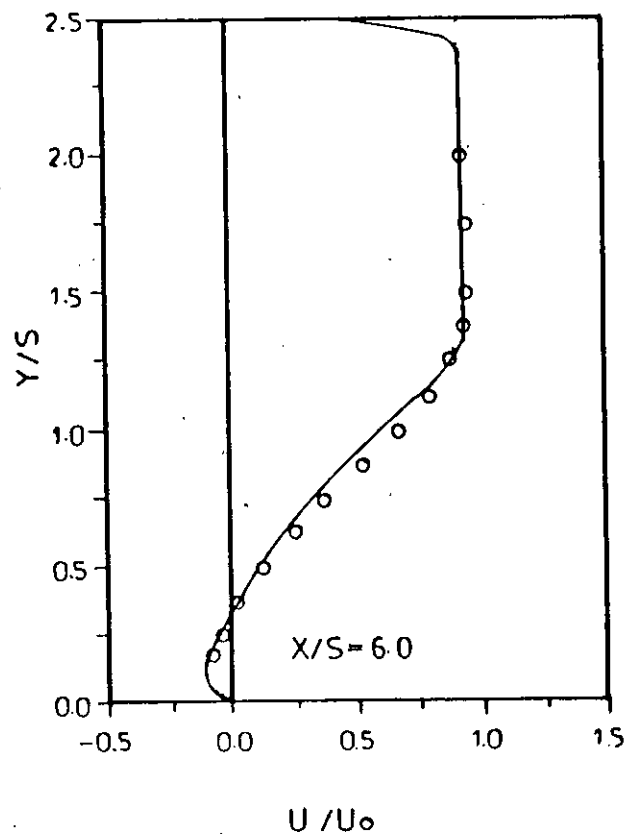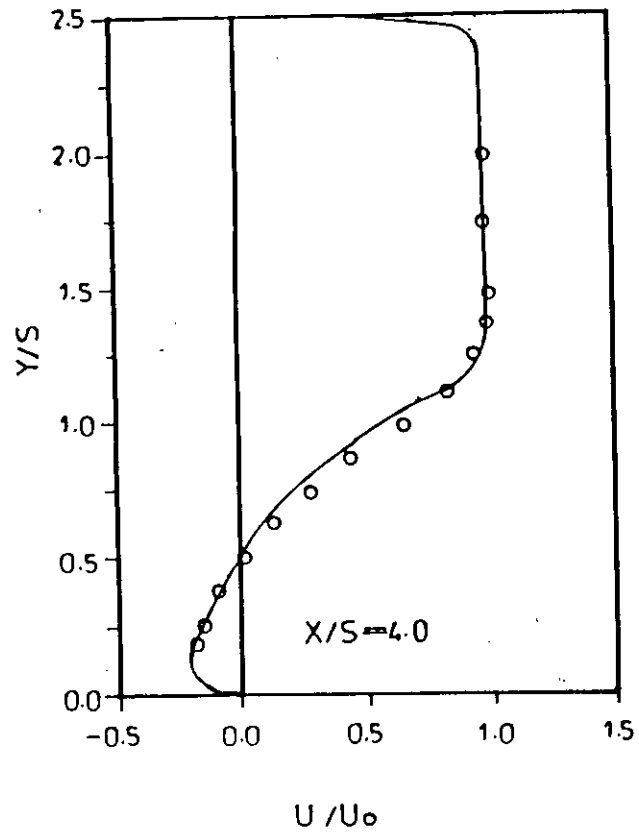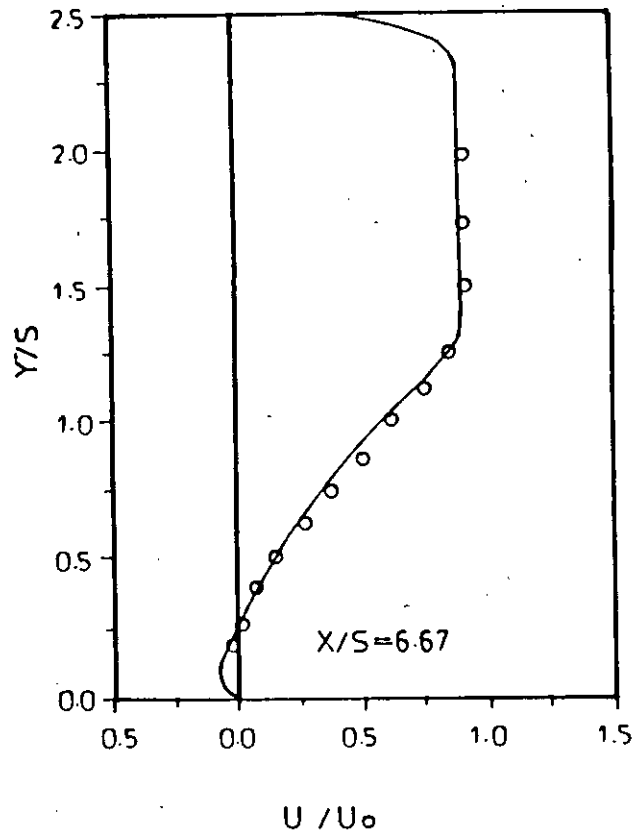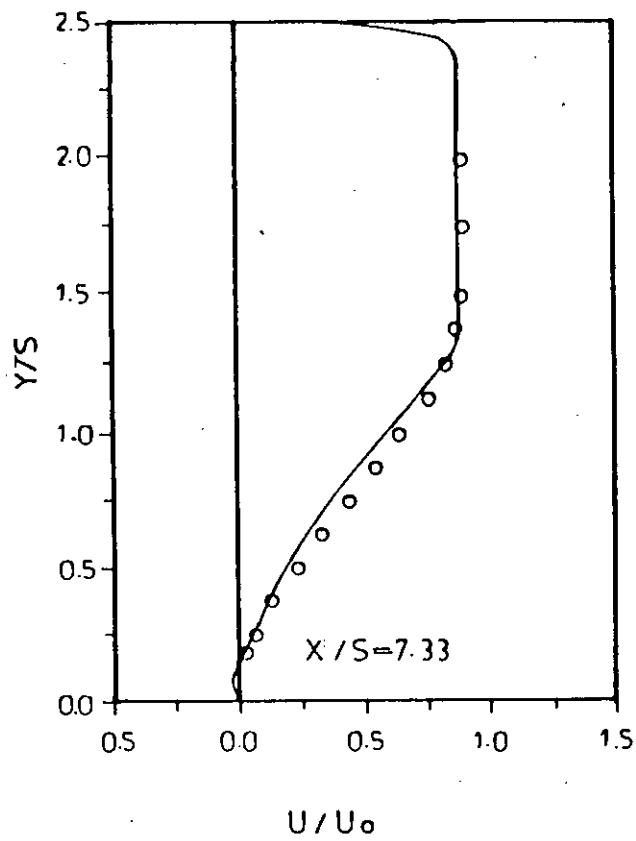
Fig. 4.1    Contd.
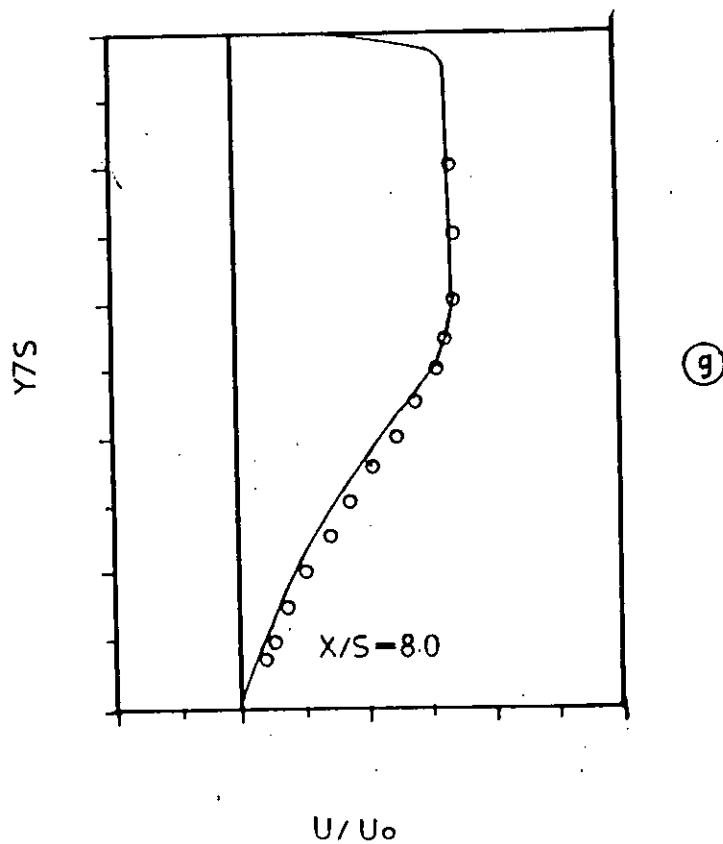
Fig. 4.1: Mean velocity profiles at different
axial locations for $Re_s = 40000$
——Present prodiction;
O Expt. (Ecton & Johnston, 1980)

X/S = 3.2

Y/S

U/U_o

(a)

X/S = 4.55

Y/S

U/U_o

(b)

Fig. 4.2 Contd.

(c)

X/S = 5.87

(d)

X/S = 7.2

Fig. 4.2   Contd.
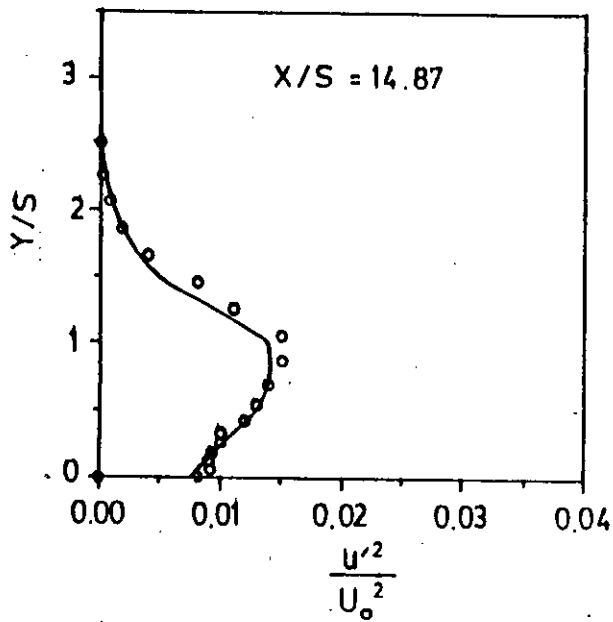
X/S = 9.53

(e)

X/S = 12.2
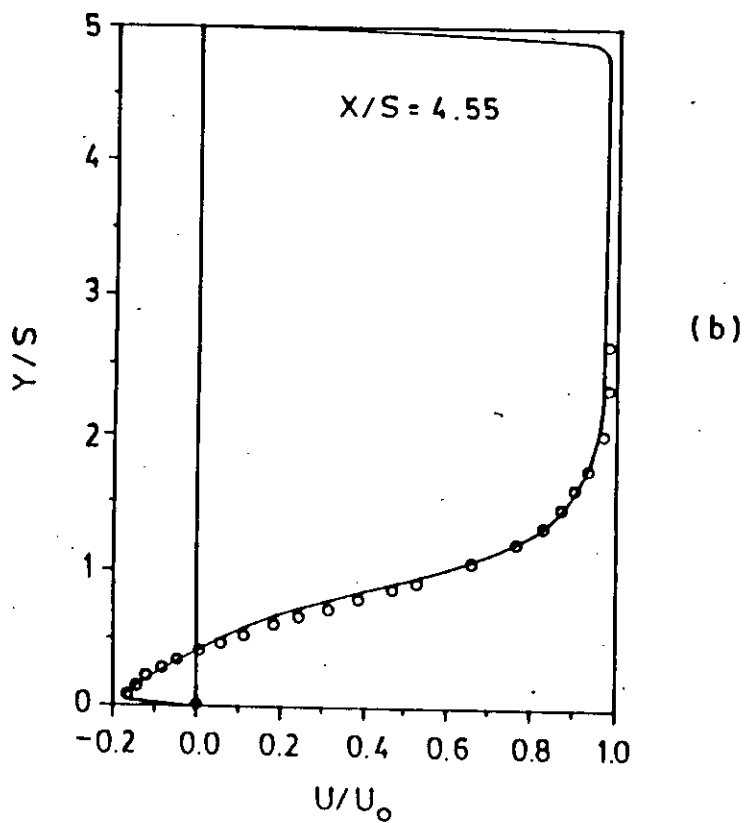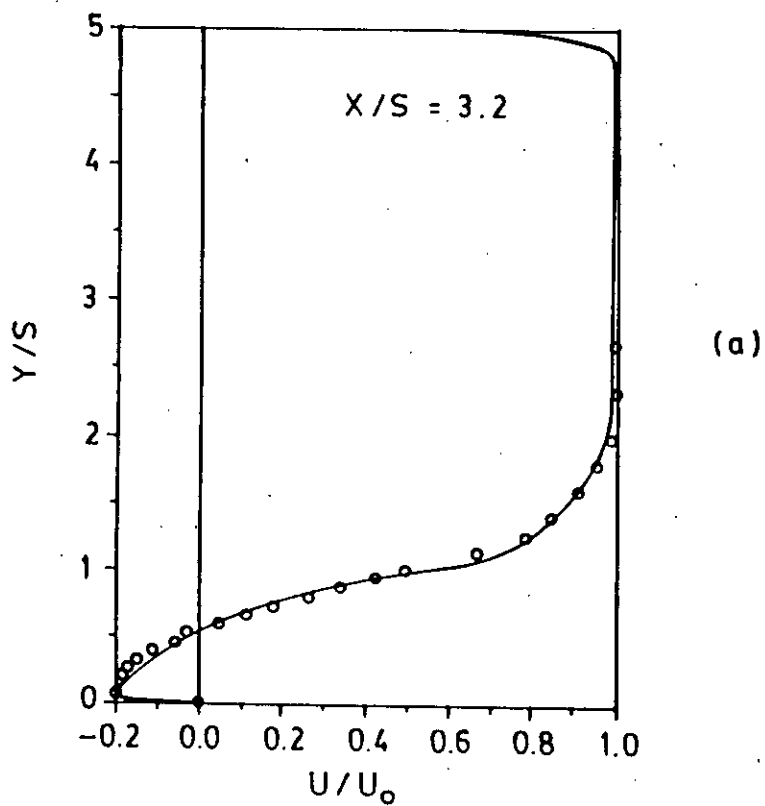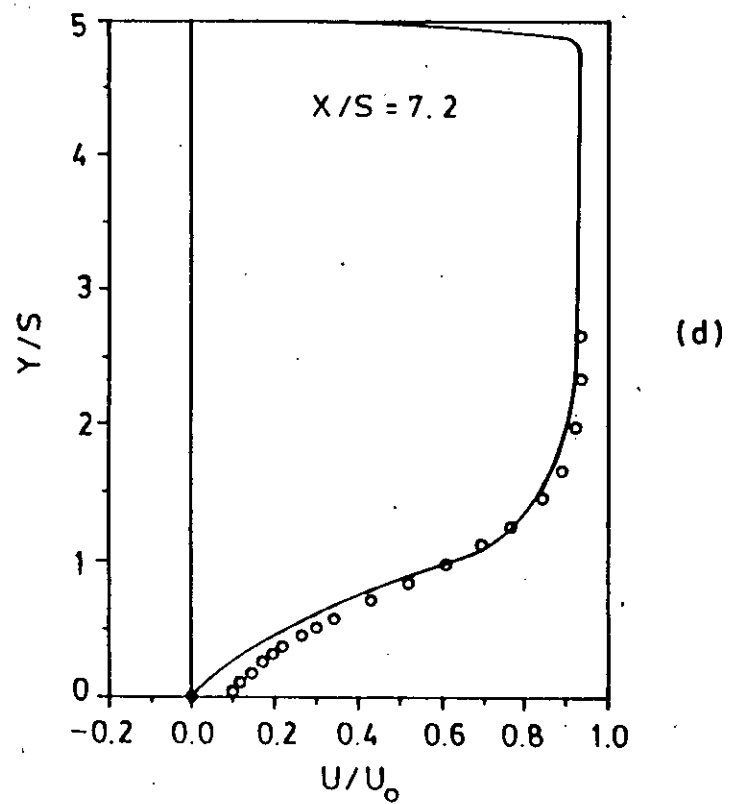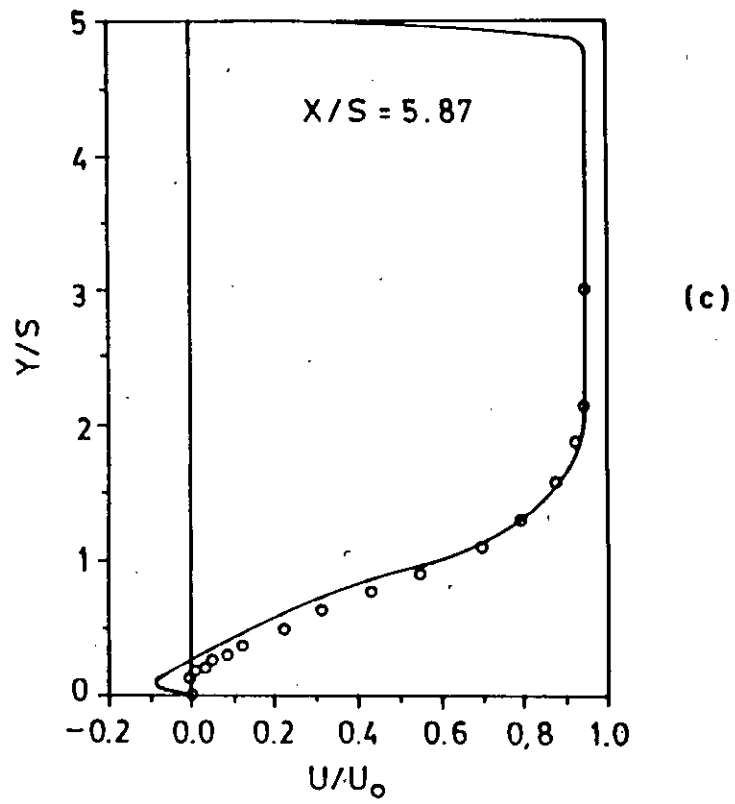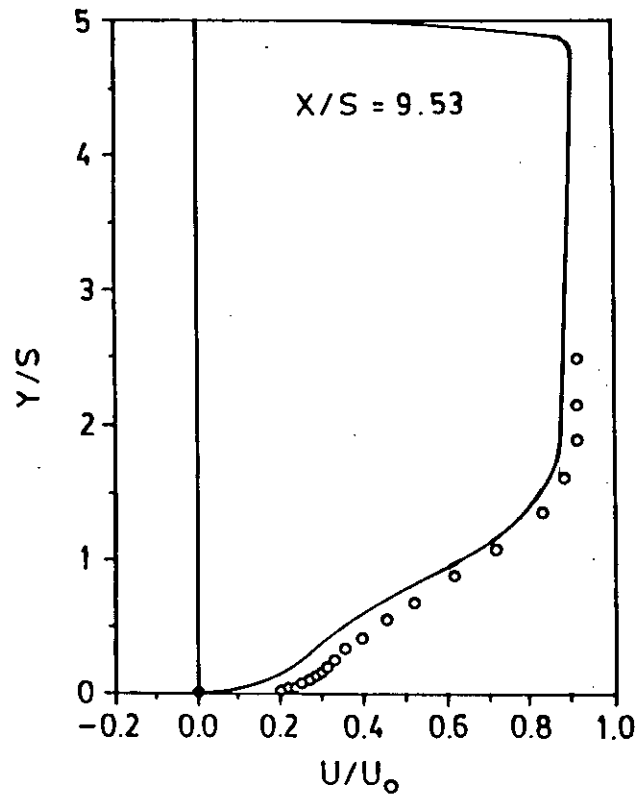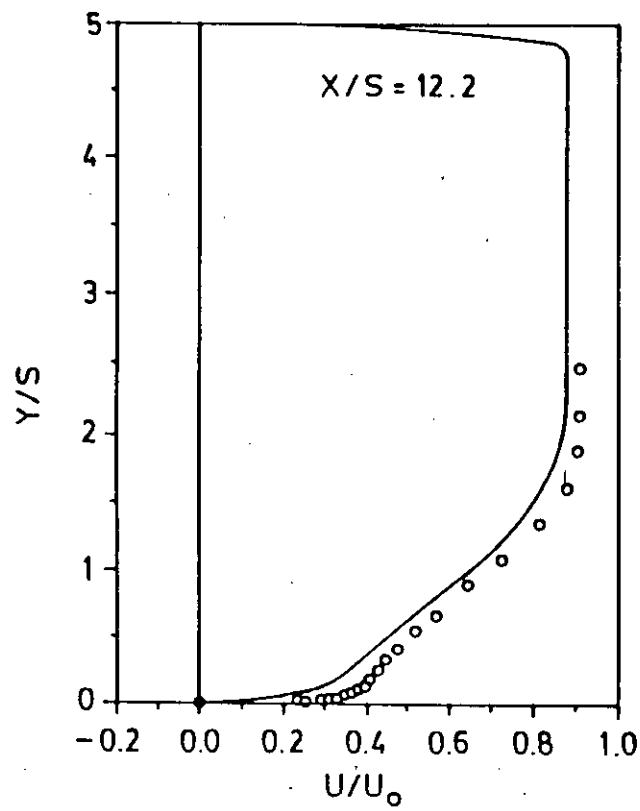
(f)

Fig. 4.2 Co'ntd.
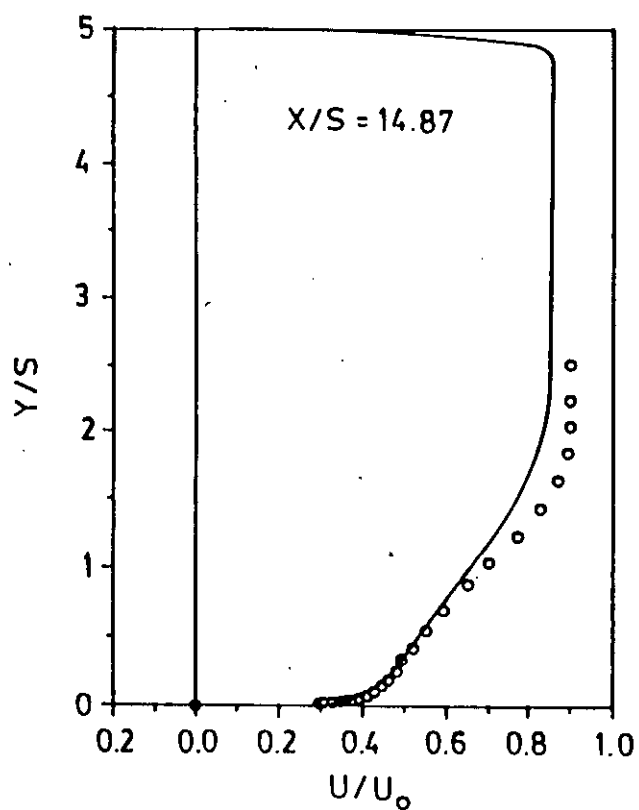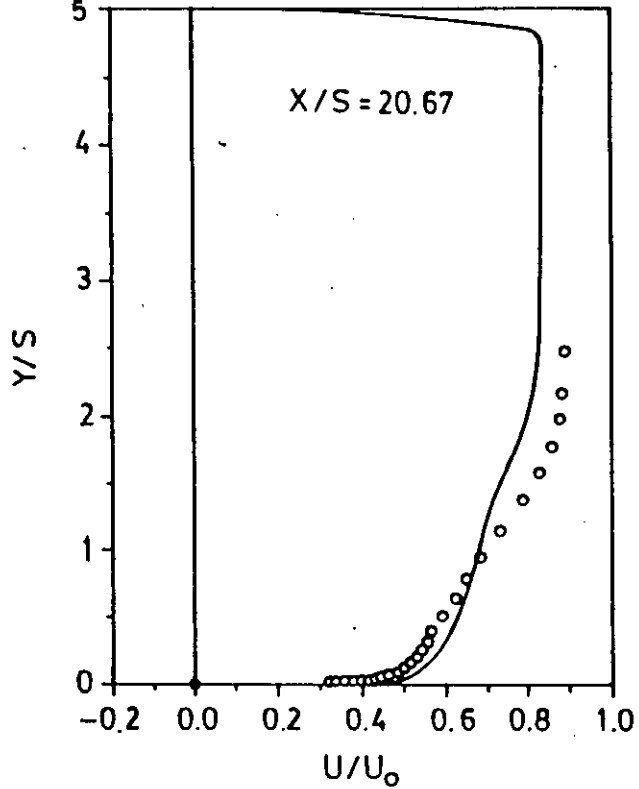
Fig. 4.2 Mean velocity profiles at different
axial locations for $Re_S$ = 28,000

——— Present prediction

o      Expt. ( Vogel and Eaton, 1984 )

(a)

X/S=1.0

U / Uo

(b)

X/S=2.0

U / Uo
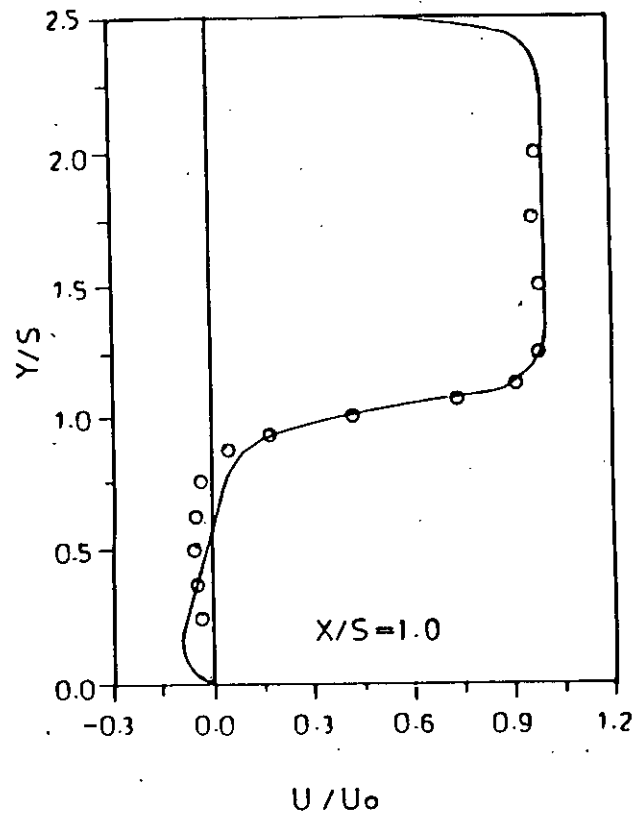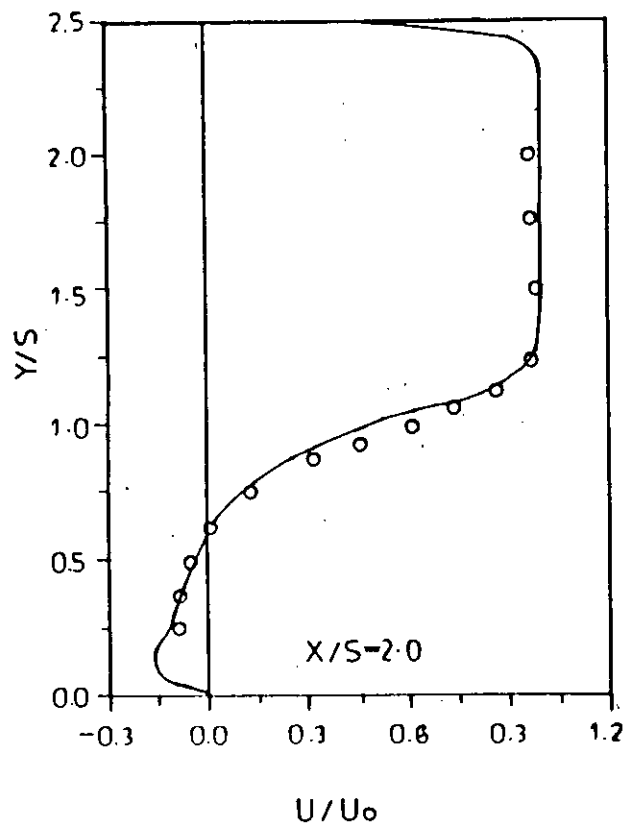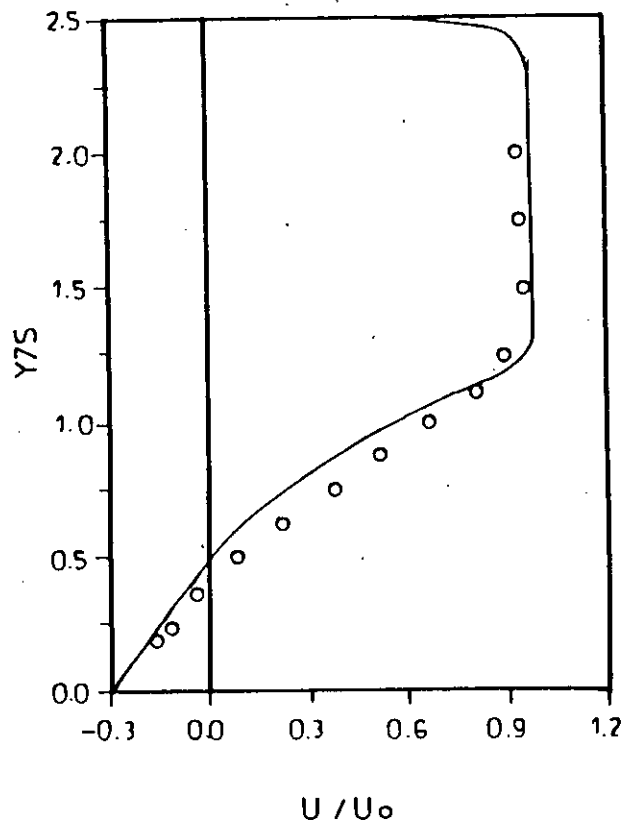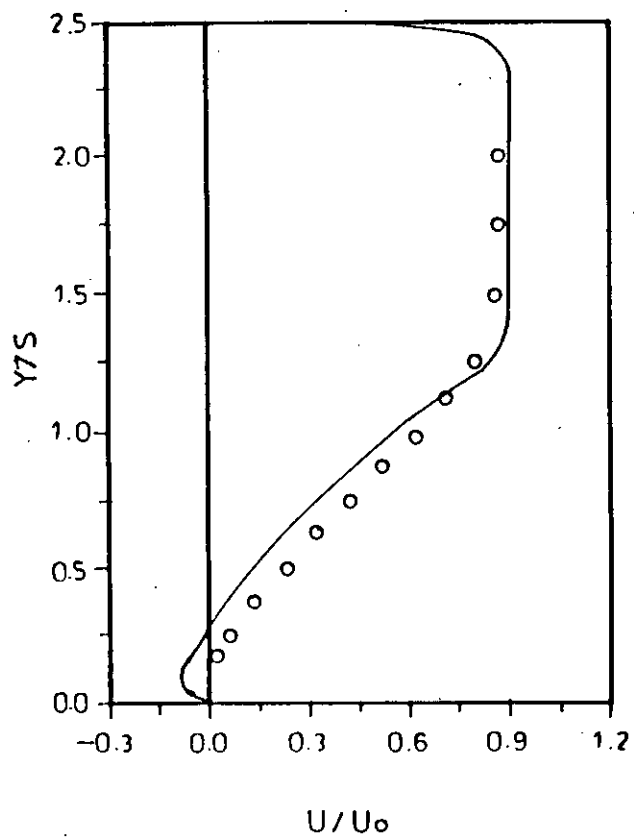
Fig. 4.3    Contd.
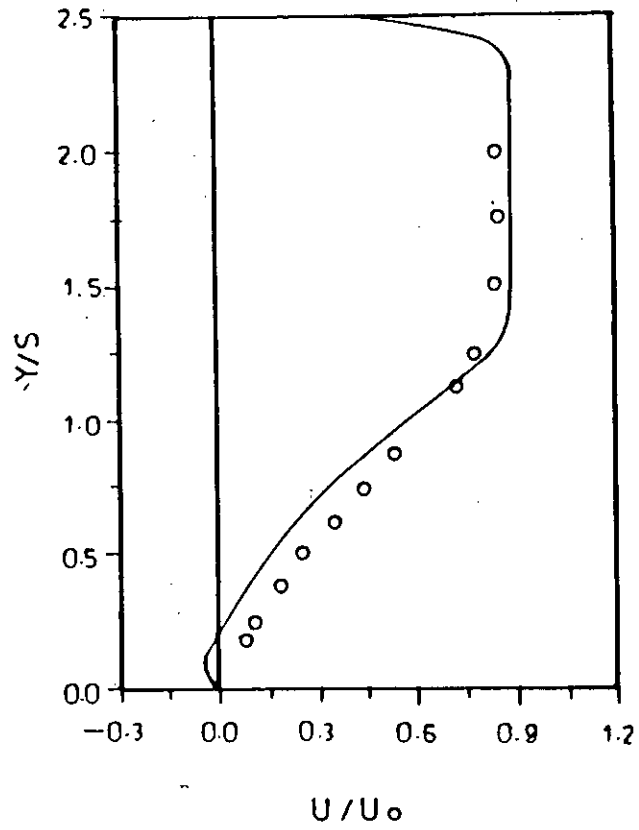
Fig. 4.3    Contd.

(e)
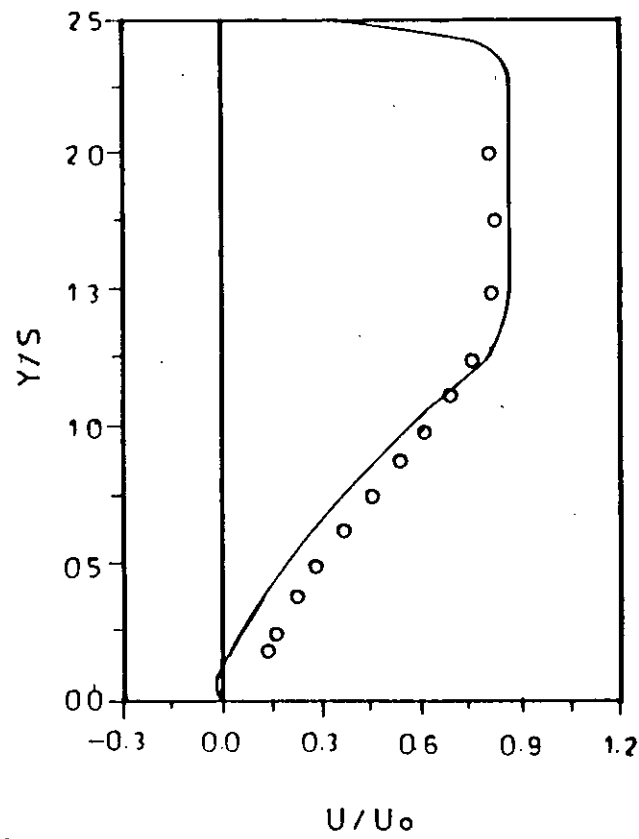
(f)

Fig. 4.3    Contd.
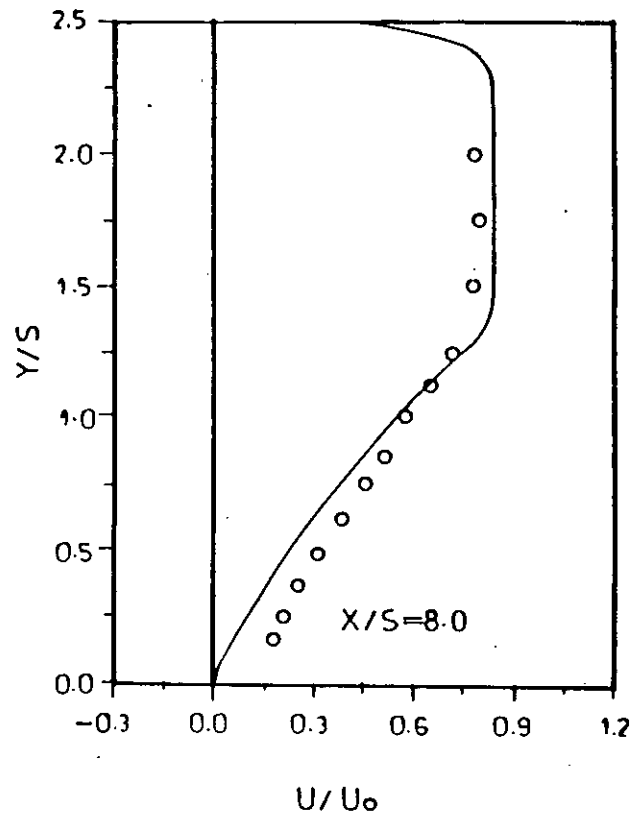
Fig. 4.3 Mean velocity profiles at different
axial locations for Res.= 11000
———Present prediction:
O Expt. (Eaton & Johnston, 1980)
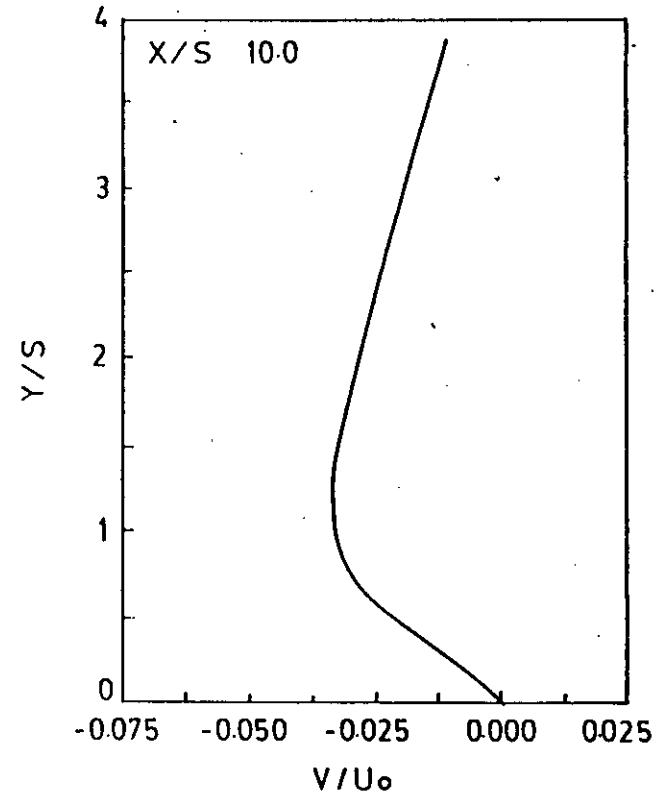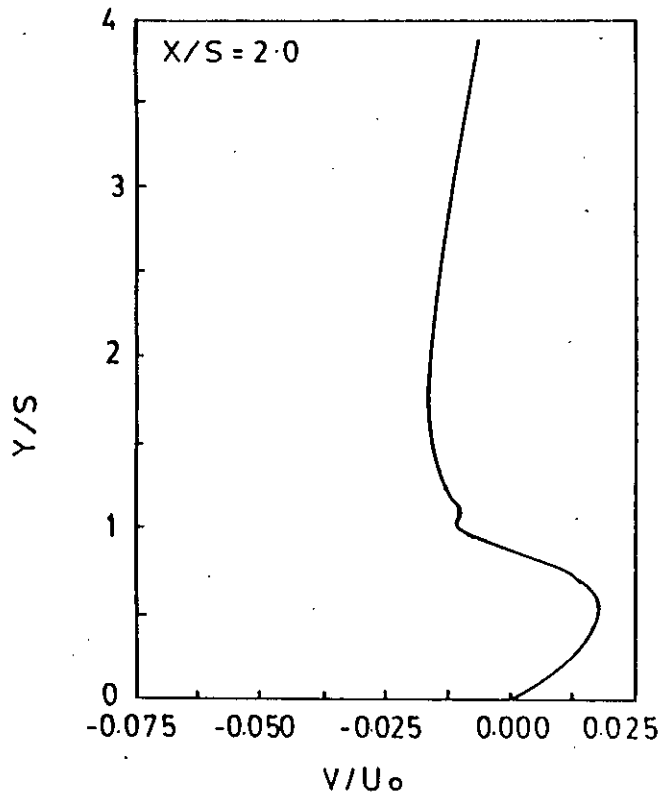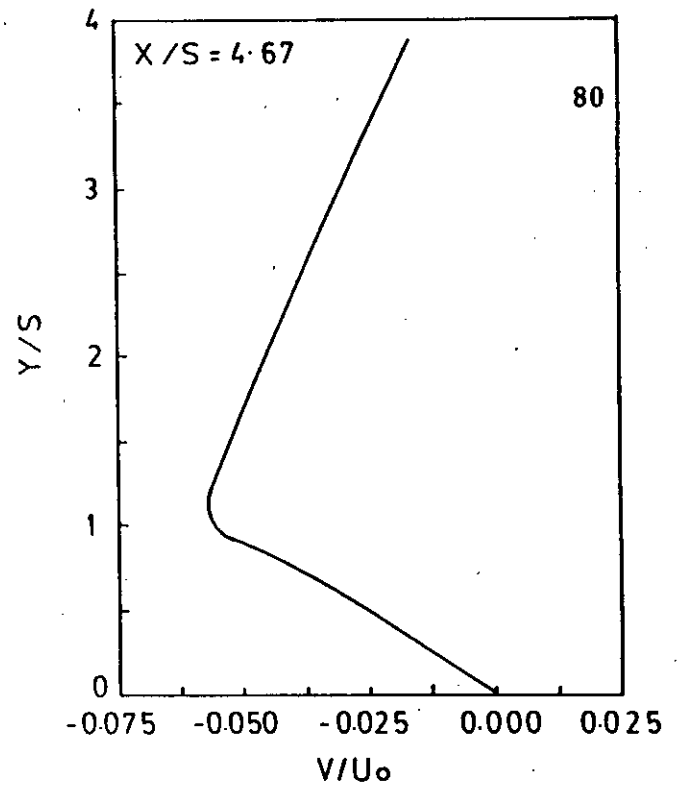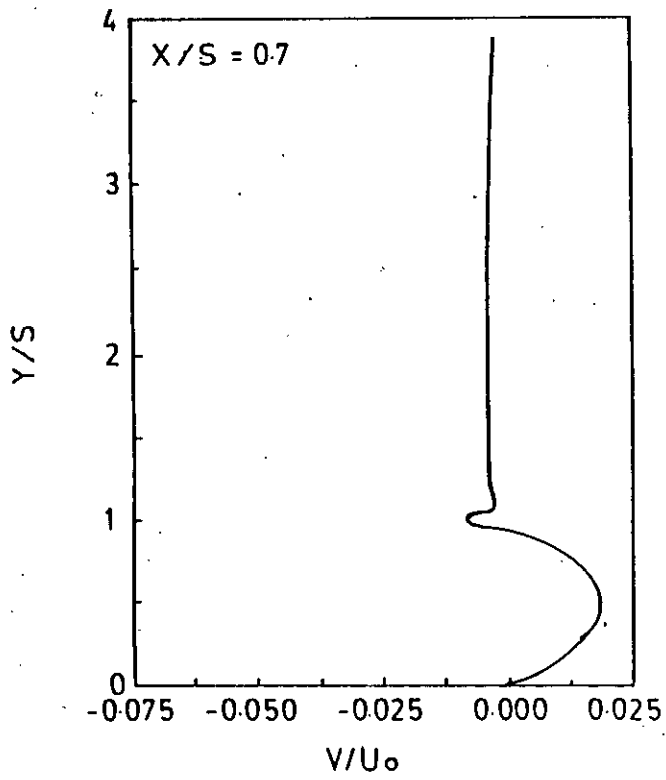
FIG. 4·4  PREDICTED MEAN NORMAL VELOCITY PROFILES AT DIFFERENT
AXIAL LOCATION  FOR Re$_S$=28,000
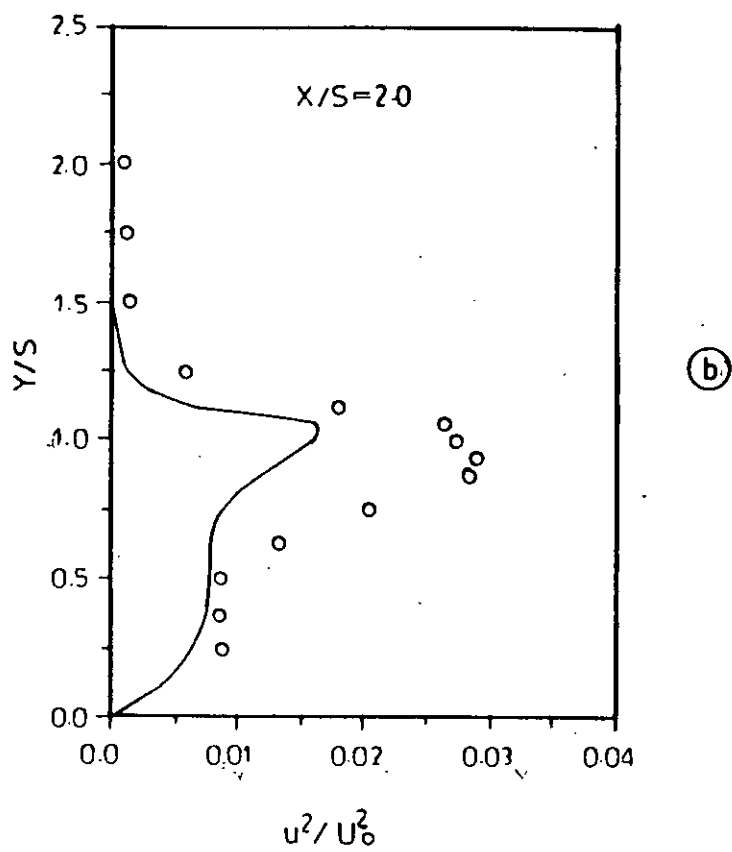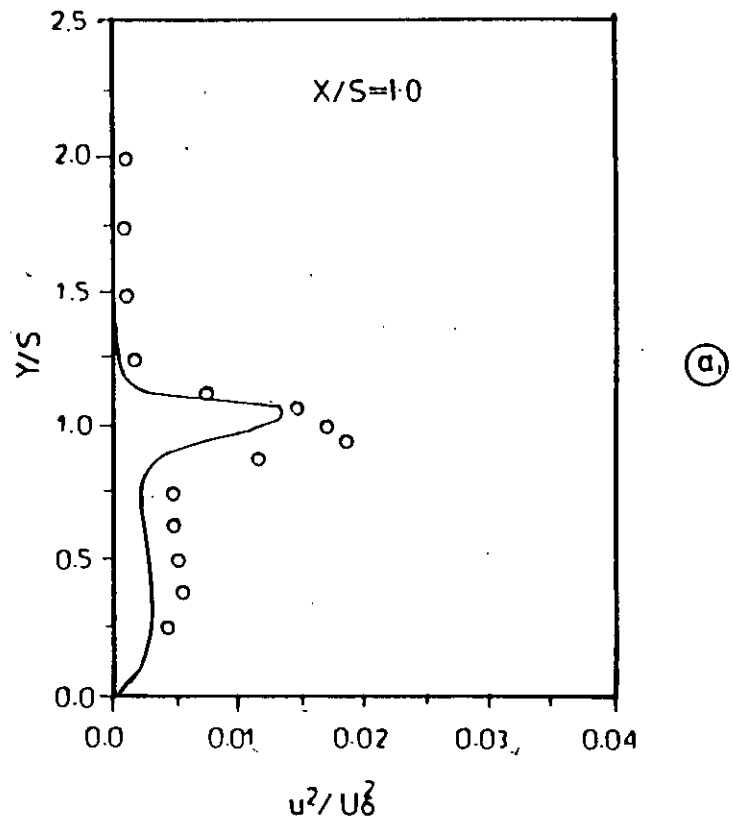
Fig. 4.5        Contd.
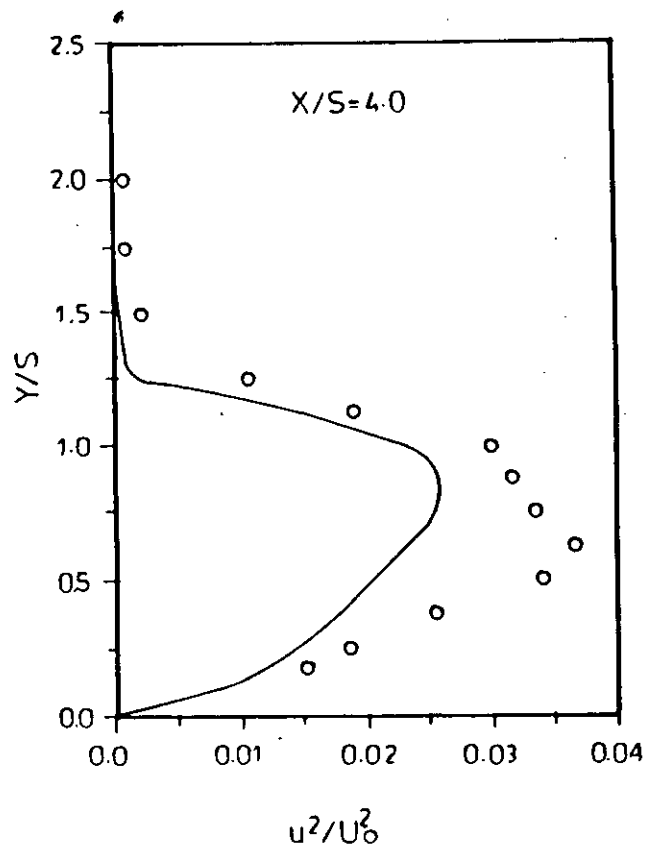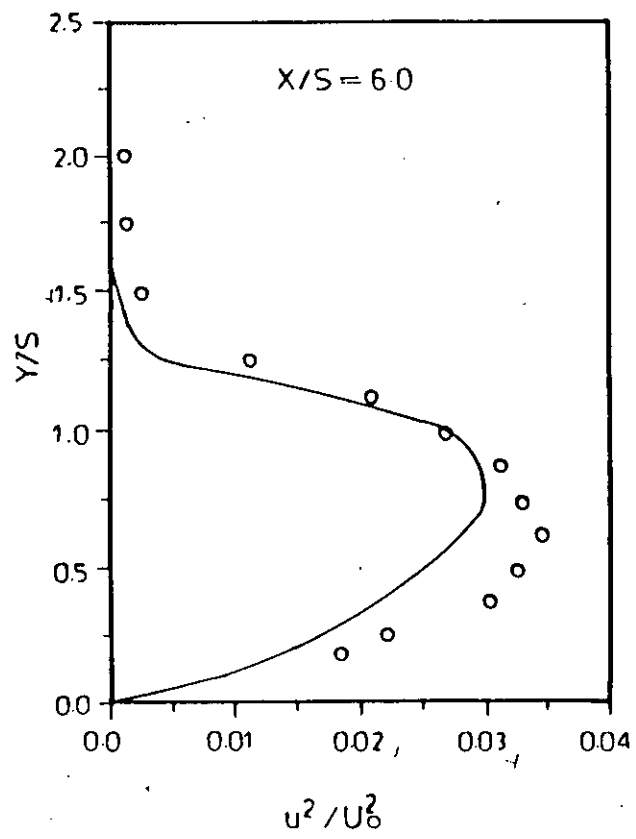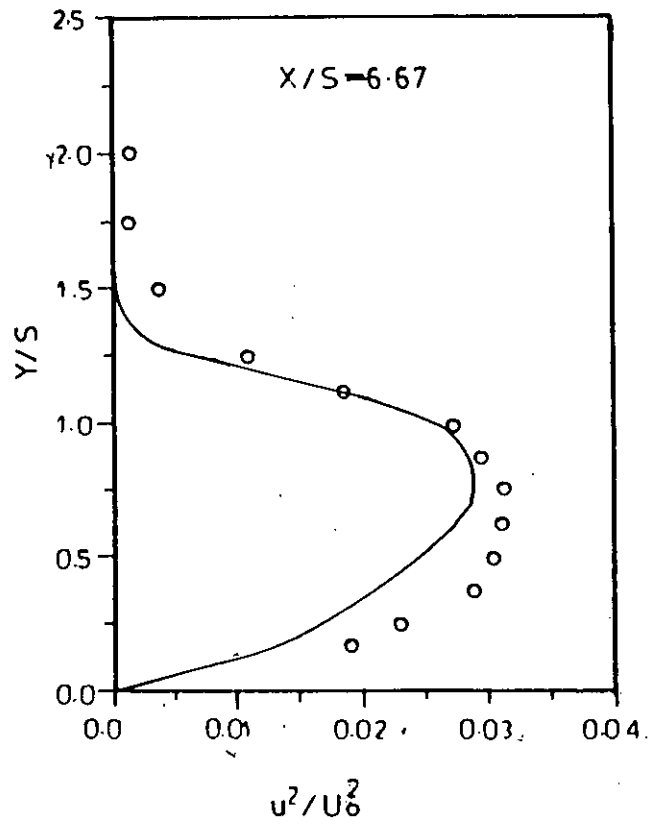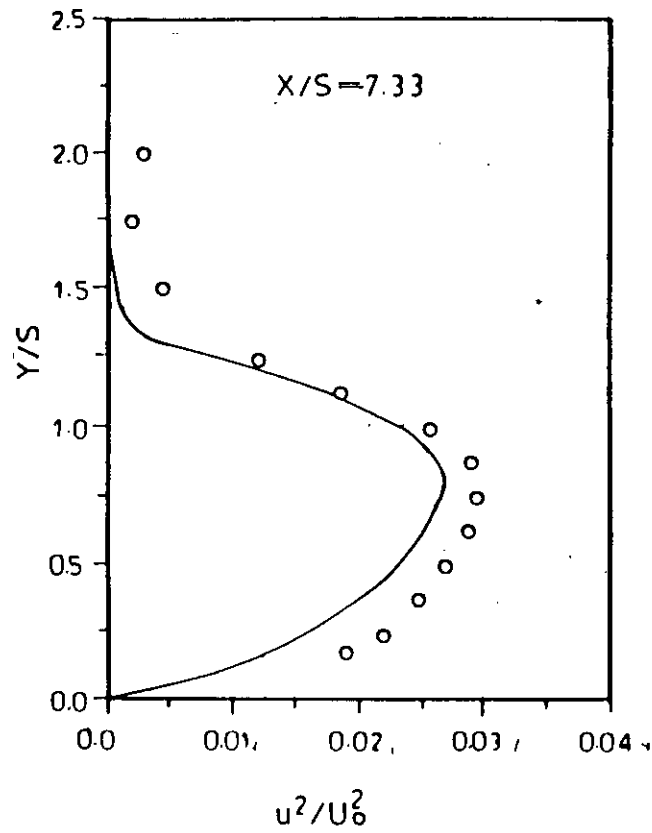
Fig. 4.5    Contd.

Fig. 4.5 Contd.
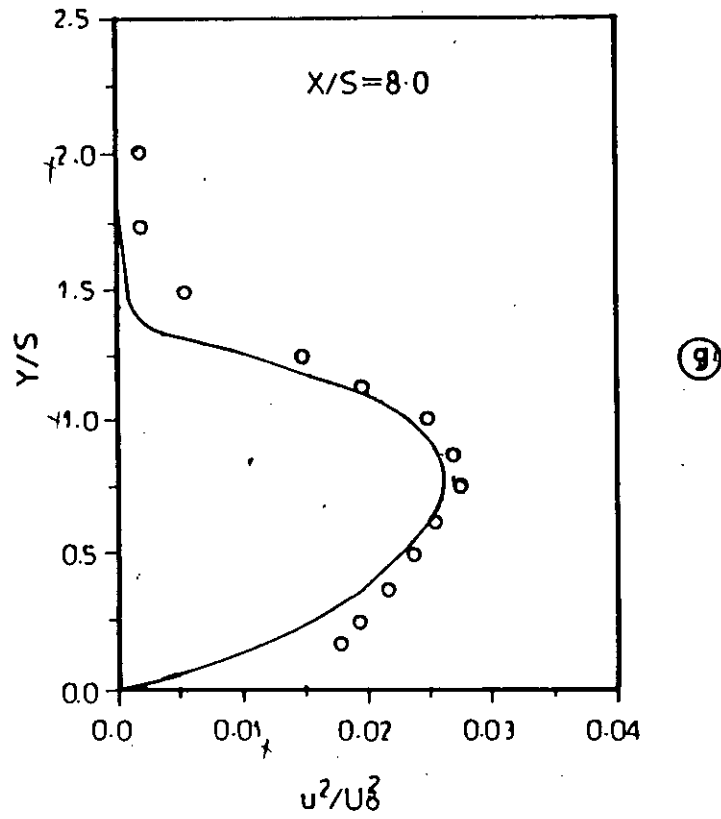
Fig. 4.5. Turbulent normal stress profiles at
different axial locations for Res=11000
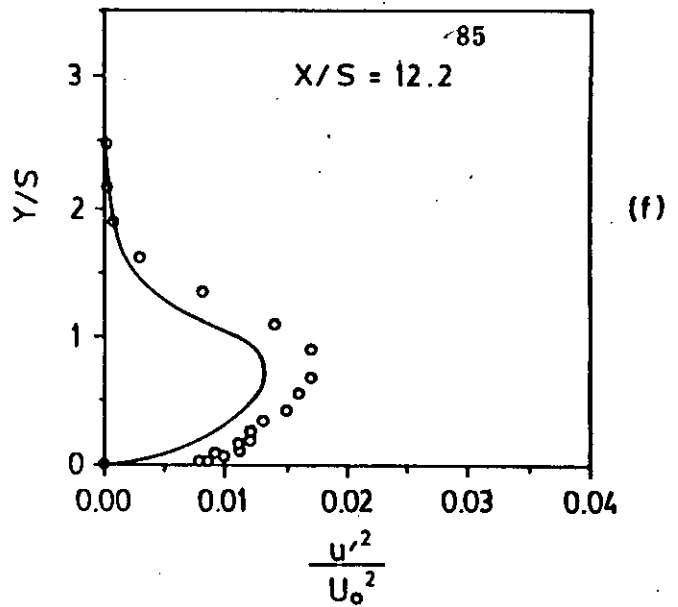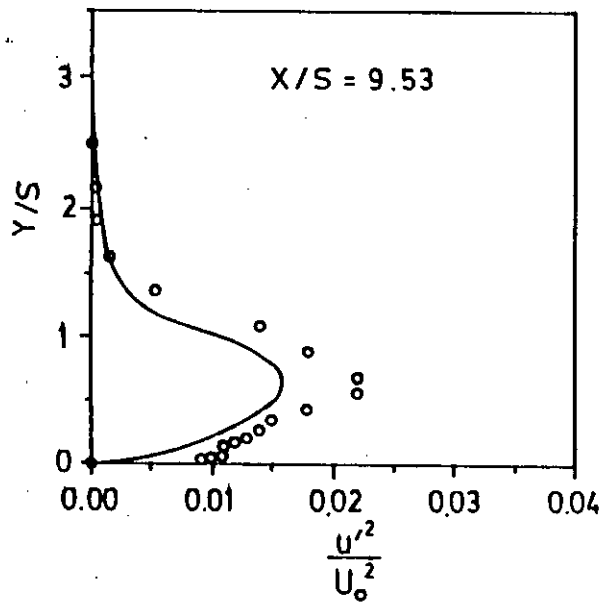____Present prediction;.
O Expt.(Eaton & Johnston, 1980 )
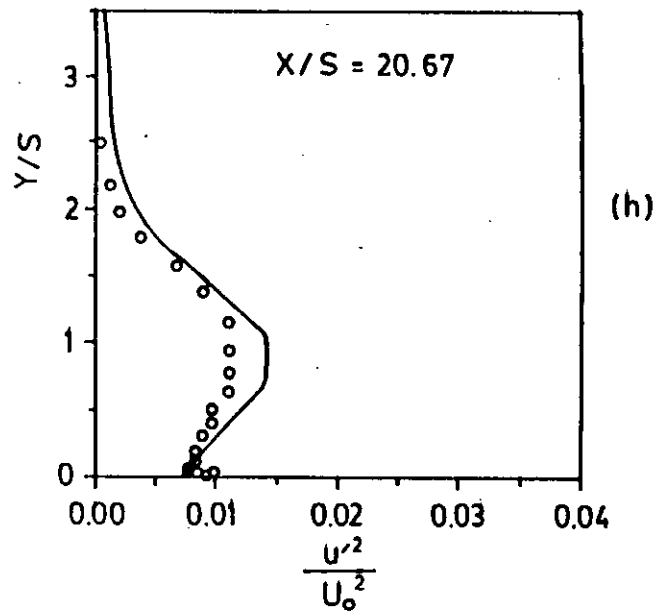
Fig. 4.6 Turbulent normal stress prfiles at different axial locations for $Re_S = 28,000$
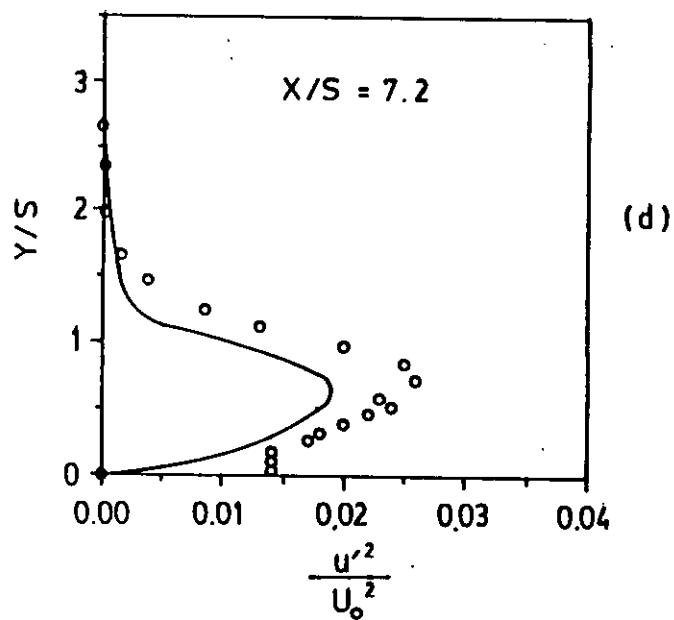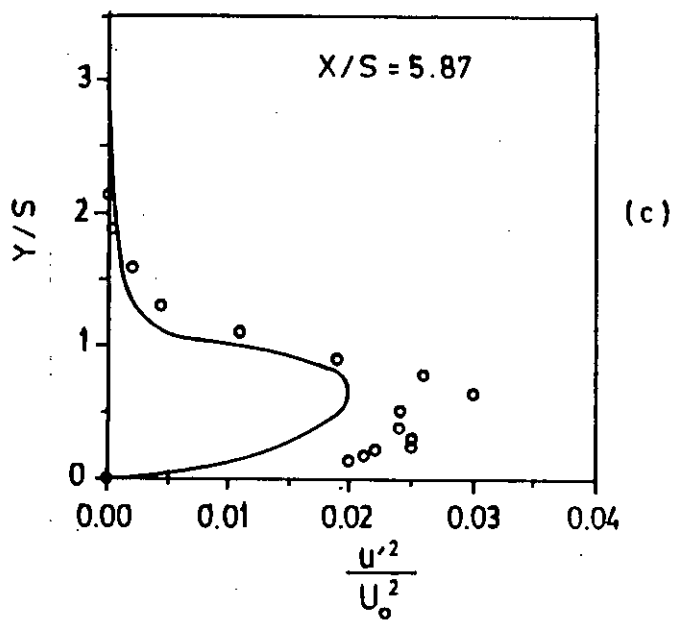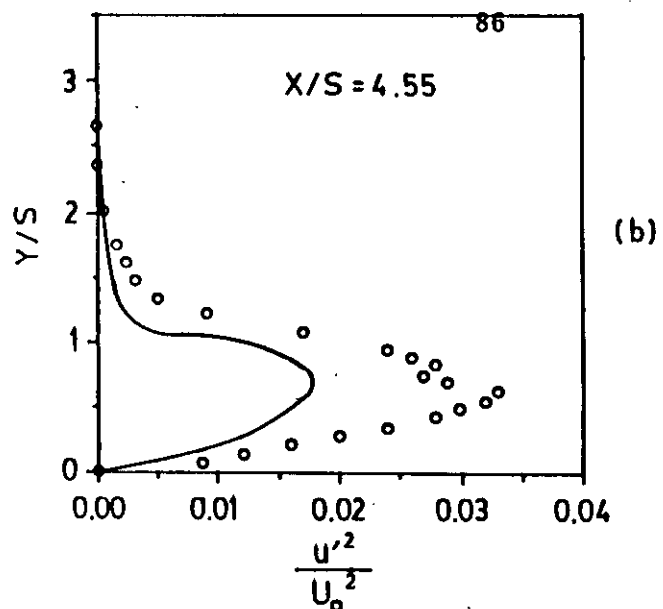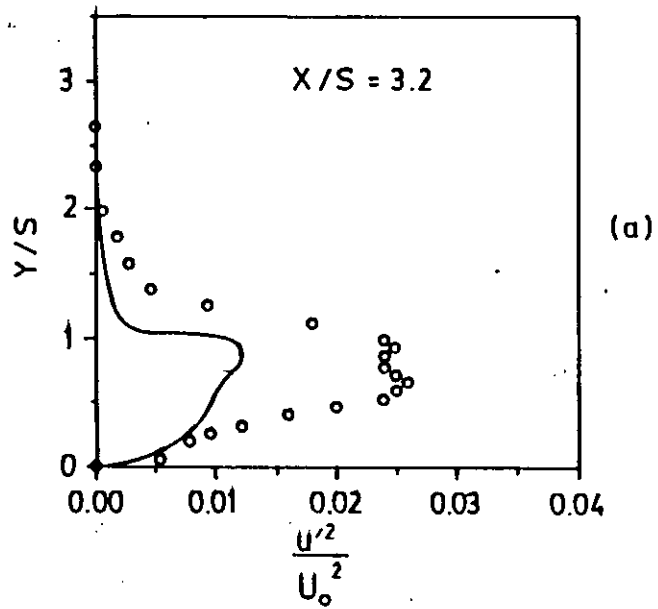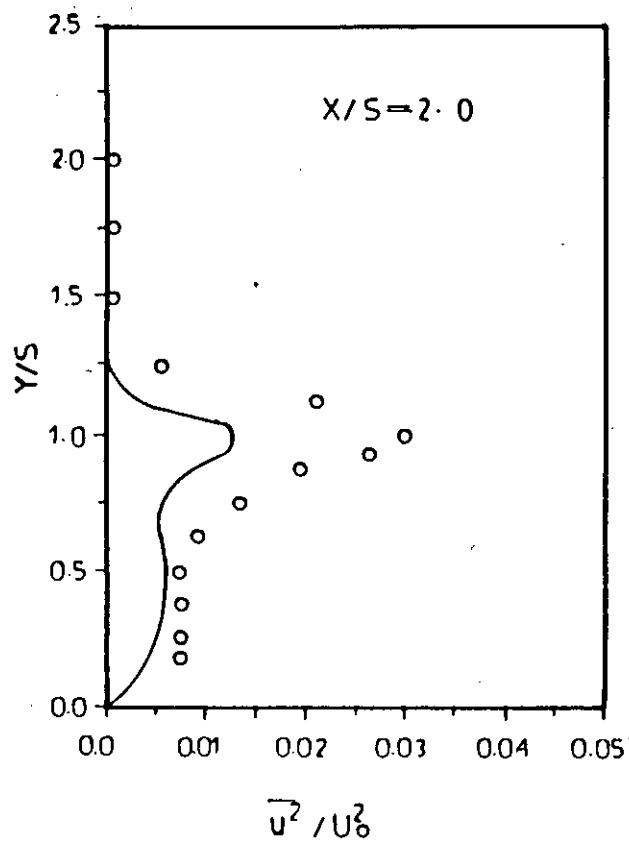
——— Present prediction

o    Expt. (Vogel and Eaton, 1984)

Fig. 4.6 Contd.

Fig. 4.7    Contd.
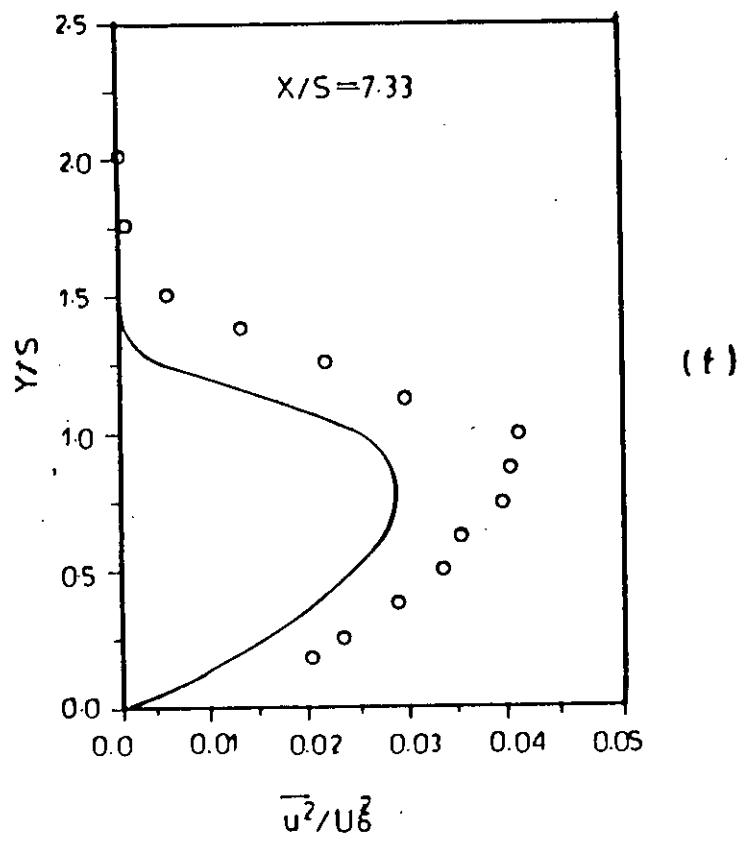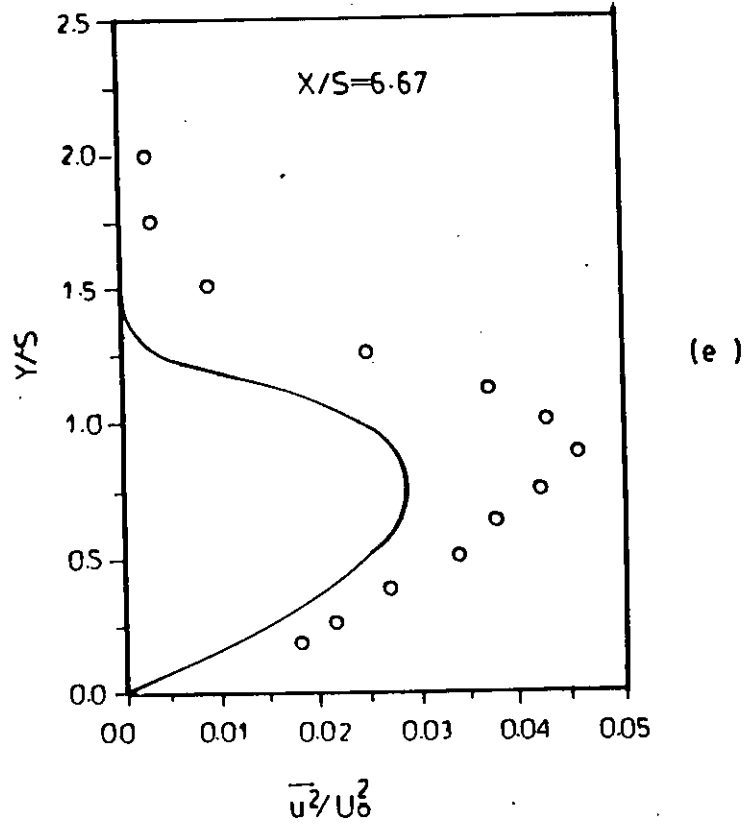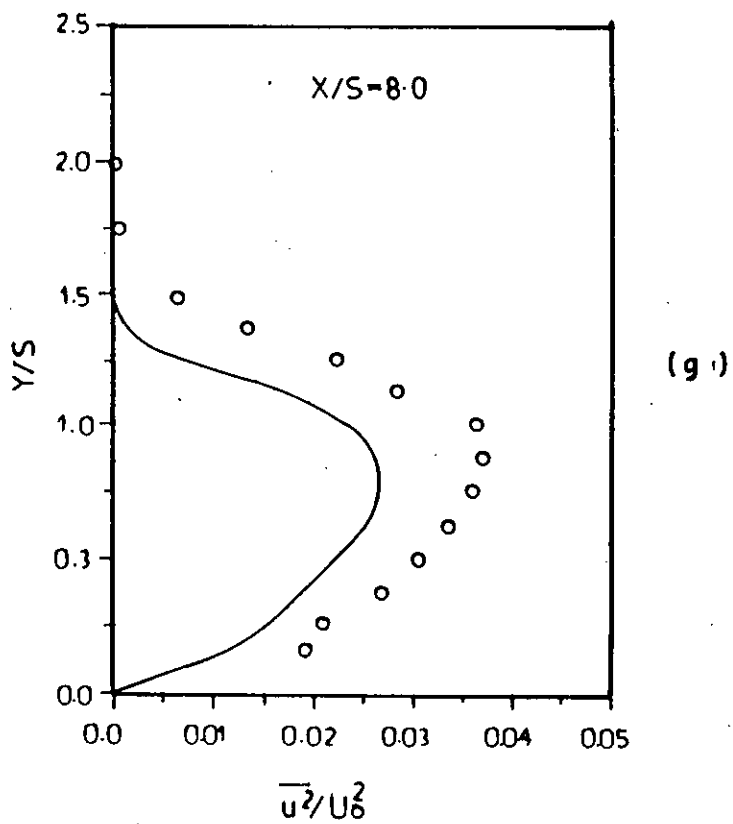
(c)

$$u^2/U_0^2$$



(d)

$$\overline{u^2}/U_0^2$$

Fig. 4.7    Contd.

(e)

(f)

Fig. 4.7    Contd.

(g ·)

Fig. 4:7 . Turbulent normal stress profiles at different axial locations for Res=40000.

_____Present 'prediction,

O Expt. (Eaton & Johnston, 1980)

(a)

$X/S = 1.0$

Y/S

$-\overline{uv}/U_o^2$



(b)

$X/S = 2.0$

Y/S

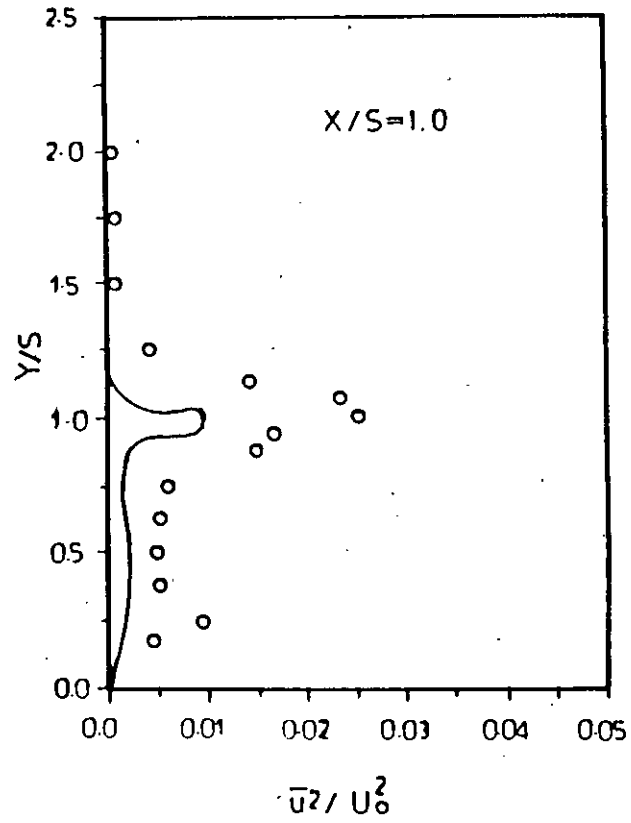$-\overline{uv}/U_o^2$

Fig. 4.8    Contd.

X/S=4.0

(c)

$-uv/U_o^2$

X/S=6.0

(d)

$-\overline{uv}/U_o^2$
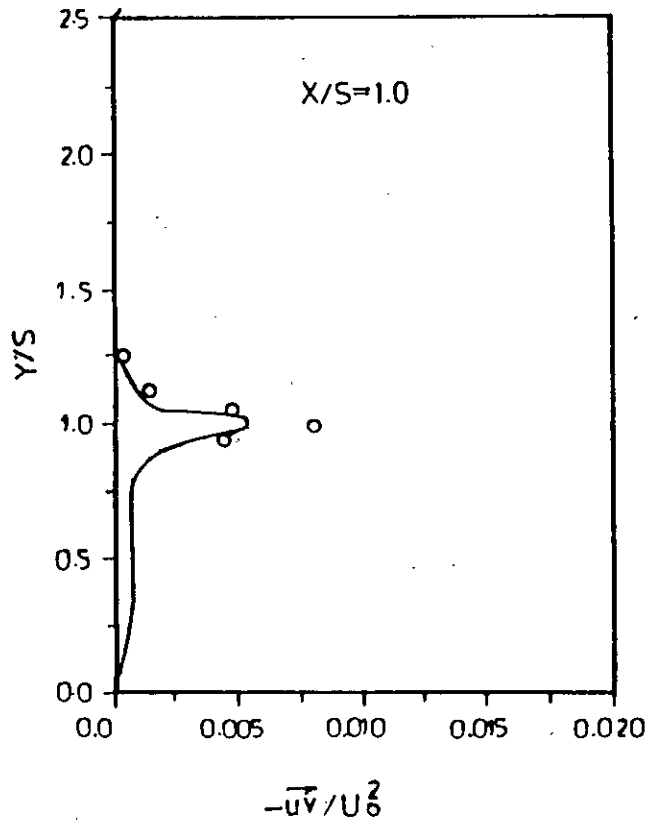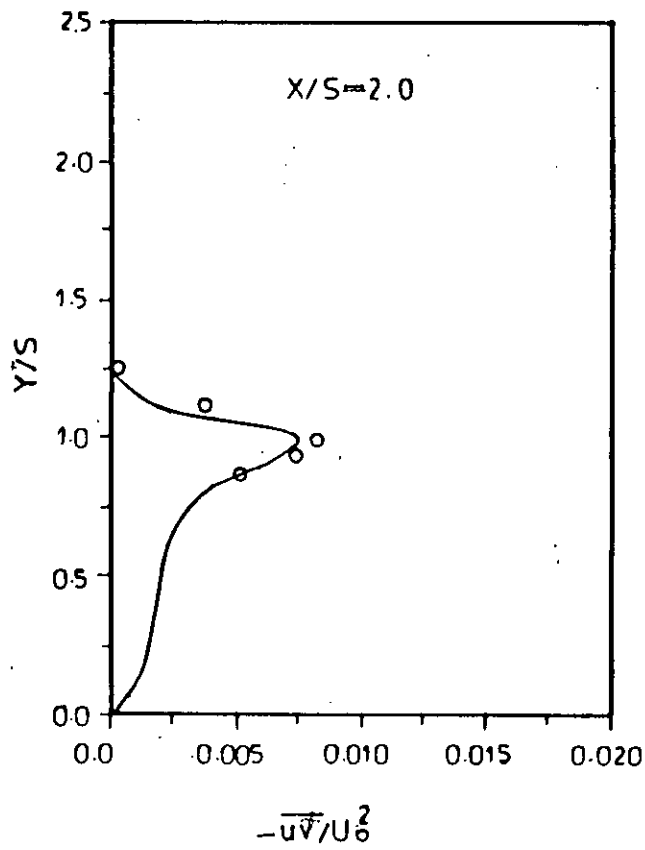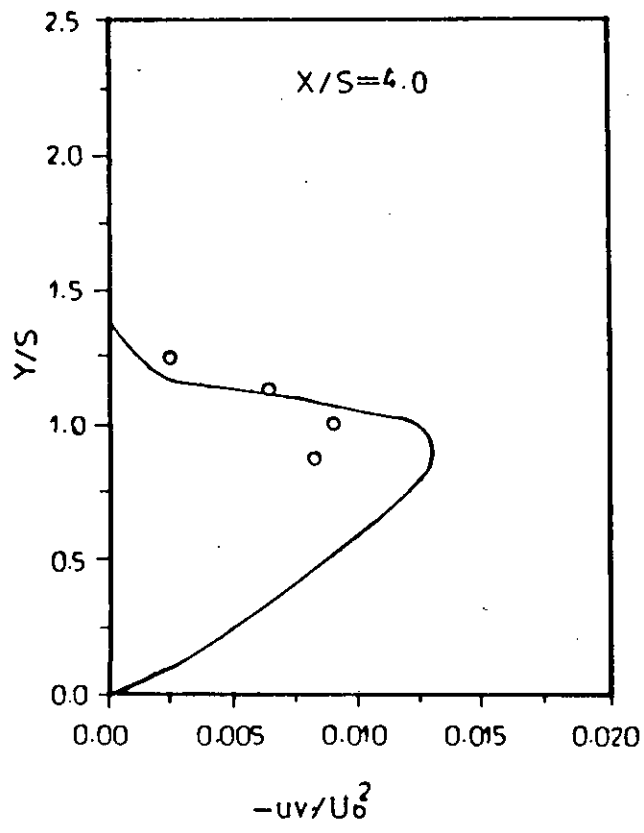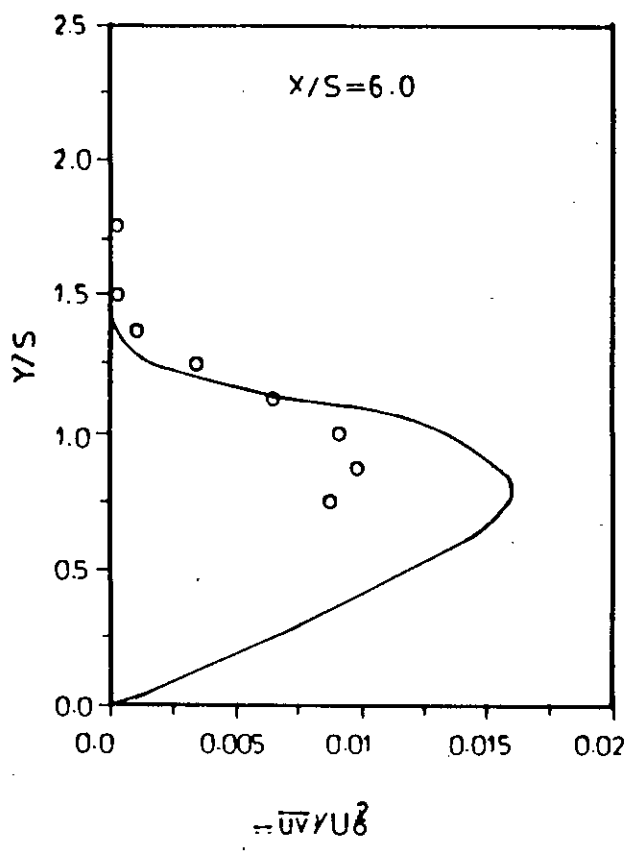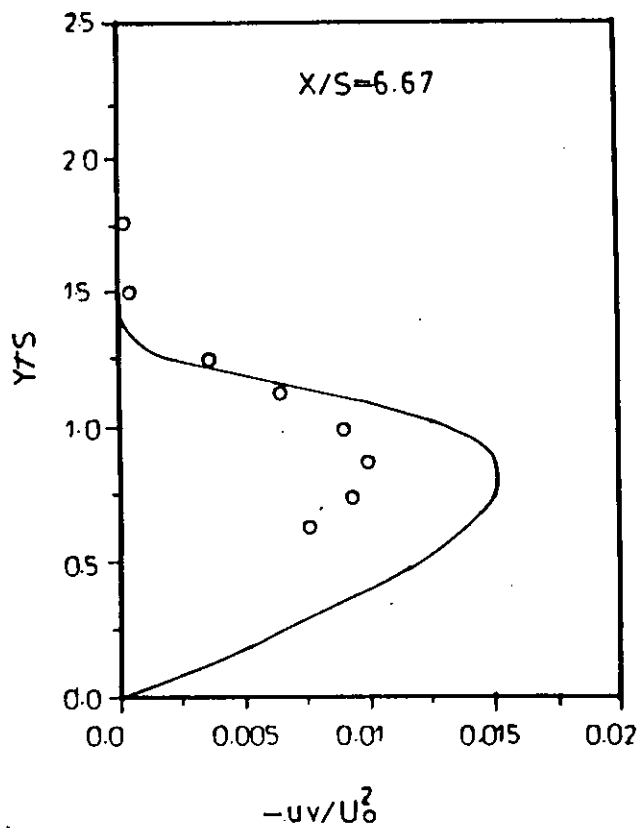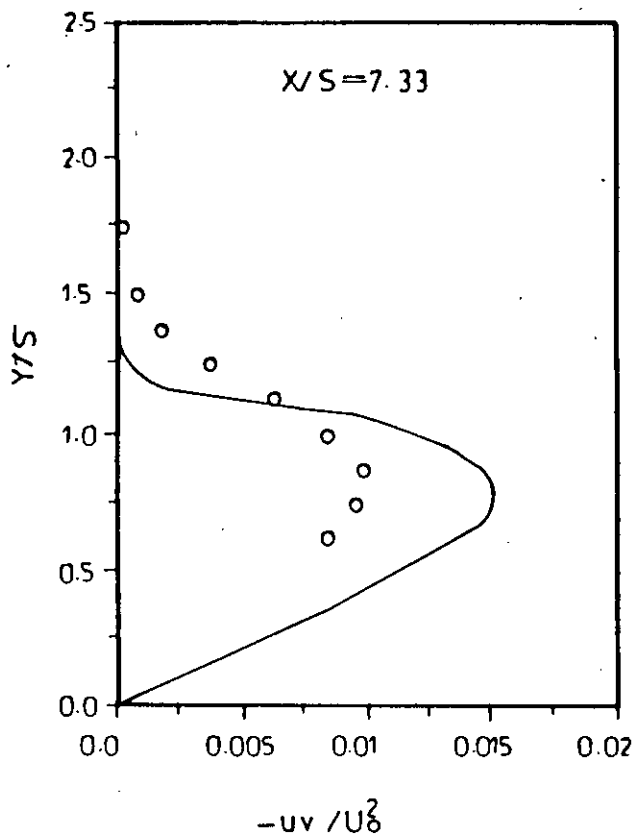
Fig. 4.8 Contd

Fig. 4.8 Contd.
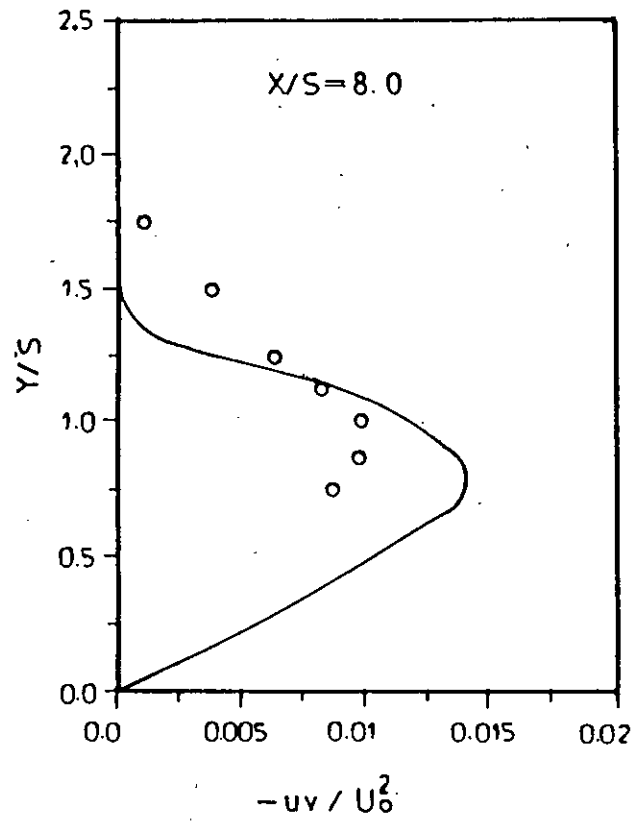
Fig. 4.8. Turbulent shear stress profiles at
different axial locations for $Re_S = 40000$
——— Present prediction,
o Expt. (Eaton & Johnston 1980)
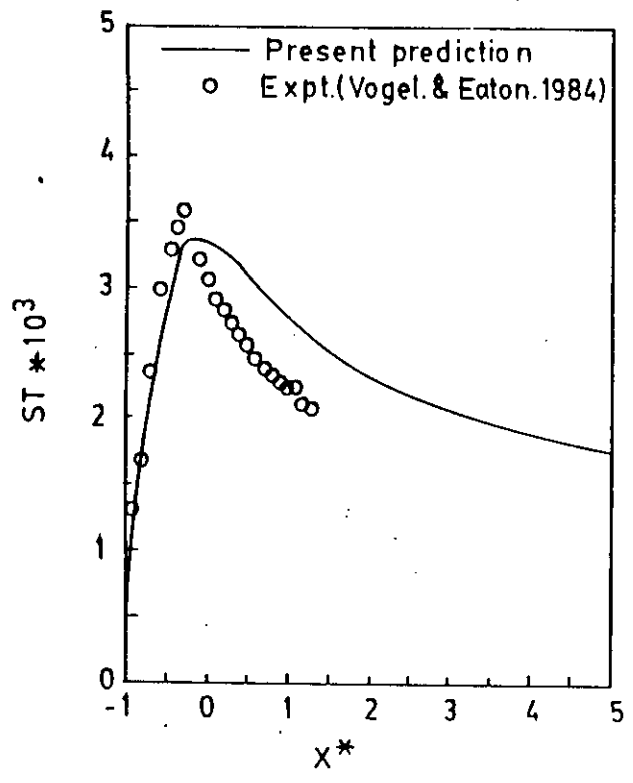
FIG. 4.9 HEAT TRANSFER COEFFICIENT
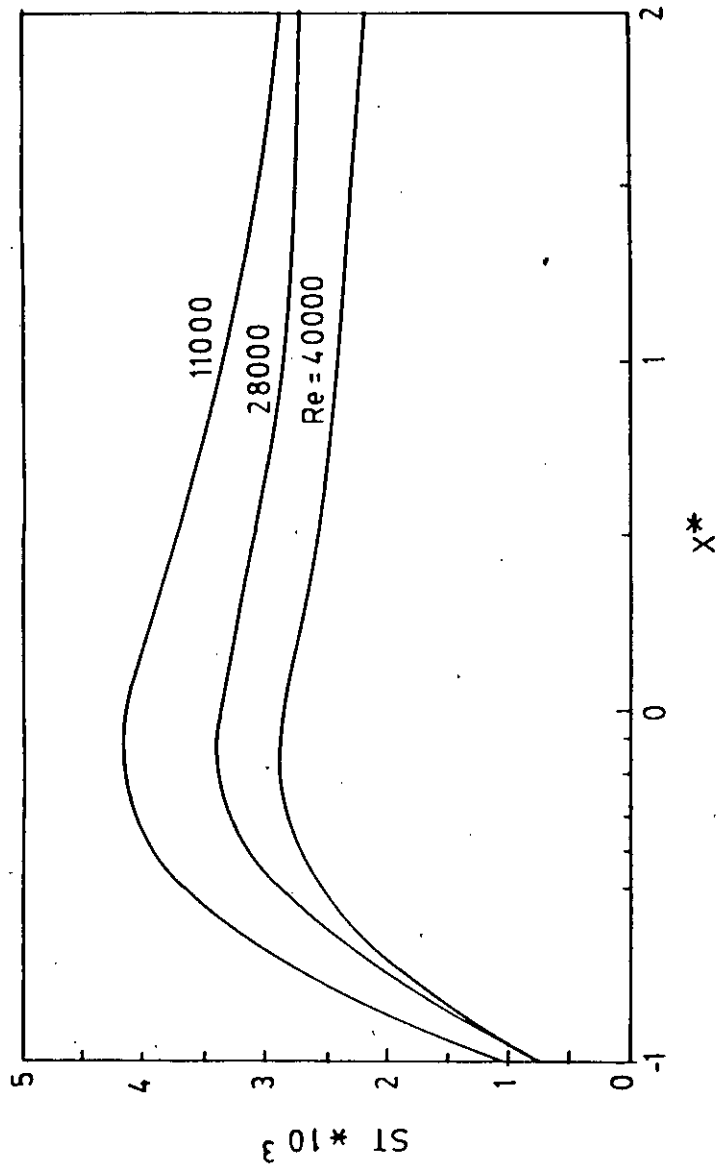
FIG. 4.10  STATON  NUMBER  VARIATIONS  FOR  DIFFERENT  REYNOLDS  NUMBER
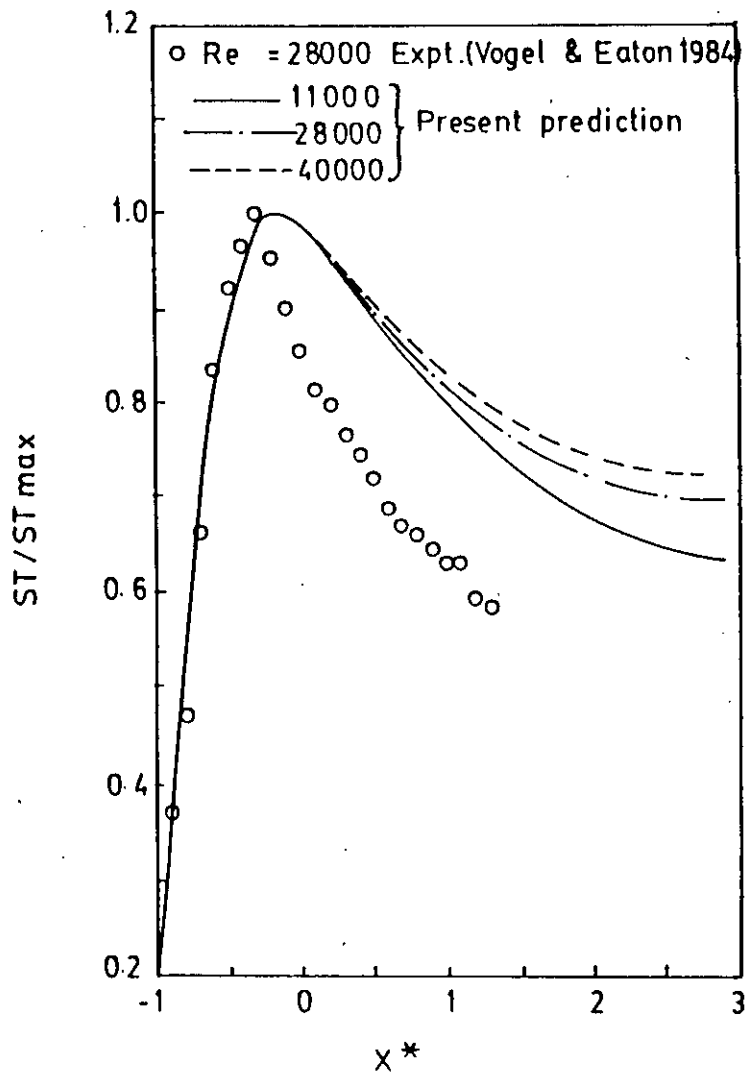
FIG. 4.11 STATON NUMBER PROFILES VARYING WITH
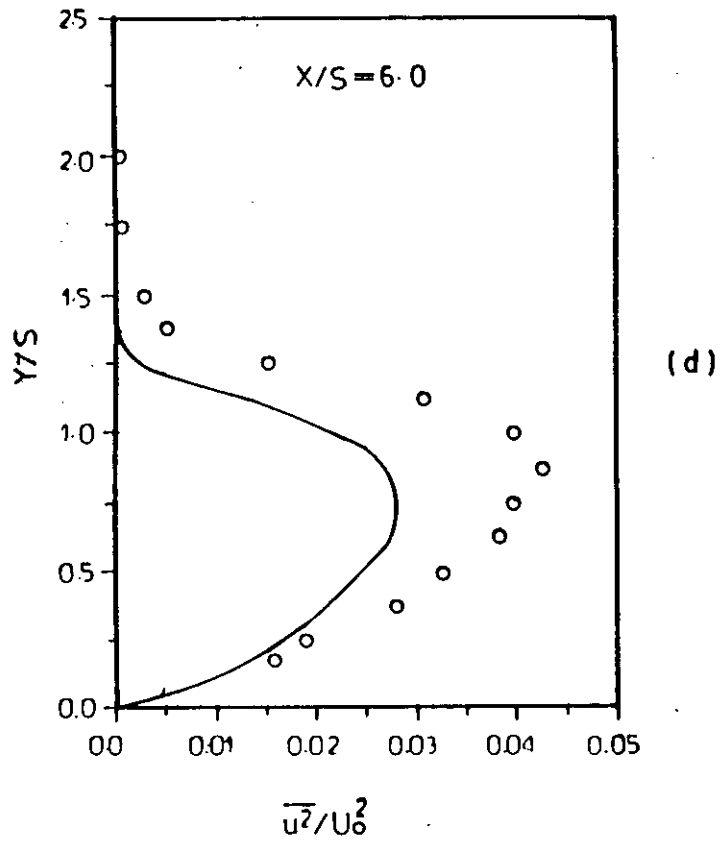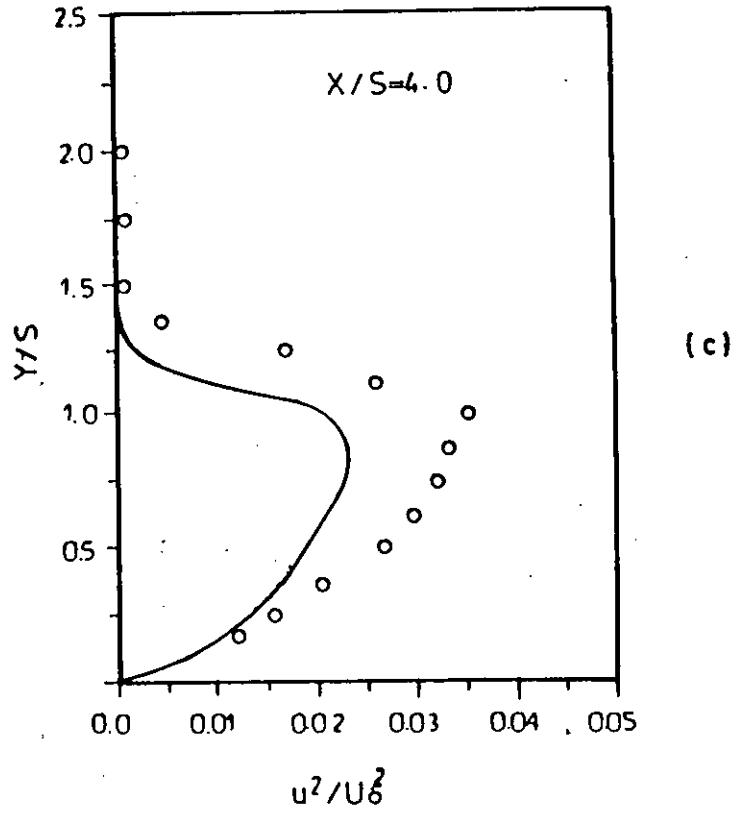REYNOLDS NUMBER NORMALISED ON THE
MAXIMUM STATON NUMBER

(a)

(b)
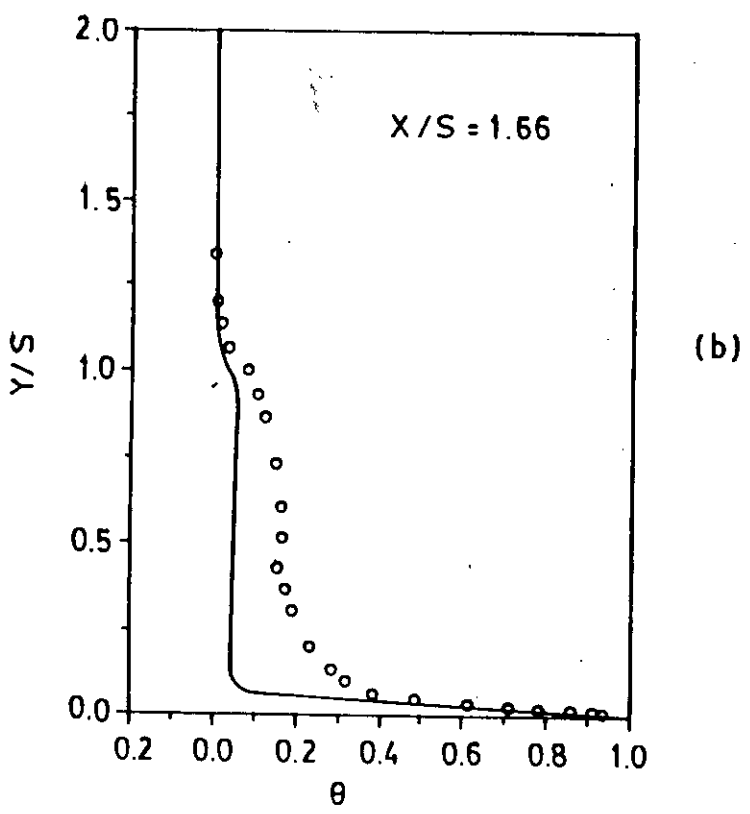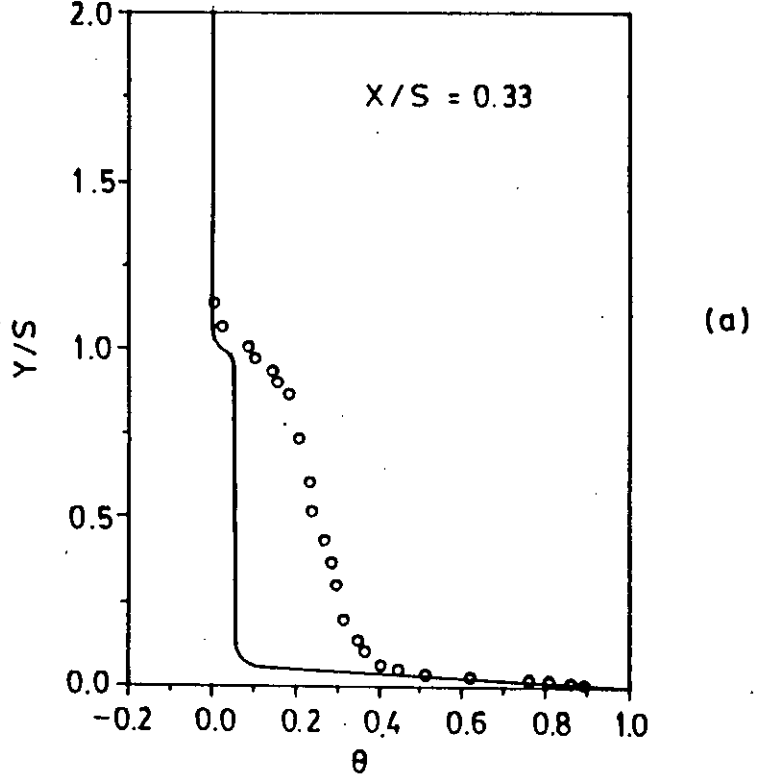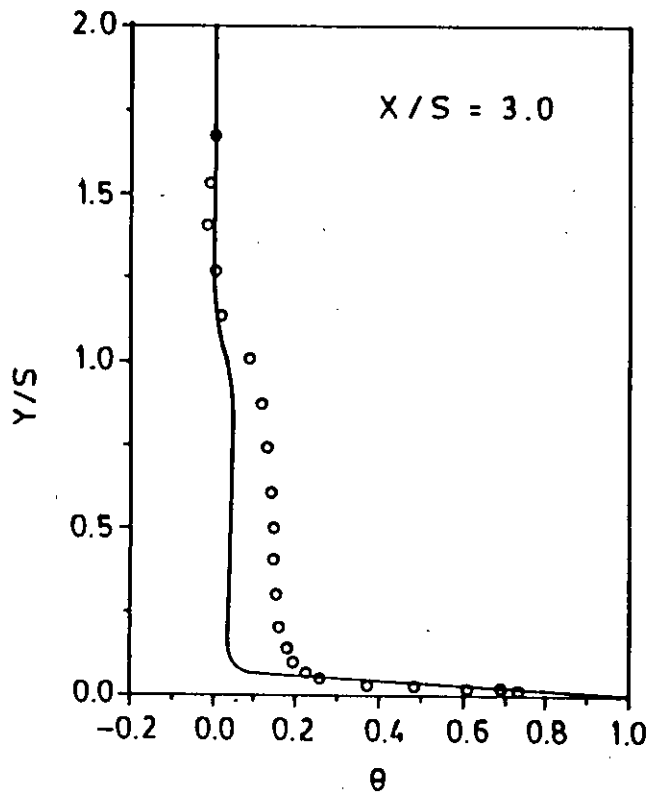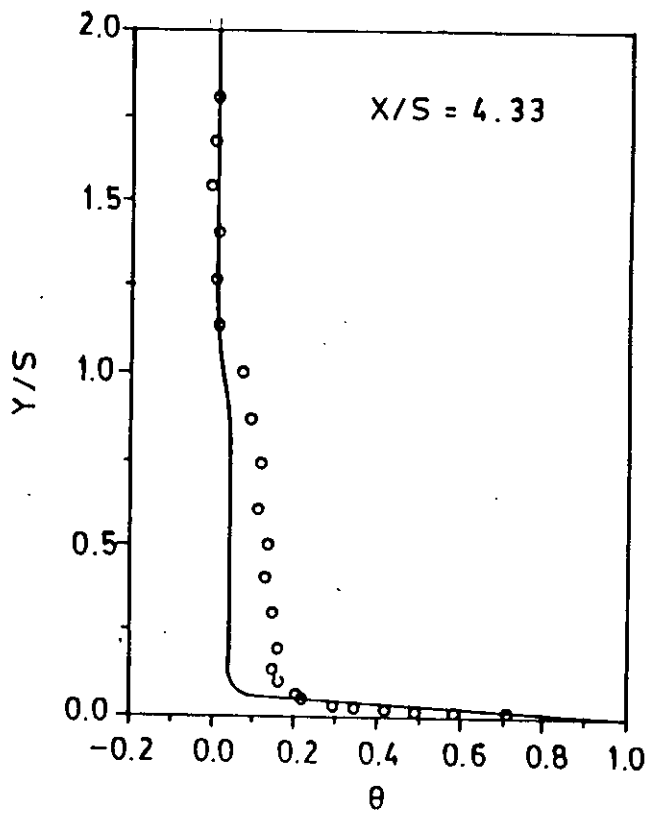
Fig. 4.12  Contd.
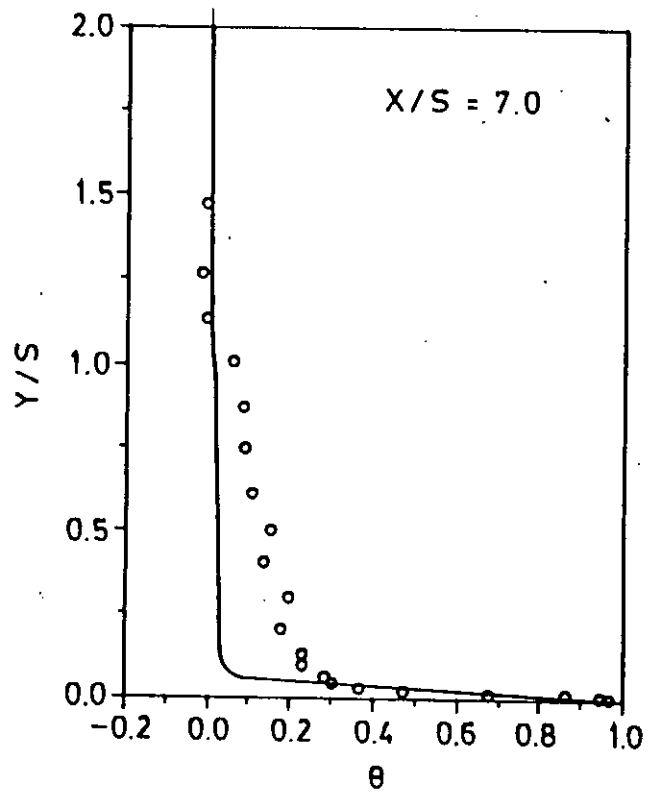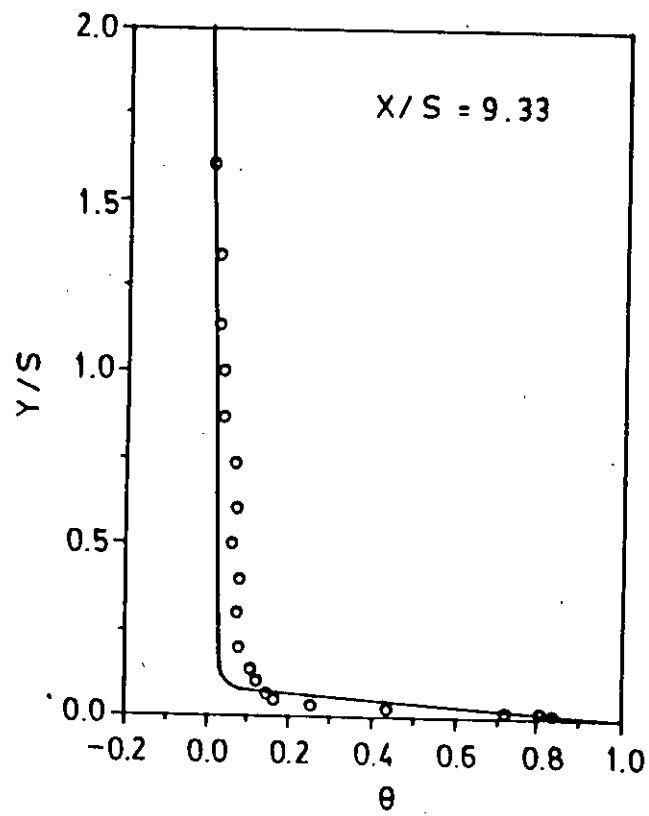
Fig. 4.12 Contd.

Fig. 4.12  Contd.
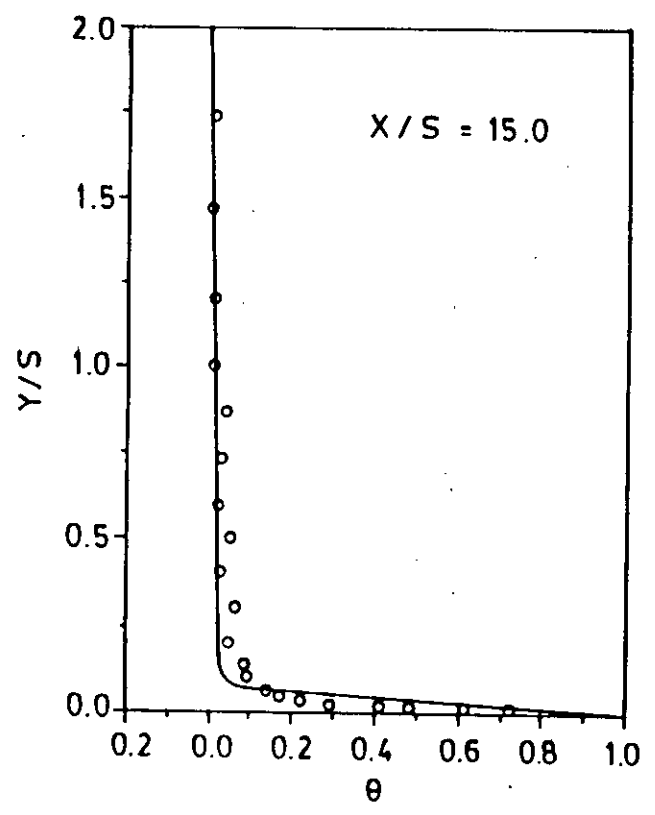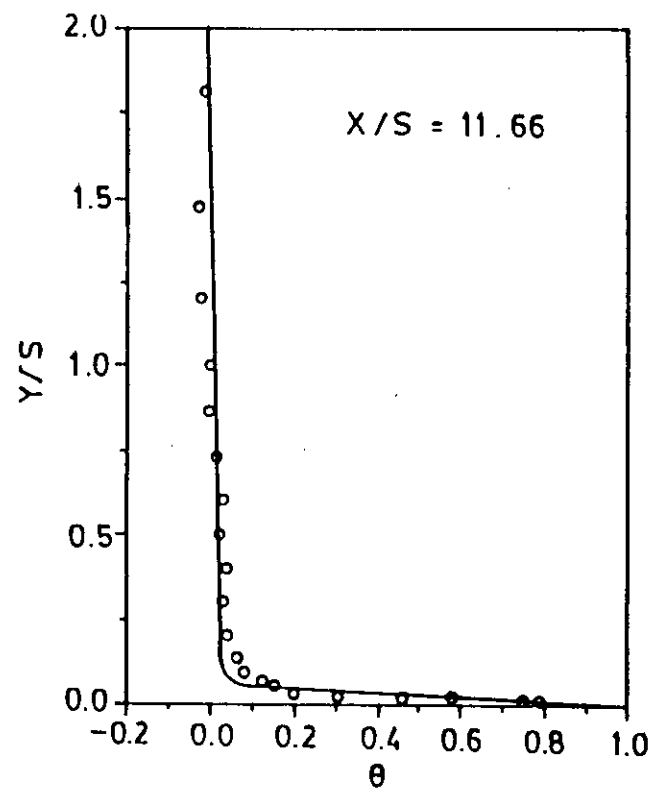
Fig. 4.12   Temperature profiles at different axial
locations for  $Re_S = 28,000$

——   Present prediction
o    Expt. (Vogel and Eaton, 1984)

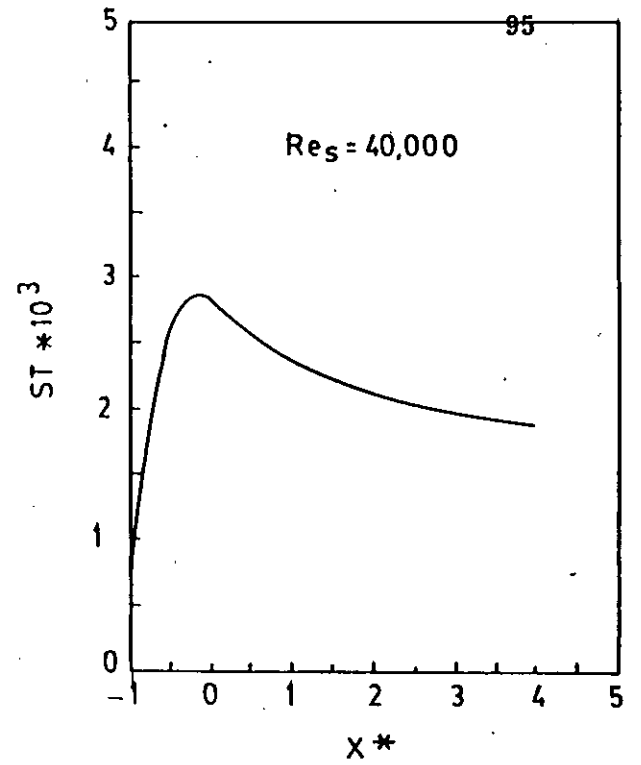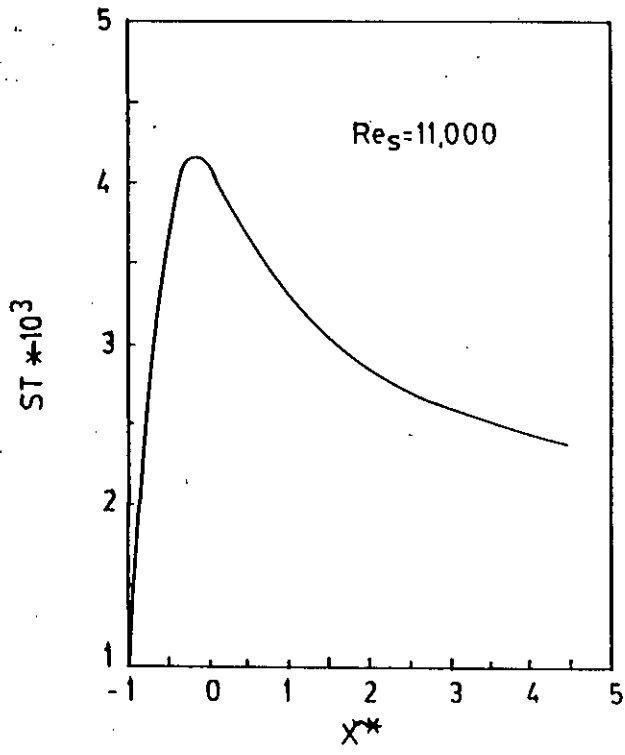# REFERENCES

Abbott, D. E. and S. J. Kline (1962), "Experimental Investigation of Sub-sonic Turbulent Flow Over Single and Double Backward Facing Steps", Trans. ASME, J. Basic Engineering, Vol. 84D, Series D, 1962, pp. 317-325.

Adams, E. (1984), "Experiments on the Structure of Turbulent Reattaching Flow", Ph. D. thesis, Thermosciences Div., Mech. Engg. Dept., Stanford Univ., Stanford, CA 94305 (available as Adams, Johnston, and Eaton, Termosciences Division Report MD-43, May 1984.

Amano, R. S. (1982), "Turbulent Transport Modeling of Shear Flows Around an Aerodynamic Wing", Semi-Annual Progress Report #1, ME Dept., Univ. of Wisconsin-Milwaukee, Milwaukee, WI.

Amano, R. S.,M. K. Jensen, and P. Goel (1983), Jensen, and P. Goel (1983), "Turbulent Heat Transport Downstream from an Abrupt Pipe Expansion", ASME-JSME Thermal Eng. Joint conf., Honolulu, Ha, Vol. 3:63, p. 71.

Amano, R (1983), "A Study of Turbulent Flow Downstream of An Abrupt Pipe Expansion", AIAAJ., Vol. 21, #10, Oct., pp. 1400-1405.

Armaly (1982), "Experimental and Theoretical Investigation of Backward - facing Step Flow", Institute of Hydromechanics Section III: Mechanics of Turbulent Flows, University of Karlsruhe, F.R.G.

Aung, W., and R. J. Goldstein (1972), "Heat Transfer in a Turbulent Separated Flow Downstream of a Reaarward-Facing Step", Israel J. of Tech., Vol. 10, No. 1-2, pp. 35-44.

Aung, W., and C. Watkins (1978) "Heat Transfer Mechanisms in Separated Forced Convection", Turbulent Forced Convection in Channels and Bundles: Theory and Applications to Heat exchangers, Turkey, July 20 Aug. 2.

Aung, W. (1983), "An Experimental Study of Laminar Heat Transfer Downstream of backsteps", J. Heat Transfer, Vol. 105, No. 4, pp. 823-829.

Aung, W., and R. Goldstein (1972), "temperatur Distribtion and Heat Transfer in a Transitional Separated Shear Layer", Proc. IV International Heat-Transfer Conference, Paris & Versailles, FC-1.5.

Bradshaw, P. and F. Y. P. Wong (1972) the reattachment and relaxation of a turbulent shear layer, J. Fluid Mech., Vol. 52, pp. 113-115.

Bradbury, P., and F. Y. F. Wong (1972), "The Reattachment and

Relaxation of a Turbulent Shear Layer", J. Fluid Mech. Vol. 52, Part I, pp. 113-135.

Chieng, C. C., and B. E. Launder (1980)_, "On the Calculation of Turbulent Heat Transport Downstream from an Abrupt Pipe Expansion", Dept. of Mech. Engg., UC-Davis, March.

Chilcott, R. E. (1967), "A Review of Separated and Reattaching Flows with Heat Transfer", Int. J. Heat and Mass Transfer, Vol. 10, pp. 783-797.

Chandrasuda, C. (1975), "A Reattaching turbulent Shear Layer in Incompressible Flow", Ph. D. Thesis, Dept. of Aeronautics, Imperial College of Science and Technology.

Driver, D. M., and H. L. Seegmiller (1982), "Features of a Reattaching Turbulent Shear Layer Subject to an Adverse Pressure Gradient, Paper #AIAA-82-1029, AIAA/ASME 3rd Joint Thermophysics, Fluids, Plasma and Heat-Transfer Conference, June 7-11, St. Louis, MO.

Durst, F., and C. Tropea (9181), "Turbulent, Backward-Facing Step Flows in Twoo-Dimensional Ducts and Channels", Proc. 3rd Symp on Turbulent Shear Flows, UC-Davis, Sept. 9-11, pp. 18.1.18.6.

de Brederode, V. and P. Bradshaw (1972), "Three-Dimensional flow in Nominally Two-Dimensional Separation Bubbles I. Flow Behind a Rearward Facing Step", I.C. Aero Report 72-19, 1972.

Eaton, J. K., a. H. Jeans, J. Ashjaee, and J. P. Johnston (1979), " A Wall-Flow Direction Probe for Use in Separating and reattaching flows," J. Fluids Engrg., Vol. 101, pp. 364-366.

Eaton, J. K., (1980), "Research Initiation : Heat Transfer in a Subsnic Trubulent Reattaching Flow", Thermosciences Div., Mech. Engg. Dept., Stanford Univ. Stanford, CA 94305, Nov.

Eaton, J.K , and J. P. Johnston (1980), "Turbulent Flow Reattachment : An Experimental Study of the Flow and Structure Behind A Backward-Facing Step," Report MD-39, Stanford Univ. Stanford, CA, 94305, June.

Eaton, J. K., J.P. Johnston and a. H. Jeans (1979), "Measurements in a Reattaching turbulent Shear Layer", Proceedings of the 2nd Symposium on Turbulent Shear Flows, London.

Eaton, J. K. and J. P. Johnston (1980b), "A Review of Research on Subsonic Turbulent Flow Reattachment", to be presented at AIAA 13th Fluid and Plasma Dynamics Conference, Snowmass, CO.

Eaton, J. K. and J. P. Johnston (1980a), "An Evaluation of Data for the Backward-Facing Step Flow", Report prepared for the

1980-81 Conferences on Complex Turbulent Flows, Stanford University.

Filetti, E. G., and W. M. Kays (1967), "Heat Trnsfer in Separated, Reattached, and Redevelopemnt Regions Behind a Double Step at Entrance to a Flat Duct", J. Heat Transfer, May, p. 163.

Golstein, R. J., V. L. Eriksen, R. M. Olson, and E. R.G. Eckert (1970), "Laminar Separation, Reattachment, and Transition of the Flow Over a Downstream-Facing Step", Trans. of the ASME, J. Basic Engrg., Dec., Vol. 92, pp. 732.

Gould, R., W. H. Stevenson, and H. D. Thompson (1983), "Laser Velocimeter Measurements in a Dump Combustor," Paper 83-HT-47, ASME Winter Annual Meeting, Nov., Boston, USA.

Goldstein, R. J., V. L. Eriksen, R. M. Olson, and E. R. G. Eckert (1970), "Laminar Separation, Reattachment and Transition of Flow Over a Downstream-Facing Step", trans. ASME, J. Basic Engineering, Vol. 92D, No. 4, pp. 732-741.

Hsu, H. C. (1950), "Characteristics of Mean Flow and turbulence at an abrupt Two-Dimensional Expansion," Ph.D. thesis, Dept. of Mechanical and Hydraulics, State Univ. of Iowa.

Hussain, A. K. M. F. and M. F. Zedan (1978), "Effects of the Initial Condition on the Axisymmetric Free Shear Layer: Effect sof the Initial Moemtum Thickness", Phys. Fluids, Vol. 21, No. 7, pp. 1100-1112.

Jayatilleke, C. L. V. (1969), Prog. Heat and Mass Transfer,Vol. 1, p. 193.

Kays, W. M., and M. E. Crawford, Convective Heat and Mass Transfer, McGraw-Hill Book Co., 2nd ed., 1980.

Kim, J., S. J. Kline, and J. P. Johnston (1978), "Investigation of Separation and Reattachment of a Turbulent Shear Layer: Flow over a Backward-Facing Step", Rept. No. MD-37, Thermosciences Div., Mech. Engrg. Dept., Stanford University.

Kottke, V. (1984), "Heat, Mass, and MOmentum Transfer in Separated Flows", Int. J. Chem. Eng., Jan. Vol. 24, No. 1. pp. 86-94.

Launder B.E. & Spalding D.B. (1972), Mathematical Model of Turbulence, Academic Press, London.

Leonard B. P. (1979), A Stable and Accurate Convection Modelling procedure Based on Quadratic Upstream Interpolation, Comp. Mehtods in Appli. Mech. and Eng., Vo; 19, pp. 59-98.

Leschzinev, M. A. & Rodi W. (1981), Calculation of Annular and

Twin Parallel Jets Using Various Discretisation Schemes and Turbulence Model Variations, J. Fluid Eng., ASME, Vol. 103, pp. 352-360.

Narayanan, M. A. B., Y. N. Khadgi, and P. R. Viswanath (1974), "Similarities in Pressure Distribution in Separated Flow Behind Backward-Facing Steps", Aero Quarterly, No., pp. 305-312.

Pronchick, S. W. and S., J. Kline (9183), "An Experimental Investigation of the Structure of a Turbulent Reattaching Flow behind a Backward-Facing Step", Report MD-42, Thermosciences Div., Mech. Engrg. Dept., Stanford Univ., Stanford, CA 94305, June.

Rashed, M.I.I., R. M. El-Taher and M. A. Ghazy (1978), "Experimental Investigation of the Effect of Surface Discontinuity on Step-Backward Flow", J. Engineering Sciences, Vol. 4, No. 2, Riyadh Univ., Saudi Arabia.

Seban, R. a., A. Emery, and A. Levy (1959), "Heat Transfer to Separated and Reattached Subsonic Turbulent Flows Obtained Downstream of a Surface Step", J. Aero/Space Sciences, Dec., p. 809.

Seban, R., and G. Caldwell (1966), "The Effect of a Spherical Protuberance on the local Heat transfer to a Turbulent Boundary Layer", J. Heat Trnafer, Nov., p. 408.

Seban, R. (1966), "The Effect of Suction and Injection on the Heat Transfer and Flow in a Turbulent Separated Airflow", J. Heat Transfer, Aug., p. 226.

Seban, R. A. (1964), "Heat Transfer to the Turbulent Separated Flow of Air Downstream of a Step in the Surface of a Plate", May, p. 259, J. Heat transfer.

Seki, N., S. Fukusako, and T. Hirata (1976), "Turbulent Fluctuations and Heat Trnasfer for Separated Flow Associated with a Double Step at Entrance to an Enlarged Flat Duct", J. Heat Tranfer, Nov., p. 588-593.

Seki, N., S. Fukusako, and T. Hirata (1976), "Effect of Stall Length on Heat Transfer in Reattached Region Behind a Double Step at Entrance to an Enlarged Flat Duct", Int. J. Heat and Mass Transfer, Vol. 19, pp. 700-702.

Simpson, R. L. (1981), "Review-A Review of Some Phenomena in Turbulent Flow Separation", Trans of the ASME Vol 103, Dec. p. 520.

Simpson, R. L., Y. T. Chew, and B. G. Shivaprased (1981), "The Structure of a Separating Turbulent Boundary Layer. Part I: Mean Flow and Reynolds Stress", J. Fluid Mechanics, Vol. 113, pp. 23-51.

Simpson, R. (1983), "A Model for the Backflow Mean Velocity Profile", AIAA J., Vol. 21, #1, Jan., pp. 142-143.

Simpson, R. L. (1976), "Interpreting Laser and Hot-Film Anemometer Signals in a Separating Boundary Layer", AIAA J., Vol. 14, No. 1, pp. 124-126.

Smyth, R. (1979), "Turbulent Flow Over a Plane Symmetric Sudden Expansion," Trans. ASME, J. Fluids Engineering, Vol. 101, No. 3, pp. 348-353.

Sirdir, M. (1983), "Effects of Expansion Ratio on the Calculation of Parallel-Walled Backward-Facing Step Flows: Comparison of Four Models of Turbulence", Paper 83-FE-10, ASME Winter Annual Meeting, Nov., Boston, USA.

Sirdir, M. (1983), "Calculation of Deflected-Walled Backward-Facing Step Flows: Effects of Angle of Deflection on the Performance of Four Models of Turbulencee", Paper 83-FE-16, ASME Winter Annual Meeting, Nov., Boston, USA.

Tani, I., M. Iuchi and H. Komoda (1961), "Experimental Investigation of Flow Separation Associated with a Step or Groove", Report No. 364,Aero. research Institute, Univ. of Tokyo.

Watkins, C., and A. Gooray (1982), "Numerical Calculatiuons of Turbulent Recirculating Heat Transfer beyond Two-Dimensional Backsteps and Sudden Pipe Expansions," Dept. of Mech. Engg. Howard University, Wash. D. C., Aug.

Vogel, J.C. and Eaton J. K. (1984), "Heat Transfer and Fluid Mechanicsl Measurements in the Turbulent Reattaching Flow Behind a Bakward-Facing Step, Transactions of the ASME, Vol. 107, Nov. 1985.

Walterick, R. E., J. I. Jagoda, C.R.J. Richardson, W. A. DeGroot, W. C. Strahle, and J. E. Hubartt (1984), "Experiments and Computations Paper AIAA-84-0013, AIAA 22nd Aerospace Sciences Meeting, Jan. 9-12, Reno, Nevada.

Westphal, R. (1982), "Experimental Study of Flow Reattachment in a Single-Sided Sudden Expansion", Ph.D. Dissertation, Dept. of Mech. Engrg., Stanford Univ. Stanford, CA, 94305, Dec. (available as NASA Contractor Report 3765, Jan. 1984.

Zemanick, P., and R. Dougall (1970), "Local Heat Transfer Downstream of Abrupt Circular Channel Expansion", J. Heat transfer, Feb., p. 53.

APPENDIX A

CONTROL VOLUME FOR U

CONTROL VOLUME FOR V
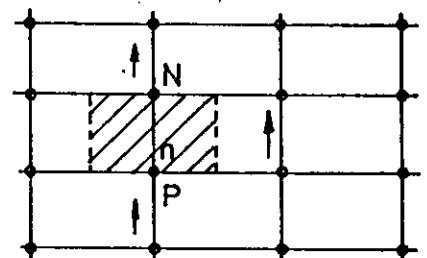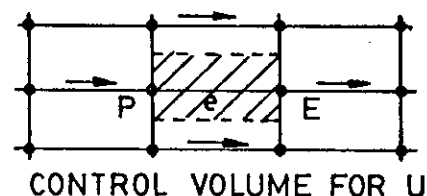
## DISCRETIZED EQUATIONS:

The momentum equations:

U-momentum equation:

$$a_e u_e = a_{nb} u_{nb} + b + (P_P - P_E) A_e \quad \ldots\ldots(1)$$

V-momentum equations:

$$a_n v_n = a_{nb} v_{nb} + b + (P_P - P_N) A_n \quad \ldots\ldots(2)$$

where    $(P_P - P_E)$ is the pressure difference

$A_e$ is the area on which the pressure difference acts

and    $(P_P - P_N) A_e$ is the pressure force acting on U control volume

The momentum equation can be solved only when the pressure field is known or is somehow estimated. Unless the correct pressure field is employed, the resulting velocity field will not satisfy the continuity equation. Such an imperfect velocity field based on a guessed pressure field * is denoted by $u^*, v^*$. This 'starred' velocity field will result from the solution of the following discretization equations:

$$a_e u_e^* = a_{nb} u_{nb}^* + b + (P_P - P_E) A_e \quad \ldots\ldots\ldots\ldots(3)$$

$$a_n v_n^* = a_{nb} v_{nb}^* + b + (P_P - P_N) A_N \quad \ldots\ldots\ldots\ldots(4)$$

## The Pressure and Velocity Corrections

Let the corrected pressure 'P' is obtained from:

$$P = P^* + P' \quad \ldots\ldots\ldots\ldots\ldots\ldots\ldots\ldots\ldots\ldots\ldots\ldots(5)$$

where $P'$ is the pressure correction.

The corresponding velocity corrections $u'$, $v'$, $w'$ can be introduced as:

$$u = u^* + u' \; ; \; v = v^* + v' \; ; \; w = w^* + w' \quad \ldots\ldots\ldots\ldots(6)$$

Subtracting (3) from (1), we have

$$a_e u_e' = a_{nb} U_{nb}' + (P_P' - P_E') A_e \quad \ldots\ldots\ldots\ldots\ldots\ldots(7)$$

Dropping $a_{nb} u_{nb}'$ for computational convenience,

$$a_e u_e' = (P_P' - P_E') A_e \quad \ldots\ldots\ldots\ldots\ldots\ldots\ldots\ldots\ldots(8)$$

$$u_e' = d_e (P_P' - P_E') \quad \ldots\ldots\ldots\ldots\ldots\ldots\ldots\ldots\ldots(9)$$

where $d_e = A_e/a_e$

Equation (9) is the velocity-correction formula.

APPENDIX B

## SOLUTION PROCEDURE

SIMPLE (Semi-Implicit Method for Pressure-Linked Equation) algorithm is used for the calculation of the flow field. The important operations, in order of their execution, are:

1.   Guess the pressure field $P^*$.
2.   Solve the momentum equations to obtain $u^*$ and $v^*$.
3.   Solve the $P'$ equation.
4.   Calculate P by adding $P'$ to $P^*$.
5.   Calculate u, v from their starred values using the velocity-correction formulas.
6. Solve the discretization equation for other variables (such as temperature and turbulence quantities) if they influence the flow field through fluid properties, source terms etc.
7.   Treat the corrected pressure P as a new guessed pressure $P^*$, return to step 2 and repeat the whole procedure until a converged solution is obtained.

TABLE 1.1

SUMMARY OF BACKWARD FACING STEP DATA SETS

| Author/s | B.L. Thickness at sep. $\delta_B/S$ | $R_\delta$ sep. | B.L. state at sep. | $Re_\delta$ | Free Stream Turbulence $u'/U_o$ | Aspect ratio | Reattachment length $x_r/S$ | Turbulence data | max $\overline{u'v'}/U_{ref}^2$ | max $\overline{u'^2}/U_{ref}^2 \times 100$ | Configuration | last data $x/S$ |
|---|---|---|---|---|---|---|---|---|---|---|---|---|
| Abbott & Kline | .16-1.97 | 800-1600 | Turb. | $2\times10^4$ $-5\times10^4$ | | 2-15 | 7±1 | hot-film dubious results | – | – | sudden expansion double-sided | 10 |
| Baker | .71 | 3550 | Turb. | $5\times10^4$ | .15% | 18 | 5.7 – 6.0 | u' PWA u'v' x-wire | 1.1 | 4.2 | small step in large tunnel $y_1/y_o$=1.10 | 9 |
| Bradshaw & Wong | .13 | 730 | Lam | $4.2\times10^4$ | | 30.5 | 6 | – | – | – | sudden expansion with shaped upper wall | 52 |
| Chandrsuda | 0.04 | 570 | Lam | $1.1\times10^5$ | 0.07% | 15 | 5.9 | $\overline{u'}$ u-wire $\overline{v'}$, $\overline{u'v'}$ x-wire | 1.1 | 2.7 4.0 w/ u-wire | sudden expansion top wall sloped down at 1.7° | 14.3 |
| Denham | .5 | ~150 | Lam/ Turb | $3\times10^3$ | – | 20 | 6 | u' laser | – | 5 | sudden expansion 2:3 | – |
| Eaton & Johnston | .23 | 890 | Turb. trans. | $3.9\times10^4$ | .3% | 12 | 7.97 | u' pulsed wire anemometer | – | 4.5 | sudden expansion 3:5 | 12 |
| Eaton & Johnston | .23 | 510 | Trans | $2.3\times10^4$ | 1.0% | 12 | 8.2 | u' pulsed wire anemometer | – | 3.4 | sudden expansion 3:5. | 12 |
| Eaton & Johnston | .18 | 240 | Lam | $1.1\times10^4$ | .3% | 12 | 6.97 | u' pulsed wire anemometer | – | 3.7 | sudden expansion 3:5 | 12 |

[Taken from Eaton & Johnston, 1980]

TABLE 1.1

SUMMARY OF BACKWARD FACING STEP DATA SETS

| Author/s | B.L. Thickness at sep. $\delta_s/h$ | $R_\theta$ sep. | B.L. state at sep. | $Re_h$ | Free Stream turbulence $\overline{u}/U_0$ | Aspect ratio | Reattachment length $x_r/h$ | Turbulence data | max $\overline{u'v'}/U_{ref}^2$ × 100 | max $\overline{u/2}/U_{ref}^2$ × 100 | Configuration | last data $x/h$ |
|---|---|---|---|---|---|---|---|---|---|---|---|---|
| Etheridge & Kemp | 2.0 | 600 | Trans. turb. | | 2% | | 5.0 | Frequency shifted LDV $\overline{u'}, \overline{v'}, \overline{u'v'}$ | 1.7 | 4.2 | Free surface water channel Distance to surface = 14.5 h. | 8.26 |
| Grant | – | – | Turb. | $3.4 \times 10^3$ | – | 23 | – | laser u' | – | 4.5 | small step in large tunnel | 4.5 |
| Haminh & Chaissing | .05 | – | Turb. | $1 \times 10^5$ | .1% | 6 | ~6 | – | – | – | sudden expansion 5.5-6.6 | 15 |
| Hsu | .13 | 3300 | Turb. | $2.5 \times 10^5$ | 3.5% | 4.5 | >6.0 (6.3) | hotwire $\overline{u'}, \overline{u'v'}$ | 50 | 3.6 | sudden expansion 2:3 | 10.5 |
| Kim et al. | .45 | 1400 | Turb. | $3.0 \times 10^4$ | ~.6% | 24 | 7±1 | $\overline{u'}, \overline{v'}$ $\overline{u'v}$ x-wire | .95 | 2.47 | sudden expansion 3:4 | 16 |
| Kim et al. | .30 | 1400 | Turb. | $4.5 \times 10^4$ | .6% | 16 | 7±1 | $\overline{u'}, \overline{v'},$ $\overline{u'v'},$ x-wire | 1.00 | 2.84 | sudden expansion 3:4.5 | 16 |
| Kuehn | – | 4950/12,000 | Turb. | – | – | 6 | 7 | – | – | – | sudden expansion 3"-4" | |
| Kuehn | – | 4950/12,000 | Turb. | – | – | 12 | 6.74/6.51 | – | – | – | sudden expansion 3.5"-4" | |
| Narayanan et al. | 3.33-.2 | 1800 | Turb. | – | .03% | 166-10 | 5.6-6 | – | – | – | small step in large wind tunnel | – |

TABLE 1.1

SUMMARY OF BACKWARD FACING STEP DATA SETS

| Author/s | B.L. Thickness at sep. $\delta/S$ | $R_\theta$ sep. | B.L. state at sep. | $Re_S$ | Free Stream Turbulence $\overline{u'}/U_o$ | Aspect ratio | Reattachment length $x_r/S$ | Turbulence data | max $\overline{u'v'}/U^2_{ref}$ x 100 | max $\overline{u'^2}/U^2_{ref}$ x 100 | Configuration | last data $x/S$ |
|---|---|---|---|---|---|---|---|---|---|---|---|---|
| Rashed et al. | – | – | – | $3.9\times10^4$ | .3% | 10 | 6 | u' hotwire | – | – | sudden expansion 2.4:2.8 | 12 |
| Rothe and Johnston | .5 | <900 | Trans. turb. | – | 5.5% | 15 | 7 | – | – | – | – | – |
| Seki | – | – | '– | $3.3\times10^4$ | ? | ? | ? | hotwire u' very dubious results | .6 | 1.1 | sudden expansion double sided | – |
| Smyth | fully developed channel | – | Turb. | $7.0\times10^3$ | – | 30 | 6 | laser $\overline{u'}$, $\overline{v'}$ $\overline{u'v'}$, $\overline{w'}$ | 1.1 | 2.8 | double sided expansion 1:1.5 | 4b |
| Tani | .28 | 2100 | Turb. | $6\times10^4$ | ? | 47.5 | 6.5-6.9 | $\overline{u'}$ u-wire $\overline{u'v'}$ rotatable slant-wire | 1.3 | 3.5 | small step in large channel $y_1/y_o = 1.07$ | 16 |
| Tropea and Durst | 2 | 1080 | Trans. turb. | $5.5\times10^3$ | 2% | | 15 | laser $\overline{u'}$, $\overline{v'}$ $\overline{u'v'}$ | – | 2.8 | free surface water channel 7.5:1 | 35 |